POLITECNICO DI MILANO

School of Industrial and Information Engineering

Department of Chemistry, Materials and Chemical Engineering "Giulio Natta"

Master of Science in Chemical Engineering – Process Engineering

Thermal Degradation of PVC-PET Plastic Mixtures

in collaboration with

Ghent University - Faculty of Engineering and Architecture

Department of Materials, Textiles and Chemical Engineering

Laboratory for Chemical Technology (LCT)

Supervisor:

Prof. Alberto CUOCI

Co-supervisor:

Prof. Kevin VAN GEEM

Author:

Emanuele MONTANARI – 921103

Academic Year 2019/2020

Contents

List of figures

List of tables

Abstract

Plastic materials play a significant role in the world today due to their countless applications. They are used to produce valuable products such as protective packaging, clothing, insulation materials, medical devices, and key components for different applications. However, with the fast increase in plastic consumption, there is also an inevitable increase in plastic waste that causes significant environmental pollution due to its low degradability in nature.

The most widespread treatment trend remains landfilling or incineration, although, especially for the former, attempts have been made to limit its use over the years. In fact, neither of these routes is completely accepted from an environmental point of view by the current international legislation. Moreover, this kind of waste is difficult to be treated or mechanically recycled, mostly due to its complex nature and composition that strongly affects the degree to which this waste can be effectively recycled.

On the contrary, chemical treatment processes, such as pyrolysis or gasification, are promising alternatives for waste valorization. In particular, plastic mixtures pyrolysis makes it possible to treat different types of plastics together, exploiting their properties to decompose at different temperatures. Therefore, in order to minimize polymer waste, nowadays, there is a greater interest in better assessing the chemical phenomena governing plastic mixtures thermal degradation.

Among these polymers, polyvinyl chloride (PVC) and polyethylene terephthalate (PET) play a significant role during the pyrolysis of mixed plastic waste since they are found in

significant quantities. For this reason, modeling the thermal degradation of these two polymers mixture is of extreme importance and leads to quite a few challenges due to the existence of chemical interactions between them. Furthermore, the presence of PVC in the mixture makes the selection of reaction conditions more complex due to the large chlorine content within its molecular structure, becoming a source of an important release of HCl.

This work aims to study and understand an existing detailed kinetic model describing the thermal degradation of neat PVC and PET, followed by the study of the thermal degradation of PVC-PET plastic mixtures, with special emphasis on the chemical interactions occurring between these two polymers. The planned work includes various simulations and comparisons with experimental data at different operating conditions and sensitivity analysis of the model itself to the main parameters affecting the thermal process. The collected experimental results are compared with the results obtained from the existing model in order to highlight the strengths and weaknesses of the model, comparing both the thermogravimetric curves and the distribution of the products.

The results showed the reliability of the model in the operating conditions investigated. However, further studies will be necessary to obtain more precise predictions, especially regarding the distribution of the products. The work carried out represents a starting point for future activity to obtain a clearer and more reliable kinetic scheme of the current PVC and PET neat polymers model and PVC-PET mixtures. This model, combined with the previously developed kinetic schemes of other plastic polymers, can be used to simulate real plastic mixtures collected in municipal solid waste, i.e. *plasmix*, and for the design of pyrolysis plants.

Sommario

Le materie plastiche rivestono un ruolo significativo nel mondo di oggi date le loro innumerevoli applicazioni. Sono utilizzate, infatti, per la produzione di prodotti come imballaggi protettivi, indumenti, materiali isolanti, dispositivi medici e componenti chiave per svariate applicazioni. Tuttavia, il rapido aumento del consumo di plastica porta anche ad un inevitabile aumento della produzione di rifiuti plastici che, a causa della bassa degradabilità in natura, provoca un considerevole inquinamento ambientale.

La tendenza più diffusa per trattare questi rifiuti plastici rimane quella del deposito in discarica o dell'incenerimento, anche se, soprattutto per la prima, si è cercato di limitarne l'uso nel corso degli anni. Infatti, nessuno dei due sistemi risulta completamente accettabile da un punto di vista ambientale dalle attuali politiche internazionali. Inoltre, questo tipo di rifiuti risulta difficile da trattare o riciclare meccanicamente, soprattutto a causa della sua complessa natura e composizione che ne influenzano l'effettivo grado di riciclo.

Al contrario, processi di trattamento chimico, come la pirolisi o la gassificazione, risultano essere una promettente alternativa per una valorizzazione del rifiuto. In particolare, la pirolisi di miscele plastiche è in grado di trattare diversi tipi di plastiche insieme, sfruttando le proprietà delle stesse di decomporsi a temperature differenti. Pertanto, al fine di ridurre l'accumulo di rifiuti plastici, esiste sempre più un maggiore interesse a comprendere meglio i fenomeni chimici responsabili della degradazione termica delle miscele plastiche.

Tra questi polimeri, il polivinilcloruro (PVC) e il polietilentereftalato (PET) svolgono un ruolo importante durante la pirolisi di rifiuti plastici poiché presenti in quantità significanti.

Per questa ragione, la modellazione del degrado termico di questi due polimeri e della loro miscela è di estrema importanza e porta a non poche difficoltà a causa dell'esistenza di interazioni chimiche che si verificano tra di loro durante il processo. Inoltre, la presenza di PVC nella miscela rende più complessa la scelta delle condizioni di reazione a causa dell'elevato contenuto di cloro all'interno della propria struttura molecolare, diventando fonte di un significativo rilascio di HCl.

L'obiettivo di questo lavoro è focalizzato sullo studio di un modello cinetico dettagliato già esistente che descrive la degradazione termica del PVC e PET puri, seguito dallo studio della degradazione termica di miscele plastiche PVC-PET, con particolare enfasi sulle interazioni chimiche che avvengono tra questi due polimeri. Il lavoro previsto comprende diverse simulazioni e confronti con dati sperimentali in differenti condizioni operative, oltre ad un'analisi di sensibilità del modello stesso in funzione dei principali parametri che possono influenzare il processo termico. I risultati sperimentali raccolti sono confrontati con i risultati ottenuti dal modello esistente al fine di evidenziare i punti di forza e di debolezza del modello, confrontando sia le curve termogravimetriche che la distribuzione dei prodotti.

I risultati hanno mostrato l'affidabilità del modello nelle condizioni operative indagate, anche se ulteriori studi sono necessari al fine di sviluppare un modello con migliori capacità predittive, soprattutto per quanto riguarda la distribuzione dei prodotti. Il lavoro svolto rappresenta un punto di partenza per una futura attività finalizzata ad ottenere uno schema cinetico più chiaro e affidabile dell'attuale modello per il PVC, PET e della loro miscela. Questo modello, unito agli schemi cinetici precedentemente sviluppati di altri polimeri plastici, potrà essere utilizzato per la simulazione di vere e proprie miscele plastiche raccolte nei rifiuti solidi urbani, ovvero *plasmix*, e per il design di impianti di pirolisi.

Chapter 1

1. Introduction

Plastic has rapidly become part of human life since its massive production in the early 50s. Indeed, in the past years, plastic polymers have become increasingly important and widely used in our life due to their versatility, durability, low weight, and cost. Plastic materials entirely make objects from packaging, covers, films, and bags to construction and electronic applications. Moreover, nowadays, plastic materials have substituted classic materials like wood, glass, and metals in many different applications.

Although their usefulness is well recognized worldwide, plastics became one of the main contributors to the waste management problem as a direct consequence of the enormous amounts produced every year.

1.1. Worldwide Plastic Production and Consumption

The worldwide massive production of plastic is explained by the fact that the family of plastics is composed of a wide variety of materials designed to meet the very different performance requirements of thousands of end products [1].

The chart in Fig. 1.1 shows a large increase in global plastics production from 1950 to 2018. In 2018, global plastics production reached 359 million metric tons, with 62 million metric tons produced in Europe alone.

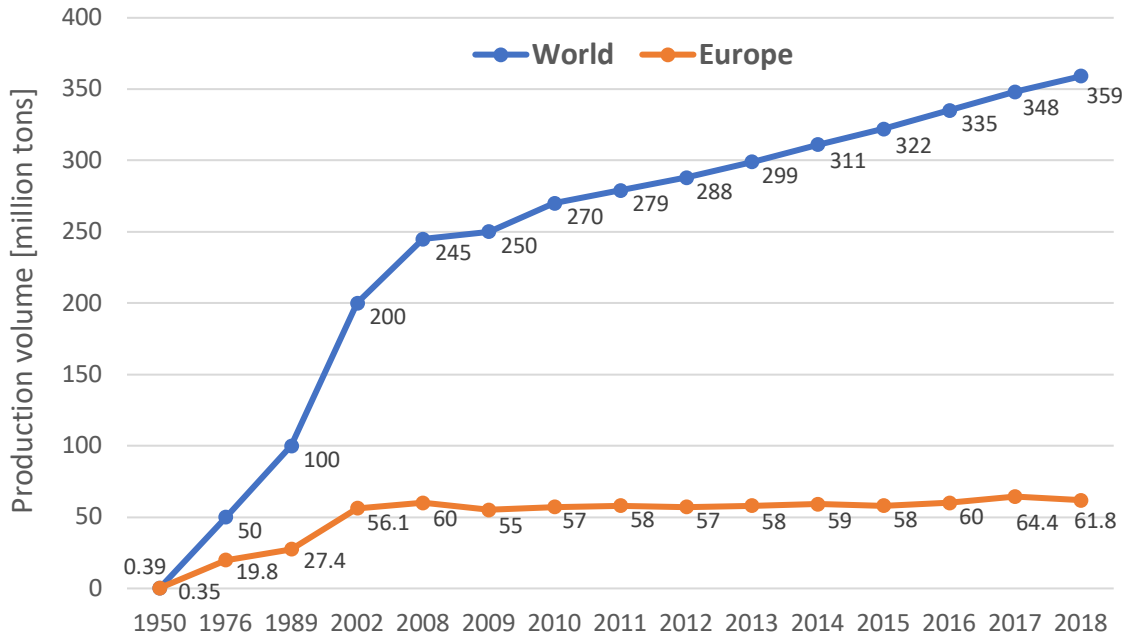

Fig. 1.1 Global plastic production from 1950 to 2018 in million tons [1].

As can be seen, the demand and consumption of plastic materials have grown further in recent years, exceeding 350 million metric tons per year.

The chart in Fig. 1.2 shows the cumulative production of plastic. By 2015, the world production of plastic materials was 7.8 billion tons, i.e. more than one ton of plastic for every person alive today.

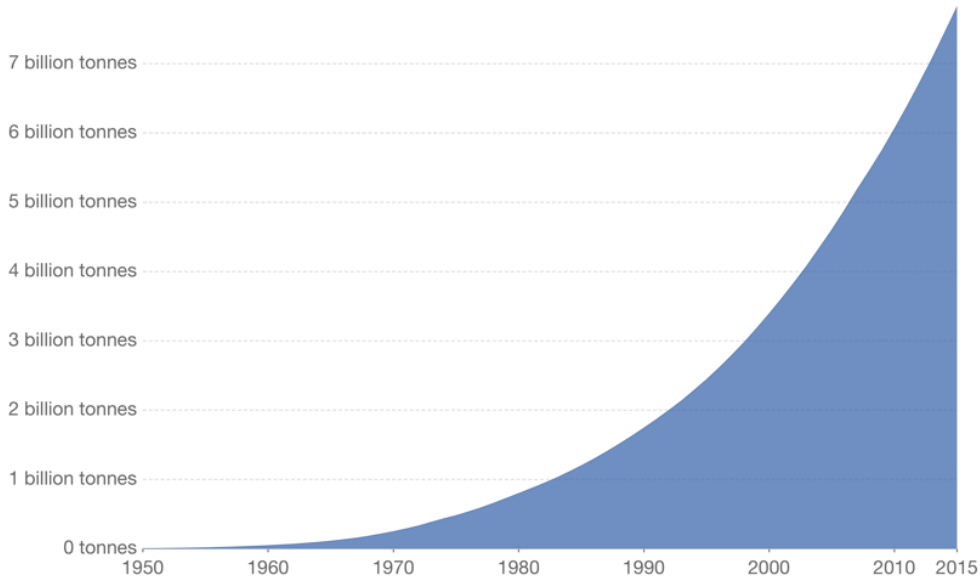

Fig. 1.2 Cumulative global production from 1950 to 2015 [2].

The distribution of global plastic production is shown in Fig. 1.3. The majority portion is covered by Asia, where China is the leader. Indeed, China is the largest producer of plastics globally, accounting for more than one-quarter of the global production (30% in 2018). It is evident how the role of China in this sector is becoming increasingly important. For example, plastic imports from China into the United States are steadily increasing as China's plastic industry grows. Moreover, plastic production in China is expected to grow further in the following years [1].

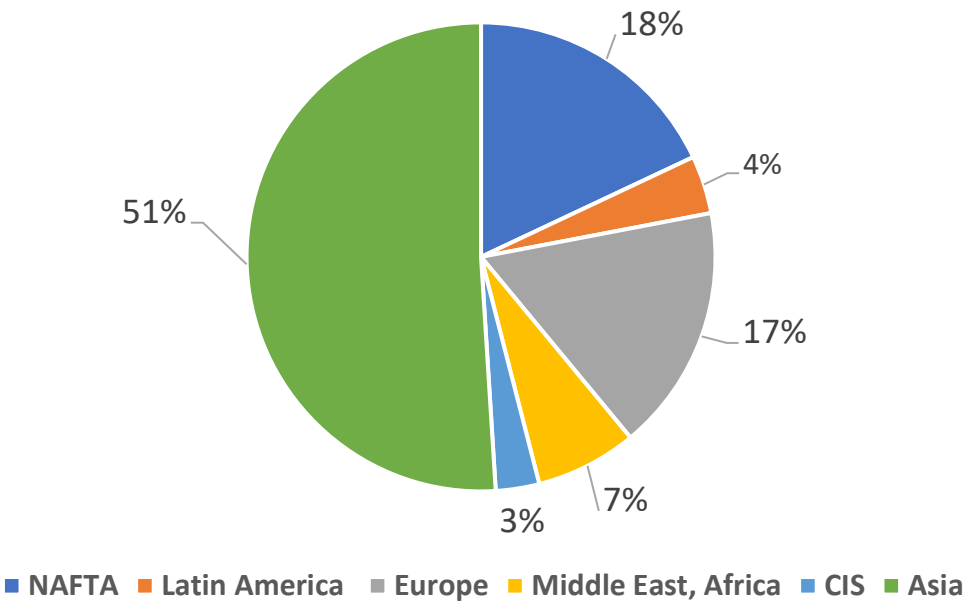

Fig. 1.3 Distribution of global plastic production in 2018 [1].

The chart in Fig. 1.4 shows the plastic production divided by the industrial sector for 2015. The packaging is the main use of primary plastics accounting for 42% of the total plastics production, followed by building and construction, which was the second largest sector utilizing 19% of the total plastic production. Primary plastic production does not directly reflect plastic waste generation since this is also influenced by the polymer type and lifetime of the end product.

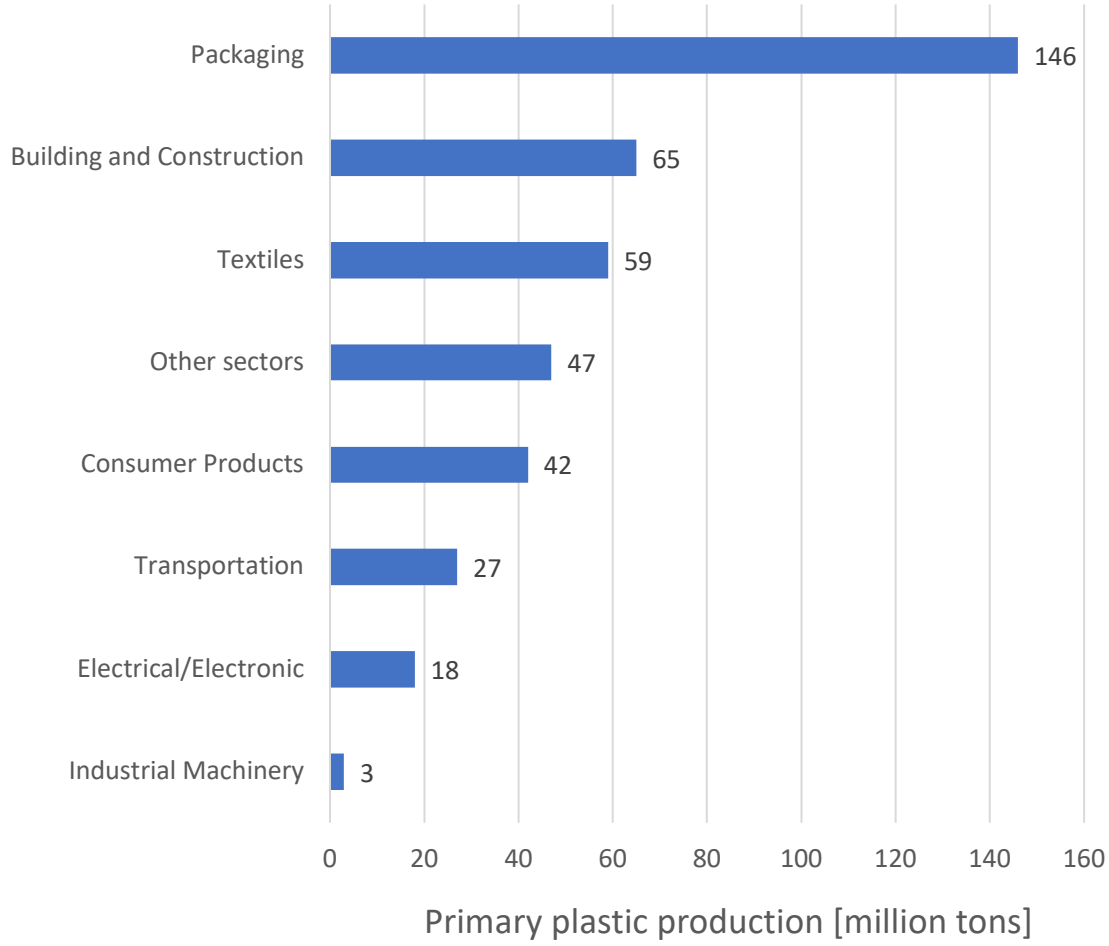

Fig. 1.4 Total plastic use by sector in 2015 [2].

It is important to notice that plastic waste generation is strongly influenced by primary plastic use and product lifetime. For example, packaging has a very short 'in-use' lifetime (typically around 6 months or less) [2]. This is in contrast to building and construction, where plastic use has a mean lifetime of 35 years [3]. Therefore, the packaging is the main generator of plastic waste, responsible for almost half of the total waste produced globally, as shown in Fig. 1.5, showing the plastic waste generation by each sector.

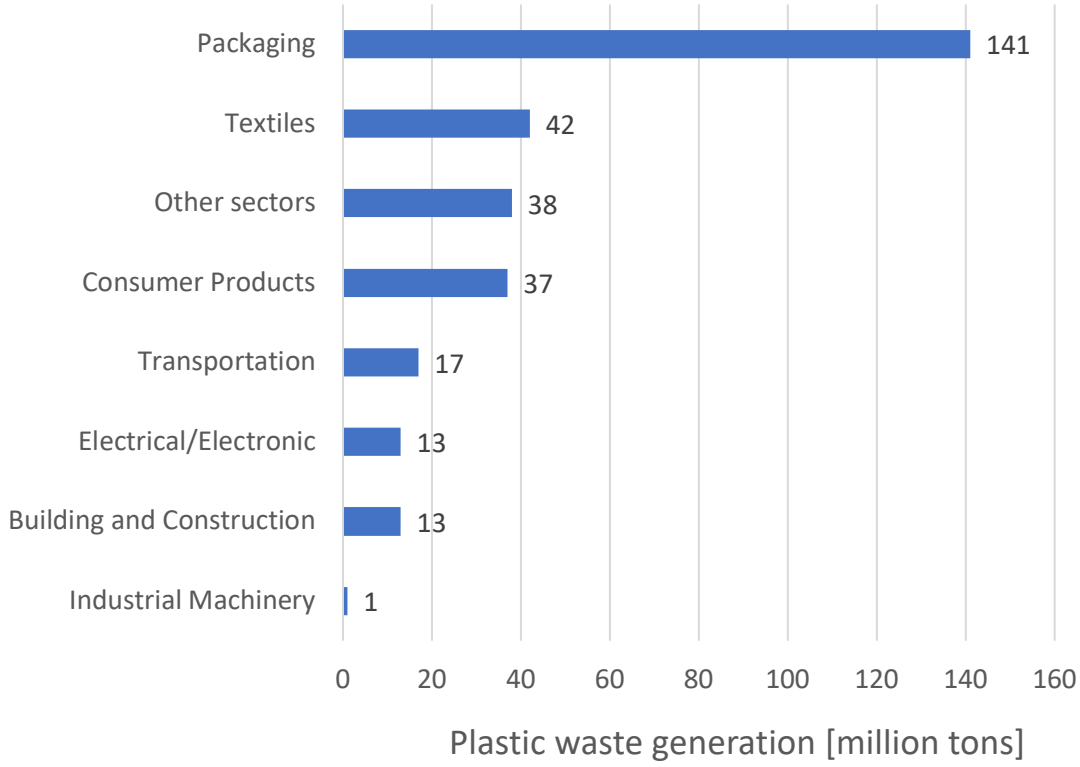

Fig. 1.5 Total plastic waste by sector in 2015 [2].

1.2. Plastic in MSW

Due to their properties and low price, the demand and consumption of plastic materials keep increasing over the years. Consequently, there was also an increasing waste generation, and plastic became one of the main contributors to the waste management problem.

Comparing Fig. 1.4 and Fig. 1.5, it is possible to see that in 2015 primary plastics production was 407 million tons, while total plastic waste generation was 302 million tons. So, around three-quarters of the plastic produced ended up as waste.

Fig. 1.6 shows the daily waste generation of plastic per person in different countries. This figure represents the total plastic waste generation and does not account for differences in waste management, recycling, or incineration among these countries.

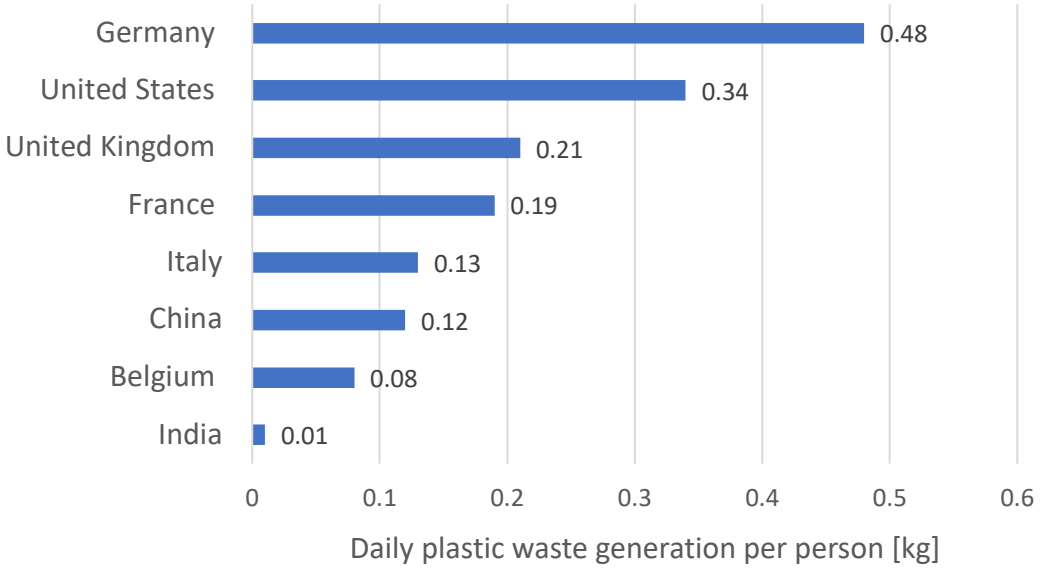

Fig. 1.6 Daily plastic waste generation per person in 2010 [2].

Also, the chart in Fig. 1.7 shows the total plastic waste generation by country, measured in tons per year. Although the following estimate is available only for 2010, the relative global picture is similar in projections to 2025 [2].

Due to the largest population, China produced the largest quantity of wasted plastic, nearly 60 million tons in 2010, followed by the United States (38 million tons) and Germany (14.5 million tons).

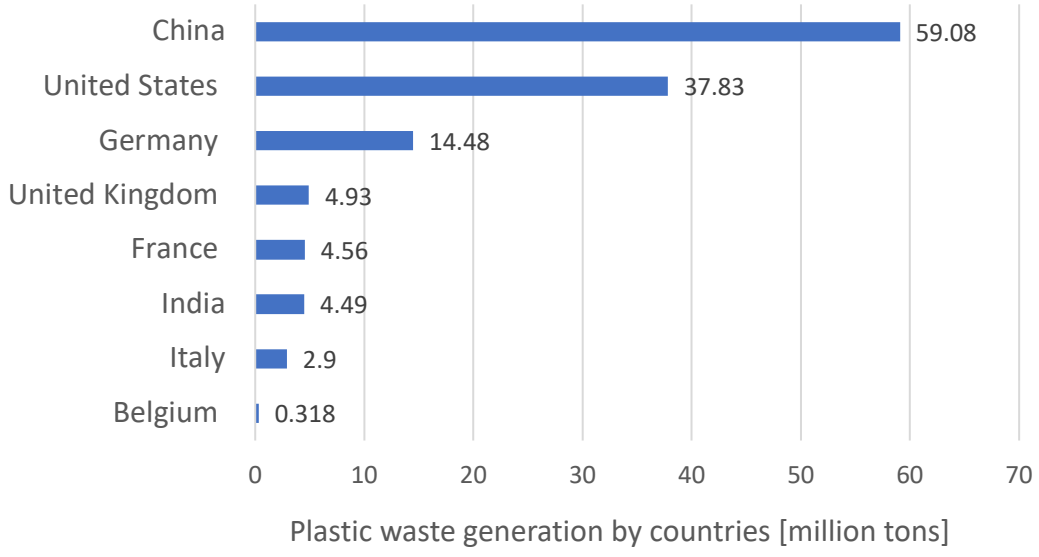

Fig. 1.7 Total plastic waste generation by countries in 2010 [2].

Consequently, the amount of waste plastics has risen widely in Municipal Solid Wastes (MSW), and plastics became one of the main contributors to the waste management problem on land, seas, and rivers [4,5]. MSW consists of different waste items of various human activities. Its composition varies greatly geographically, and it changes significantly with time. Fig. 1.8 shows the typical composition of MSW in the U.S.A, China, and Europe.

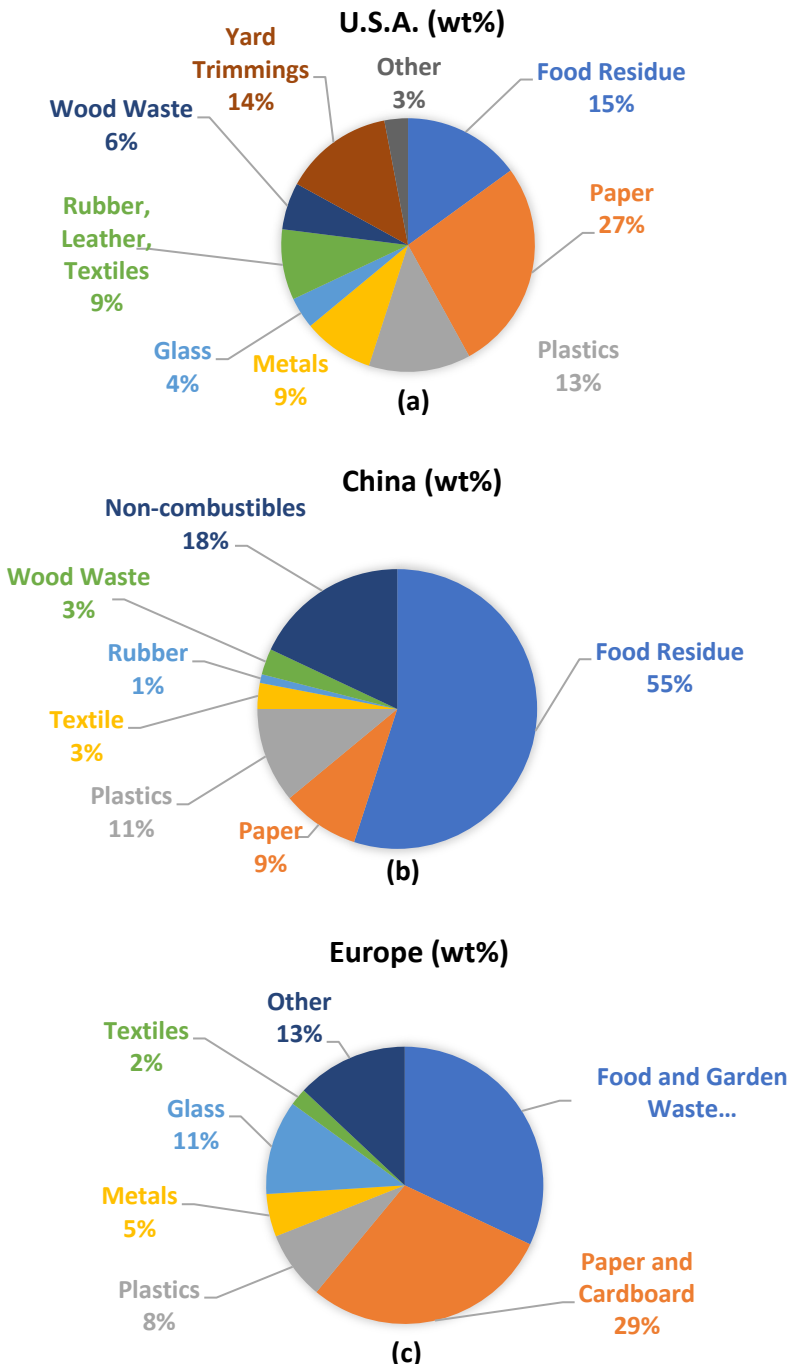

Fig. 1.8 Composition of MSW in the (a) U.S.A. [6]; (b) China [7]; and (c) Europe [8] in wt%.

Fig. 1.8 shows the weight of Solid Plastic Waste (SPW) in the MSW. Indeed, the values of SPW are in a range of 8-13% of the total MSW [6-8]. Therefore, it becomes essential to carefully separate the plastic waste from the rest of the waste, taking into account the potential contaminants after the separation.

Among plastics, low-density polyethylene (LDPE), high-density polyethylene (HDPE), polypropylene (PP), polyvinyl chloride (PVC), polystyrene (PS), polyethylene terephthalate (PET), and polyurethane (PU) account for 81% of the European plastic demand distribution in 2018 (Fig. 1.9).

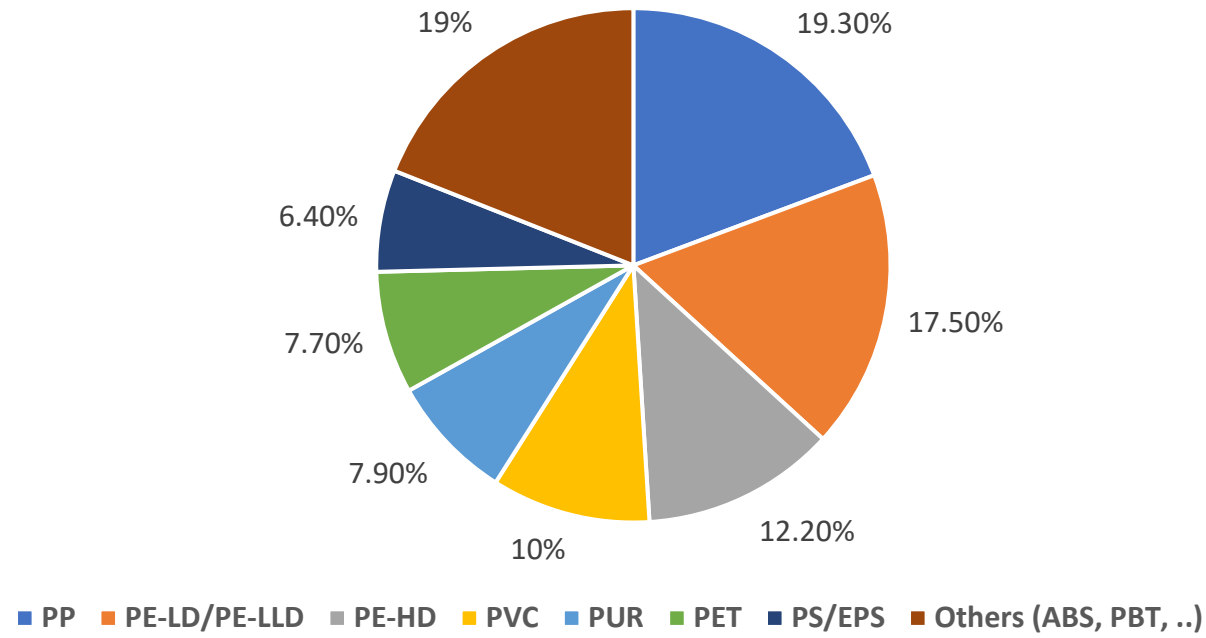

Fig. 1.9 European plastic demand distribution by resin types in 2018; PP (polypropylene), PE-LD (polyethylene low density), PE-LLD (polyethylene linear low density), PE-HD (polyethylene high density), PVC (polyvinyl chloride), PUR (polyurethane), PET (polyethylene terephthalate), PS (polystyrene), EPS (expanded polystyrene), ABS (acrylonitrile butadiene styrene), PBT (polybutylene terephthalate) [1].

1.3. PVC and PET among plastics

Among all the different kinds of plastics, both PVC and PET play a significant role in the disposal management of plastic mixtures due to their great demand worldwide. Indeed, as shown in Fig. 1.9, these two polymers account for 17.7% of the global total demand.

1.3.1. PVC

For years, PVC has been used in various applications, and it is a product in continuous development. Indeed, PVC is the third most widely produced plastic material after polyethylene (PE) and polypropylene (PP), and it made up ~10% of European polymer production in 2018. The wide use of this polymer is mainly due to its properties, such as resistance and versatility. Indeed, PVC can be produced both in rigid and flexible forms thanks to the addition of plasticizers.

The biggest PVC markets are pipes and window profiles, followed by rigid films and cables, as shown in Fig. 1.10 [9]. A wide range of additives is incorporated during PVC production, improving the mechanical properties of PVC products, and making PVC applications extensive. Even though the durable PVC products can sustain long service life compared with other plastics, they will eventually become solid waste [10].

Due to its importance and utility, the global plastics production capacity of PVC was about 61 million tons in 2013. Fig. 1.11 shows that China accounted for half of the total PVC produced in the world [9]. The consumption of PVC in 2013 reached 38.5 million tons, and it was estimated that global demand would rise by ~3.2% per year to 2021 [11].

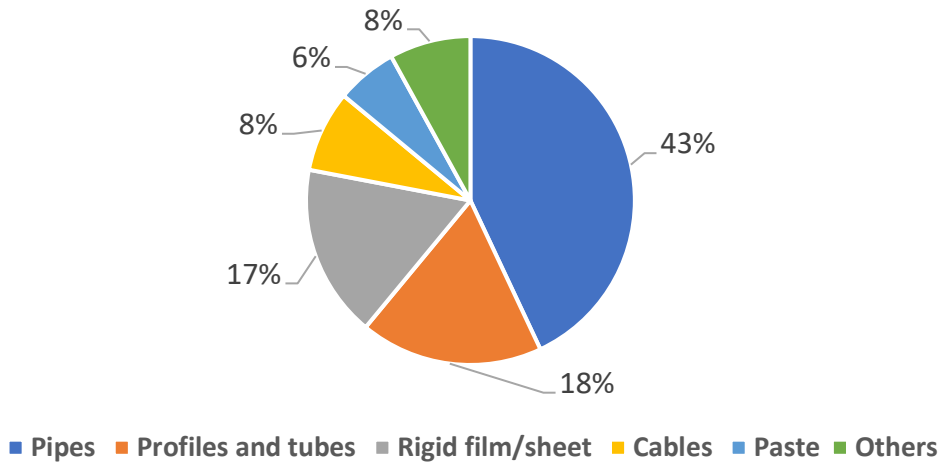

Fig. 1.10 PVC application worldwide in 2013 [9].

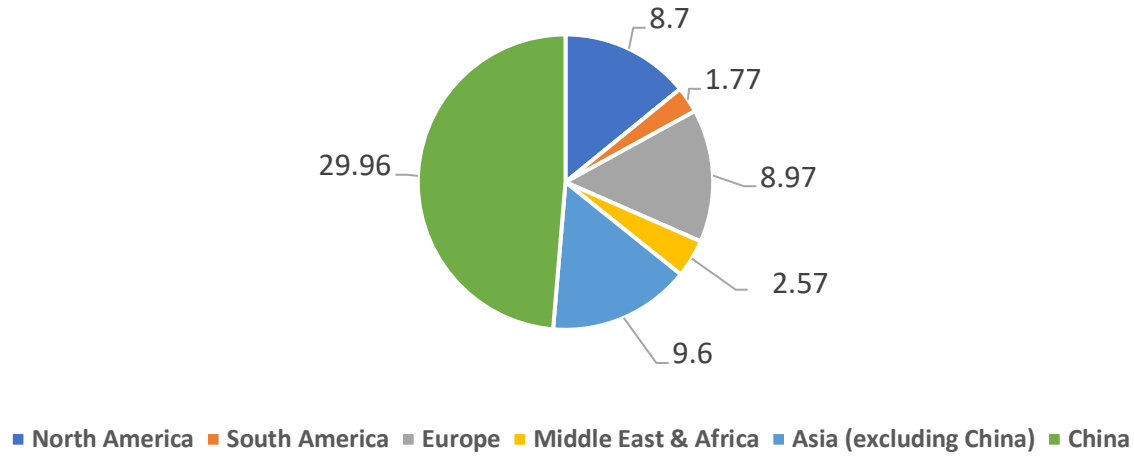

Fig. 1.11 Distribution of global PVC production by region in 2013 (million tons) [9].

1.3.2. PET

Just like PVC, PET is another of the most widely used polymer material across the world, and it is used in many different applications. It is the most common thermoplastic polymer belonging to the polyester family, a category of polymers containing the ester functional group in their main chain. It is often combined with additives and metals to modify its properties that make its recycling a tough task.

PET made up ~7.7% of European polymer production in 2018, and it is the fifth-most-produced polymer after polyethylene (PE), polypropylene (PP), polyvinyl chloride (PVC), and polyurethane (PU) (Fig. 1.9). It is widely used in the production of fibers for clothing (textile industry). Still, it is also employed for other sectors, such as in the packaging industry as containers for liquids (plastic bottles) and food, thermoforming for manufacturing, and in combination with glass fibers for engineering resins. Indeed, more than 60% of the global PET production is used for synthetic fibers, followed by bottle production (30%) [12].

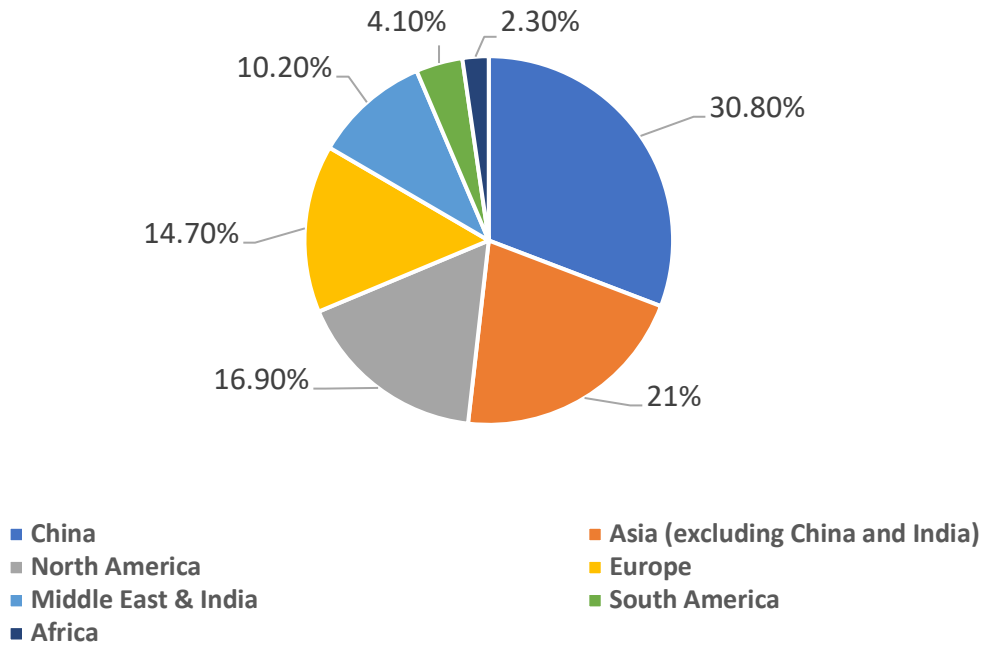

Fig. 1.12 PET production capacity distribution worldwide in 2017, by region [13].

Fig. 1.12 shows the distribution of the production capacity of PET resin worldwide in 2017 by region. The global PET production reached 30.3 million tons in 2017, with China accounting for 30.8%. China is both the largest producer of PET resin and the largest consumer of PET bottles. The European region accounted for 14.7% of the total PET

production capacity, while the global PET production capacity increased from 27.8 million tons in 2015 to 30.3 million tons in 2017 [13].

While in Europe and America the rise of PET consumption is mainly maintained by PET bottle production, in Asia the expansion of PET use is correlated to a higher production of fibers, due to the shift of fiber production from the industrialized countries to low-wage ones [14].

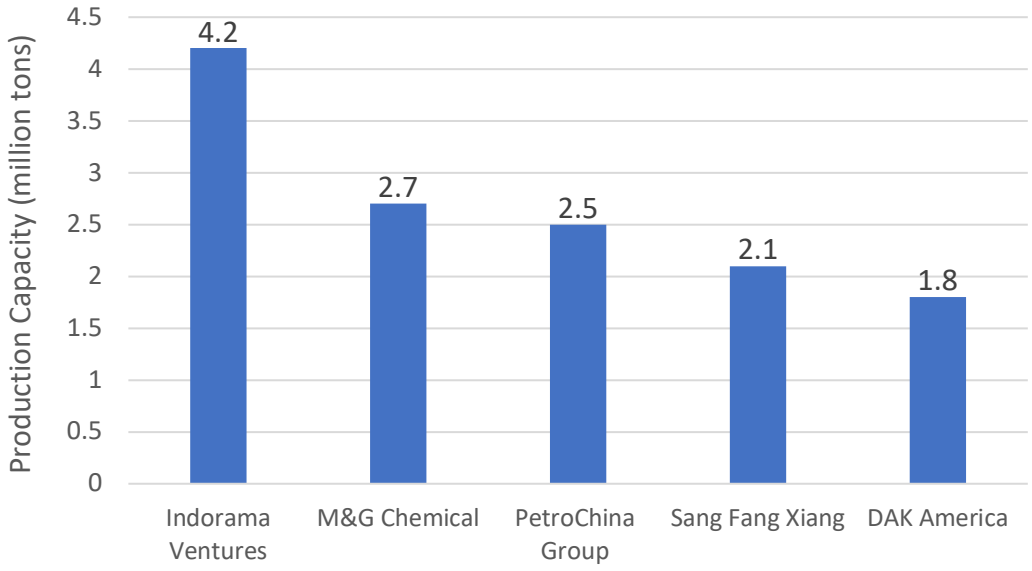

Fig. 1.13 Top 5 Companies PET resin production capacity in 2017 [13].

The production of PET polymer is mainly dominated by a few companies, as illustrated in Fig. 1.13. Indorama Ventures (Thailand) was the largest producer of PET in the world in 2017, with an installed production capacity of 4.2 million tons. The other leading companies are M&G Chemical (Luxembourg), Zhejiang Yisheng Petrochemical Co., Sang Fang Xiang, and DAK America [13].

Future growth in PET polymer consumption will continue to be driven by the two largest end-use segments, textile filament and solid-state resin, driven by further investments into new polyester fiber capacity in Asia and growing beverage markets in the emerging world [15].

1.4. Plastic Waste Disposal

As highlighted in the previous paragraphs, plastic waste is one of the current global challenges due to its huge volumes, estimated at millions of tons annually. Therefore, there is a great need to dispose it. At the end of its life cycle, the product is disposed and becomes a waste, and it could be:

- deposited in the landfill;
- valued by extrusion (mechanical recovery);
- valued by pyrolysis and gasification (chemical recovery);
- valued by incineration (energy recovery).

Typically, municipal plastic waste consists of a mixture of different types of plastics of unknown composition. Additionally, it may be contaminated by organic fractions (such as food) or non-polymer inorganic fractions (such as paper), which makes it a very complex stream to recycle [16].

From an environmental point of view, it would be better to avoid the accumulation of Solid Plastic Waste (SPW) by reducing plastic production in the first place (using smarter packaging or alternative materials, for example) or pushing towards the reuse of plastics products. Since it is impossible to avoid the production of SPW, the preferred option for the disposal of this type of waste is recycling. In this way, new raw materials are obtained via a mechanical or chemical pathway. If the polymer waste cannot be recycled, energy recovery is the preferred option, while landfill should be avoided and no longer considered [16]. Indeed, the main risks of landfilling plastic waste lie in environmental concerns, such as contamination of soil and groundwater. In contrast, plastic incineration introduces costly pollution control treatments due to the emission of toxic volatile organic compounds (VOCs).

Fig. 1.14 shows that, during the past years, recycling and energy recovery rates have steadily increased, contributing to a significant reduction of landfilling.

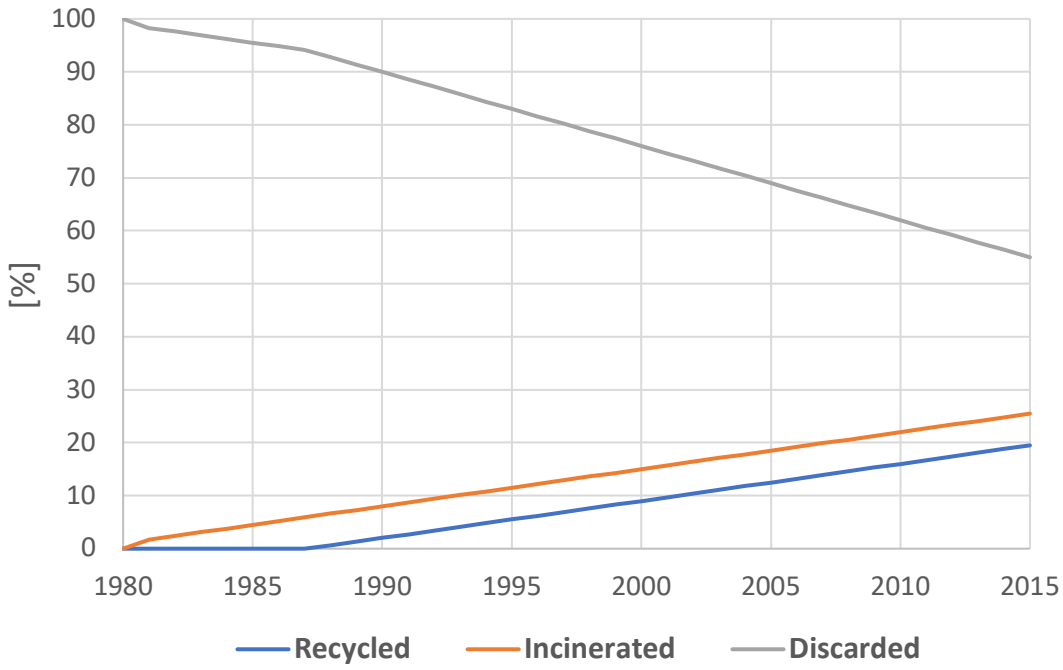

Fig. 1.14 Evolution of landfilling, recovery and recycling of SPW in EU, 1980 to 2015 [2].

Before 1980, plastic recycling and incineration were negligible, and 100% of plastic waste was landfilled. Starting from 1980, incineration and recycling rates steadily increased up to the actual values. In 2015, ~55% of global plastic waste was landfilled, 25% was incinerated, and 20% was recycled. Extrapolating the historical trends, by 2050, incineration rates would increase to 50%, recycling to 44%, and landfilled waste would fall to 6% [2].

Waste disposal policies are very different across Europe: in countries with landfill restriction implemented (Belgium, Luxembourg, Netherlands, Germany, Denmark, Switzerland, Austria, Norway, Finland, and Sweden), much less than 10% of plastic waste is landfilled, while in countries such as Hungary, Croatia, and Greece, a huge amount of over 50% of all plastic waste is still landfilled [1].

Fig. 1.15 shows the main polymers listed with their respective shares in those sectors that use the most plastics in their final products. Many industrial sectors such as packaging, building, construction, electrical and electronic, and automotive use a large number of plastics. Therefore, it is clear that a huge amount of plastic waste is unavoidably produced every year. As can be seen from the figure, the largest share of all plastic waste is from packaging [1]. Packaging products have a very short lifetime, especially compared to other sectors such as building and construction, automotive which typically have a longer lifetime. Except for PVC, all of the other more produced polymers (HDPE, LDPE, PP, and PET) have their prevalent application shares within the packaging, so it is expected that these will also dominate the composition of SPW [16].

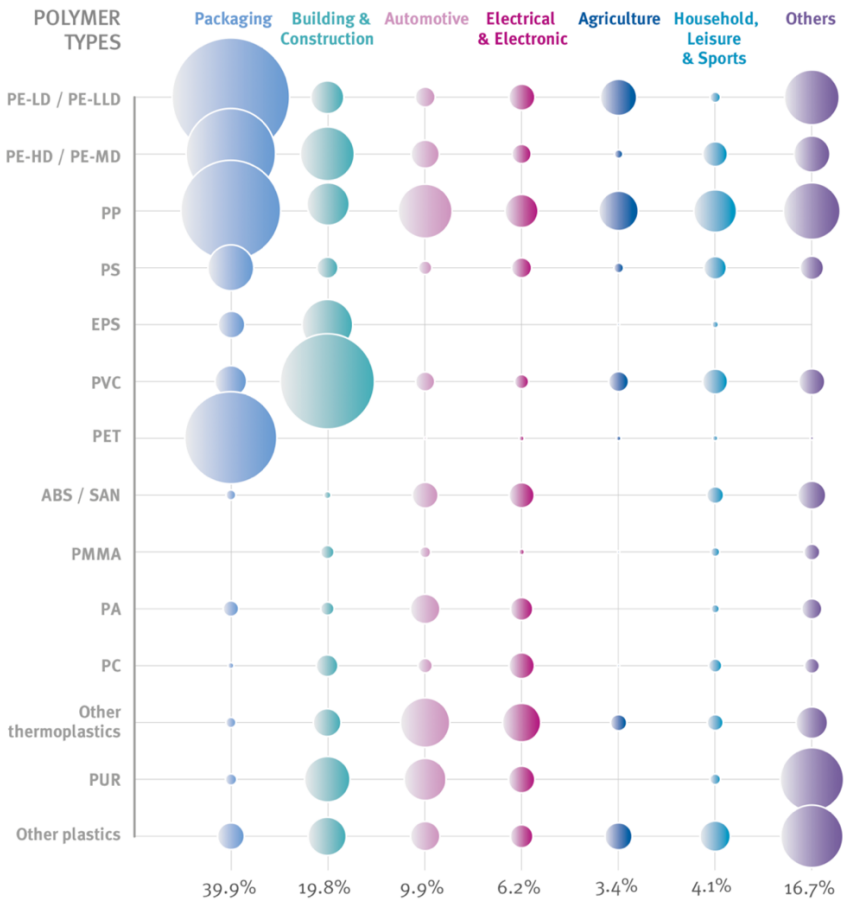

Fig. 1.15 Plastics demand by sectors and polymer types in 2018 [1].

1.5. Recycling

Circular economy and plastic waste reduction are the priorities for the European Union, resulting in stricter legislation such as landfill bans, extended producer responsibility, and specific recycling targets [17]. For example, only in 2018, the global plastics production capacity of PET and PVC reached about 28 and 36 million tons respectively [1], and the plastics used in packaging, which represent 40% of all plastic produced in the world, are the most important and continuous source of waste.

Due to its low degradability in nature, plastic waste accumulation causes environmental pollution, and the waste must be removed from the environment. Although landfill is the simplest method to dispose of plastic wastes, there are many disadvantages in following this route. For example, it occupies land, causes soil and groundwater pollution, and emits harmful materials. Also, potential resources of value-added materials may be wasted by landfill [18]. So, recycling plastic waste such as PVC and PET may be cleaner and more effective than landfills.

However, when it comes to recycling, some important properties should be taken into account, and these properties will strongly affect the degree to which this waste can be effectively recycled. First of all, it is necessary to consider if the waste is a mono-plastic (i.e. one single component) or a mixed plastic. Indeed, processing mixed polymer waste involves different challenges and, therefore, mono-plastic wastes are always preferred. Secondly, it is important to know if the plastic is clean or contaminated with inorganic or organic components or with a small fraction of other polymers. Indeed, if it is, washing and purifying steps are required before. Finally, it is necessary to consider if the composing polymers and their respective mix ratios are well known [16]. Indeed, SPW composition varies greatly geographically, and it is necessary to characterize any waste stream precisely before trying to design a process for its treatment.

1.5.1. Mechanical Recycling

The most common and widely used method for the recycling of plastic waste so far is mechanical recycling. This method aims to recover material that will be used for the production of plastic objects different from the original ones, using physical processes similar to those used for the treatment of virgin plastics.

This technique requires relatively simple technologies, but it also typically includes different pre-treatment and preparation steps: the collection, sorting, washing, and grinding of the material to guarantee a high purity. Therefore, the process is often not economically feasible. In some sectors, plastic waste is homogeneous, clean, and dry enough to allow for a good recovery and mechanical recycling of the product, but in other sectors, such as household plastics, technical difficulties, and processing costs due to the complex and contaminated waste make this route not convenient. Moreover, products coming from mechanical recycling often have lower mechanical properties, limiting their applicability and market demand.

1.5.2. Chemical Recycling: pyrolysis and gasification

Chemical recycling is a promising alternative for plastic waste recycling. This technique can treat heterogeneous and contaminated plastic waste material coming from those sectors where mechanical recycling cannot be used. It is a process that converts end-of-life plastic materials into molecules with a lower molecular weight altering the chemical structure of the polymer. It consists of a degradation process that breaks the polymer chains while the impurities are eliminated. In this way, it is possible to obtain products that, after

purification, are identical to the feedstock normally used to produce new petrochemicals and plastics or can be used as a new source of fuels [19].

From an environmental point of view, pyrolysis and gasification are considered possible techniques to thermally convert waste plastics into chemicals, reducing at the same time greenhouse gases (GHGs) and CO_2 emissions.

Gasification consists of partial and controlled oxidation, with a quantity of oxidizing agent lower than the stoichiometric one, of a liquid or solid material at temperatures above 700-800 °C in order to obtain a mixture of carbon monoxide, hydrogen, and other gaseous substances.

On the contrary, pyrolysis is a thermal decomposition process obtained by applying heat to the feedstock at temperatures between 400-800 °C in the complete absence of oxidizing elements. Pyrolysis of plastics produces three different fractions of product: an oily liquid fraction (tar) containing water and low molecular weight organic compounds, a solid product (residue, or char) consisting of residues with a higher molecular weight such as ashes and metal species, and a non-condensable gaseous fraction containing CO, CO_2, H_2O, H_2, hydrocarbons (such as CH_4, C_2H_4, C_3H_6) and other volatile compounds. The relative yields of these fractions and the degree of decomposition reached during the process depend on some important parameters:

- pyrolysis temperature;
- heating rate;
- residence time inside the reactor;
- reactor type;
- size, shape, and composition of the material to be treated;
- presence of catalysts (catalytic pyrolysis).

These parameters strongly affect the yield of the pyrolysis products, and usually pyrolysis is optimized to produce a high oil yield, which is the most relevant energetic fraction. Indeed, the product distribution shows similar trends when different operating conditions are used: increasing the operating temperature results in an increase in the gas fraction and a decrease in the wax fraction amount due to the effect of the devolatilization reaction, while an increase in residence times will result in a slight decrease in the wax fraction and an increase of gaseous species. The wax fraction decrease is explained by the wax cracking reactions, leading to an aromatic fraction [19].

The pyrolysis process is preferably carried out inside fluidized bed reactors, allowing higher conversions and a more uniform product as it is easier to obtain uniform conditions inside the reactor. Indeed, the best ideal reactor to be used should have excellent mass and heat transfer coefficients.

1.6. Presentation of the work

Plastics are usually collected and separated by employing optical detectors or gravimetric separators to be sent individually for mechanical recovery. However, the so-called *plasmix*, i.e. the set of all those plastics that are not separated from each other, should be destined for chemical recovery, even if today it is still mainly sent to waste-to-energy processes. So, in order to minimize the plastic waste and the fraction of waste going to incineration, nowadays, there is a greater interest in better assessing the chemical phenomena governing the thermal degradation process of plastic mixtures to produce fuel or raw materials for the petrochemical industry.

The present work fits exactly in this context, aiming at studying the thermal degradation of plastic mixtures on both a numerical and experimental basis. In particular, the work will be focused on the refinement and improvement of an existing detailed kinetic scheme

describing the plastics thermal degradation, with special emphasis on the possible chemical interactions occurring between PVC and PET. These polymers play a significant role during the pyrolysis of mixed plastic waste since they are found in significant quantities. Moreover, it is proved that different polymers have very low compatibility between them and, consequently, they have a very low interaction between their degradation process. In other words, their degradation can be considered independent from the presence of other polymers [20]. This is not true in PET and PVC mixtures, where chemical interaction between them exists.

The planned work will combine experimental and modeling activities. At first, the focus will be on collecting experimental data obtained from the literature about thermal degradation of PVC and PET neat polymers at different operating conditions (i.e. pyrolysis temperature and heating rate). The collected experimental data will be compared with the results obtained based on existing kinetic models developed in previous years by the CRECK Modeling Lab of the Politecnico di Milano and recently improved [20-23]. The work carried out made it possible to verify the reliability of the model itself and any existing limitations. All this information could hand towards the improvement and extension of the existing scheme, which, coupled with previously developed models for PE, PP, and PS, will make it possible to simulate real mixtures of plastic materials collected in municipal solid wastes and can be used for the design of a pyrolysis reactor for the *plasmix* treatment. Finally, a sensitivity analysis of the model for PVC-PET mixtures will be carried out in order to analyze the influence of different operating conditions on the chemical interactions between these two polymers and the product distribution.

Chapter 2

2. PVC: model description and validation

PVC is one of the most abundant plastics, and it is a special material compared to other polymers. The chlorine contained in its structure is released during the degradation in the form of chlorinated compounds, i.e. HCl and chlorinated hydrocarbons, which are very corrosive and difficult to handle. The modeling of PVC degradation is, for this reason, of great importance in view of a future chemical recovery of *plasmix*.

In this chapter it will be presented first the kinetic model of PVC thermal degradation that is developed by the CRECK Modeling Lab of the Politecnico di Milano and, then, it will follow the model validation based on the comparison between the experimental data obtained in literature and the output data coming from the simulation.

Several thermogravimetric and isothermal analyses are considered and, then, it will be investigated in deep the influence of process conditions (i.e. operating temperature and heating rate) on the product distribution, i.e. the yield of the different pyrolysis fractions, the dehydrochlorination efficiency and the formation of 2-4 rings polycyclic aromatic hydrocarbons (PAHs).

2.1. Kinetic model of PVC thermal degradation

PVC pyrolysis is a radical process that takes place in the liquid phase at temperatures above 200 °C. In this process, two successive steps occur: the dehydrochlorination step, in which chlorine is released in the form of hydrochloric acid (HCl) and where the liquid phase is

enriched in unsaturated structures (polyene chains), followed by a second step during which the polyene chains condense forming aromatic species that partly leave the liquid phase and partly reticulate through cross-linking reactions forming a fixed carbon residue. In fact, there are numerous polyaromatic hydrocarbons (PAHs), gases, and carbon residues among the species produced, where the residue represents up to ~15% of the initial sample mass. Several mechanisms have been proposed in the literature, and a semi-detailed kinetic model has been implemented by the CRECK Modeling Lab of the Politecnico di Milano.

Since the reactions that lead to the formation of degradation products are numerous and involve a large number of reaction intermediates, the approach adopted for the description of the kinetic model of PVC degradation requires the definition of *pseudo-species* that are representative of the structures present in the initial polymer and those that are formed during the degradation. Such species can be real compounds or not, representing both molecules and radicals.

According to the model, the initial PVC polymer is represented by the chlorinated reference species P-(CH_2CHCl)-P, where P represents the adjacent polymer chain. Long unsaturated chains are formed during the subsequent degradation steps, represented by the reference species P-(CH = CH)-P. Other reference species are also added in the model, with different chlorination levels. The abstraction reactions of H or Cl from these *pseudo-species* lead to the formation of the corresponding radicals. In contrast, the cross-linking reactions between the polyene molecules lead to alkyl-aromatic intermediates, which can further condense in more complex structures to form a carbonaceous residue called char. The reference *pseudo-species* of these reaction products are then introduced according to the different number of aromatic rings and the possible presence of chlorine in their structure. Therefore, the chemical processes that lead to the formation of compounds in the gas and liquid phase can be written in terms of chemical reactions between these *pseudo-species*.

The complete kinetic scheme includes ~250 reactions and 40 species. The kinetic parameters of the liquid phase reactions are directly derived from the analogous reaction parameters in the gas phase, properly corrected to take into account the switch in the liquid phase. Corrections are also applied to termination reactions to account for diffusive limitations to collisions and effective radical recombination. This means that the thermal degradation of PVC is described in terms of its intrinsic kinetics, where heat and mass transfer limitations are not included. Fig. 2.1 shows the evolution of the mass profiles with the temperature at a heating rate of 10 °C/min for the condensed phase and the main products in the vapor phase. It is also possible to note the two main degradation phases previously described. These are numerical results presented as an example to show the main characteristic of the process.

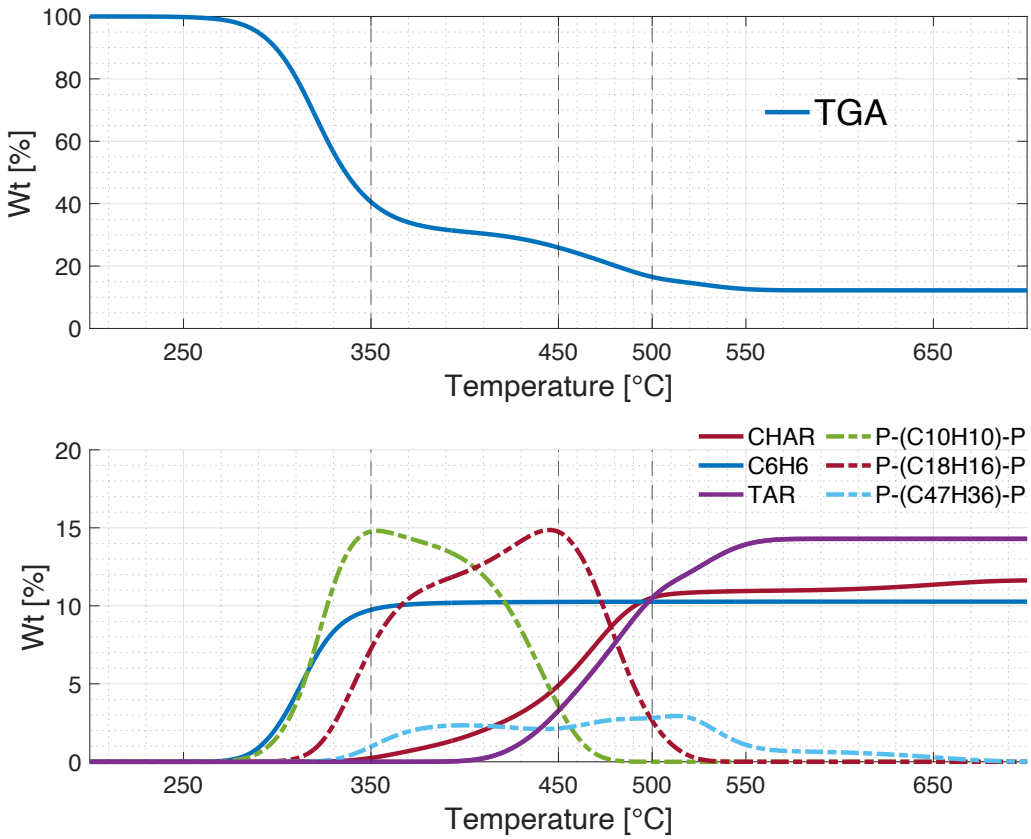

Fig. 2.1 Thermogravimetric simulation at 10 °C/min. The figure above shows the mass loss profile, while the figure below shows the profiles of the main gaseous, condensable and liquid structures formed during the degradation phases.

An analysis of the kinetic scheme allows us to better characterize the main mechanisms that determine the final mixture composition that occur during the PVC thermal treatment. First, the competition between radical initiations and terminations determines the availability of radicals in the system and, therefore, the reactivity of the system itself. The main PVC degradation initiation reaction is the homolytic breaking of the C-Cl bond. In fact, the main radical present in the system is $Cl^{\bullet}$, and it can be produced by four different initiation reactions involving as many representative species. For example, from the base polymer, the chlorine radical is obtained according to the following reaction:

$$P\text{-}(CH_2CHCl)\text{-}P \rightarrow P\text{-}(CH_2C^{\bullet}H)\text{-}P + Cl^{\bullet}$$

On the other hand, termination reactions can involve three different families of radicals present in the system: the chlorine radical (very reactive), the alkyl radicals, and the alkyl-aromatic radicals. The radical termination products can be numerous, starting with gaseous chlorine or hydrogen, the same polyvinyl chloride, polyene chains, aromatic, and polyaromatic compounds. Some of the simplest radical terminations of the system are summarized here below:

- termination to give gaseous chlorine: $Cl^{\bullet} + Cl^{\bullet} \rightarrow Cl_2$
- termination to return PVC: $Cl^{\bullet} + P\text{-}(CH_2C^{\bullet}H)\text{-}P \rightarrow P\text{-}(CH_2CHCl)\text{-}P$

2.1.1. Dehydrochlorination processes

After describing the radical initiation and termination reactions, it is now possible to analyze the steps of PVC degradation in more detail. The first phase starts from about 200 °C and corresponds to the dehydrochlorination process. The result of this phase is the formation of a polyene chain and the release of the corrosive HCl, and it explains the initial mass loss that can be observed in Fig. 2.1. In this phase, based on the temperature, both

molecular reactions and radical propagation reactions contribute to the release of HCl. In fact, at temperatures below 200 °C, molecular dehydrochlorination plays a fundamental role in the degradation of PVC. In contrast, at temperatures above 200 °C, the radical mechanism becomes dominant, including the initiation and termination reactions previously described and the propagation reactions.

Regarding the radical mechanism, which appears to be the most important one, the initiation reactions may involve the C-Cl, C-C, or the C-H bond. Since the C-Cl bond is the weakest one, it is the main reaction site, and the initiation reaction produces a very reactive chlorine radical and an alkyl radical. In turn, the Cl• radical easily extracts a hydrogen atom from the surrounding chains (abstraction reaction), generating the reference species P-(C•H-CHCl)-P, which, by decomposing, reforms chlorine radical and a double bond on the polymer chain. This process leads to the formation of the previously described polyene molecules P-(CH=CH)-P, which, through subsequent condensation and de-alkylation reactions, can explain the formation of benzene and aromatic compounds. The process just described is shown here below.

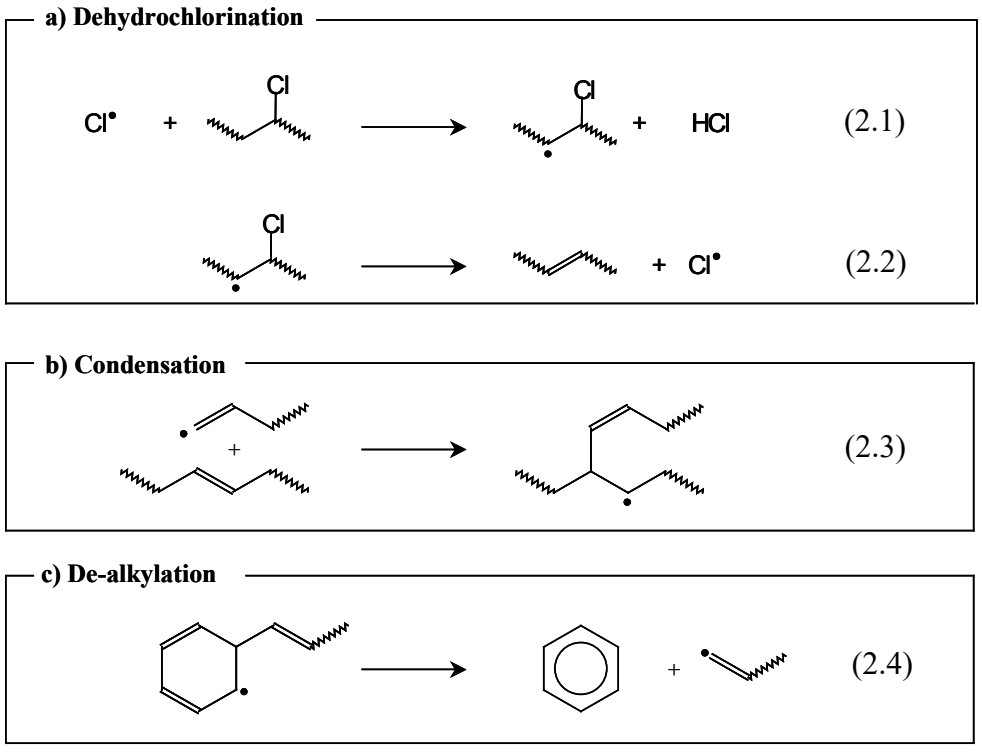

A key step in the radical process is the abstraction of H on the polymer chains by the chlorine radical. In fact, the selectivity of the hydrogen abstraction reaction in the gas phase (reaction 2.1) is much larger than the one of chlorine abstraction reaction by chlorine radical. This confirms that the gaseous chlorine is present in negligible quantities among the products, unlike HCl.

It should also be emphasized that, once the alkyl radical (P-C˙HCHCl-P) is formed, the most efficient propagation reaction is the β-cleavage of the C-Cl bond (reaction 2.2), which is much weaker than the C-C bond of the chain, thus leading to the progressive release of HCl rather than to a reduction in the average chain length.

Instead, the primary radicals formed from the cleavages of the C-C bond add to the double bonds of the already dehydrochlorinated chains, starting the cross-linking process that will become predominant in the subsequent stages of the degradation (reaction 2.3).

2.1.2. Formation of cross-linked structures and aromatic compounds

As already mentioned above, the polyene molecules formed during the dehydrochlorination process can undergo subsequent cyclization reactions, resulting in the formation of aromatic and alkyl-aromatic species and the simultaneous cross-linking of the polymeric structure. These reactions can be both intermolecular and intramolecular, and, here too, they can proceed through a molecular and radical mechanism. Some typical examples of these monomolecular and bimolecular cyclization reactions, with the subsequent dealkylation and benzene formation reactions, are reported below.

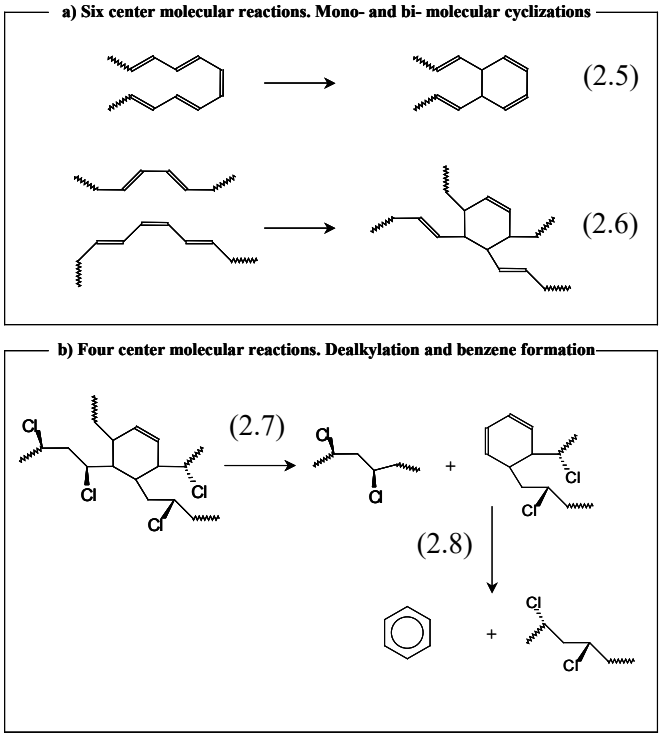

The main reaction of this category is the intermolecular cycloaddition in the liquid phase, in which, through a Diels-Alder type mechanism, two polyene chains form an alkyl-aromatic compound (reaction 2.6). This reaction can take place on portions of the chain in which the polymer has a lower degree of dehydrochlorination. In this case, the alkyl-aromatic species formed may incur in β-cleavage of the C-C bond favored by the electronegativity of the chlorine atoms still present in the chain. The consequence of this is benzene formation, which explains why benzene is formed mainly during the first stages of degradation when a reasonable amount of Cl is still present in the chain.

A further mechanism for the formation of aromatic compounds is intramolecular cycloaddition (reaction 2.5), in which the double bonds of the same molecule condense according to a Diels-Alder mechanism, forming cyclic rings. This reaction requires folding of the molecule on itself; therefore, it has higher activation energy than the intermolecular reaction. Consequently, at low temperatures, bimolecular condensation prevails, while the unimolecular reaction becomes significant only at temperatures above 500 °C. Here too, there are two possible paths:

- if the degree of dehydrochlorination of the chain is low, benzene is obtained from the starting polyene chain;
- on the contrary, if the chain's degree of dehydrochlorination is high, alkylated aromatic compounds are formed.

Therefore, when large quantities of Cl are still present in the chain, dealkylation reactions are favored, and gaseous species (e.g., partially chlorinated C_2-C_4 hydrocarbons) are released, as shown in reactions 2.7 and 2.8. However, with the progressive depletion of chlorine from the chain, molecular cyclization reactions produce alkyl-aromatic compounds, the subsequent fate of which is further condensation and growth.

2.1.3. Tar and char formation

Fig. 2.1 shows that the TGA curve undergoes a slowdown in the temperature range between 350-450 °C, where the formation of polycondensed aromatic intermediates occurs. In fact, the alkyl-aromatic species formed in the degradation step undergo a wide range of successive cycloadditions that lead to the chains rearrangement to form polyaromatic hydrocarbons (PAHs) and char (i.e. the *pseudo-species* representing the carbon residue). However, it should be considered that, if a cycloaddition of a further polyene chain occurs on an alkylated aromatic species, a Diels-Alder condensation will take place, forming a polyaromatic molecule. However, this reaction is penalized in terms of frequency factor due to the steric hindrance around the unsaturation of the aromatic species, which must be effectively impacted by the polyene chain. In particular, the *pseudo-species* representative of the primary radicals is very reactive towards double bonds. In contrast, the more complex aromatic radicals, such as those with 3 rings, are less aggressive due to the greater stabilization by resonance.

Fig. 2.1 also shows the evolution of aromatic *pseudo-species* and heavy compounds formation as a function of temperature. It can be observed how benzene is released mainly in the initial phase. At the same time, when most of the dehydrochlorination has occurred, alkyl-aromatic compounds are initially formed, which progressively condense to form polyaromatic compounds and a residue of char. The progressive growth of aromatic structures in the liquid phase is described using three different aromatic *pseudo-species* (P-(C10H10)-P, P-(C18H16)-P, and P-(C47H36)-P). These species are the representative structures of compounds with one, two, and ten unsaturated cycles.

As previously mentioned, above 350 °C, the second phase of PVC degradation begins, in which first the liquid mass reaches the *plateau* due to cyclizations (condensation phase). Subsequently, at temperatures higher than 450 °C, a new variation of the TGA slope is observed in Fig. 2.1 (fragmentation phase). This is explained by the formation of tar and volatile compounds released from the liquid phase due to the reactions of condensation, dehydrogenation, and dealkylation. Most of the resulting aromatic species are no longer bound to the polymer chains. Therefore, they can leave the liquid phase as secondary tar products, while the concentration of char increases in the liquid phase, where the hydrogen content is very low. In fact, the hydrogen-carbon ratio rapidly decreases as the degradation proceeds due to the cyclization reactions and aromatic condensation described.

Hydrogen abstraction reactions on alkyl-aromatic species are particularly selective towards benzyl sites, thus forming resonance stabilized radicals. This stability increases with the number of polycondensed rings due to the consequent delocalization of the electrons. The main pathway of these radicals is the dealkylation via β-cleavage and further condensations. Therefore, the PAHs formed have a low degree of alkylation, which is confirmed by the gas release during the formation of tar, such as ethylene, propylene, and methane, represented in the model by the *pseudo-species* C_2H_2.

2.1.4. Chlorinated systems

Finally, it remains to describe the reactions that lead to the formation of chlorinated systems, i.e. all those compounds that contain one or more chlorine atoms. As already mentioned, the Cl atoms of the polymeric chain are mainly released during the initial dehydrochlorination steps. However, the model includes the possibility that these atoms partially remain in the aromatic structures during the cyclization phase, and all the reactions previously described similarly take place also for halogenated compounds. Although they represent only ~1% of the total initial mass, it is useful to obtain information on their formation among volatile products due to their importance from an environmental perspective.

2.2. Model Validation

After the brief description of the kinetic model used for the simulations, the model accuracy and reliability can be verified by exploiting the experimental data available in the literature. The comparison between the simulated thermogravimetric curves and the experimental ones, the isothermal tests, and the product distribution is reported here below.

2.2.1. Comparison with thermogravimetric data

The model described in the previous paragraph is validated based on several dynamic experiments (TGA) found in literature carried out at different heating rates.

A first comparison was possible thanks to the experiments conducted by Yuan *et al.* [24], which carried out non-isothermal measurements, performing experiments at 10 °C/min of heating rate. In this study, chlorine (Cl) removal from polyvinyl chloride (PVC) is studied

under different operating conditions. To obtain the thermogravimetric and HCl emission curves versus temperature, PVC was put into a thermogravimetric analyzer. Then, the temperature was increased from room temperature to 500 °C at a heating rate of 10 °C/min under nitrogen (N_2) atmosphere. The results obtained are shown in the figures below.

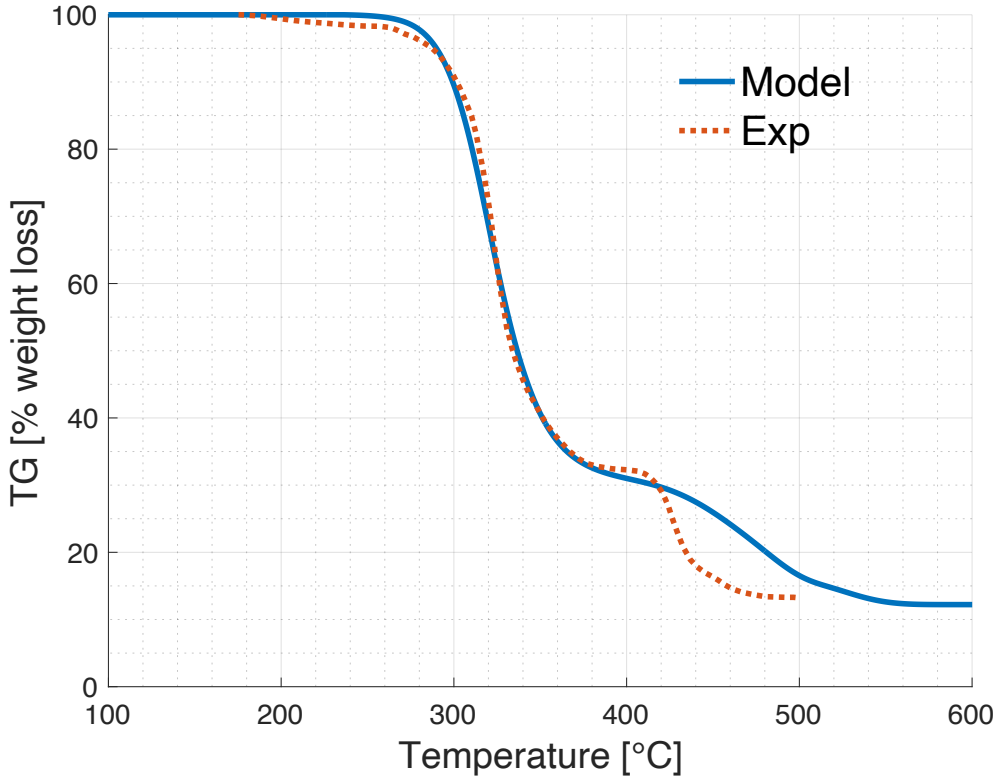

Fig. 2.2 Comparison between simulated dynamic TGA at 10 °C/min and experimental data of thermal degradation of PVC by Yuan *et al.* [24].

As already underlined in the previous paragraph, PVC presents a thermogravimetric curve different from the one of the other polymers that make up the *plasmix*. In particular, it can be noted that are present two distinct decomposition steps, separated by a small central *plateau*. The first step is the so-called dehydrochlorination phase, which begins at lower temperatures where mass loss is mainly due to HCl production. At the end of the dehydrochlorination phase, the *plateau* is reached, where there is a slowdown in the degradation process, and the chains, now chlorine-free, cyclize, forming polyaromatic hydrocarbons (PAHs), which finally degrade in the last phases of the process. Indeed, after

400 °C, the curve shows a new acceleration of mass loss with the development of volatile aromatic compounds, while beyond 500 °C, further transformations of the residue are no longer appreciable.

Fig. 2.2 shows that in both the curves, the degradation process begins near 280 °C. Then, the curves reach the *plateau* at ~30% of residue, but the *plateau* coming from the model turns out to be less flat and much longer than the one obtained from the experimental results. The biggest differences can be noted at the end of the second step. Indeed, the residual value reached at the end of the process is very similar between the two curves (where ~13% of the residue is obtained), but, as it can be seen in the figure, this value is reached at very different temperatures, i.e. ~470 °C for the TG curve obtained experimentally and ~540 °C for the TG curve obtained from the model. So, the model predicts the dehydrochlorination process with a good approximation, while in the second step, the data differ from each other. Indeed, the model curve appears to have a slight delay in the second step of the curve than the experimental one.

The HCl emission characteristic curve of PVC during the thermal gravity analysis under N_2 flow was investigated by Yuan *et al.* [24], and the results are shown in Fig. 2.3. PVC contains C–Cl bond, and its decomposition is a free radical chain reaction that can occur below 310 °C meanwhile, Cl is removed as HCl. The mechanism of PVC pyrolysis in this step can be roughly expressed as follows [24]:

$$-(CH_2 - CHCl)_n- \rightarrow -(CH = CH)_n - + nHCl$$

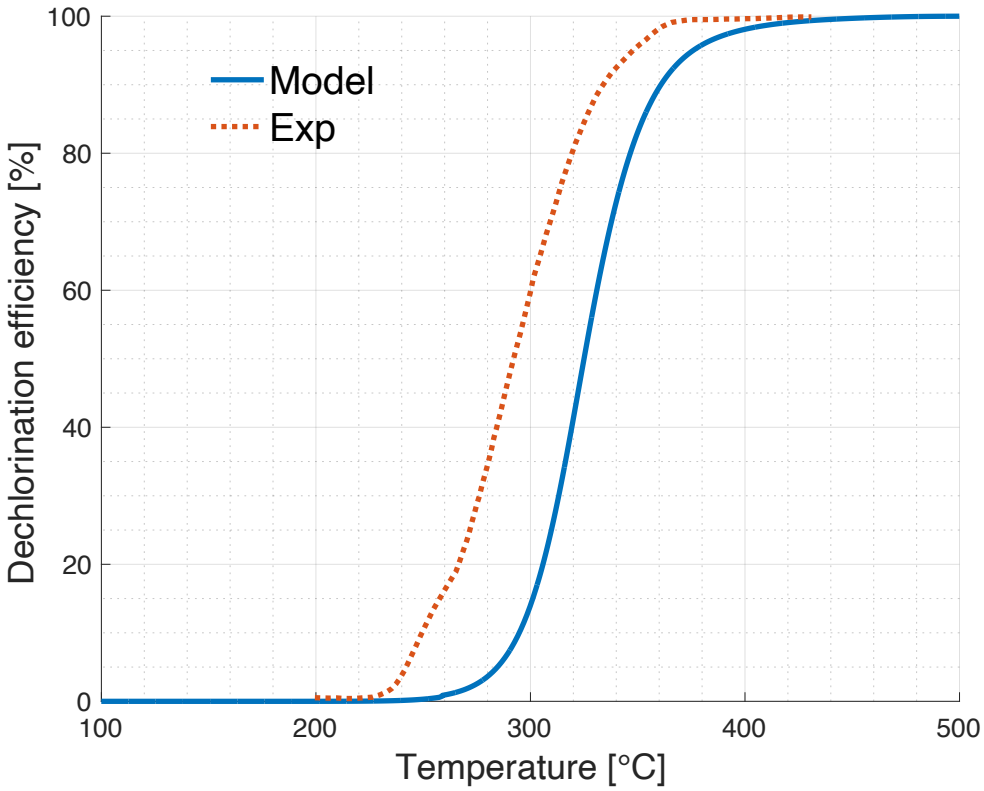

Fig. 2.3 Dechlorination efficiency of PVC: comparison between the model results and the experiment results by Yuan *et al.* [24].

The dechlorination efficiency (or Cl removal efficiency) reported in the plot is defined as:

$$\eta = \frac{Cl_{released}}{Cl_{total}}$$

Fig. 2.3 shows that the HCl release began below 250 °C, but the HCl release will last for a wide temperature span (over 350 °C) before its total removal. The trend is very similar for both the curves, but the temperature for which the relative efficiencies reach values of about 99% is very different (375 °C for the experimental data vs. 415 °C for the model). So, even in this case, there is a delay of about 40 °C of the model compared to the experimental data. Indeed, as reported in Fig. 2.4, by shifting the model curve of 40 °C, it is possible to see how both the curves match much better now.

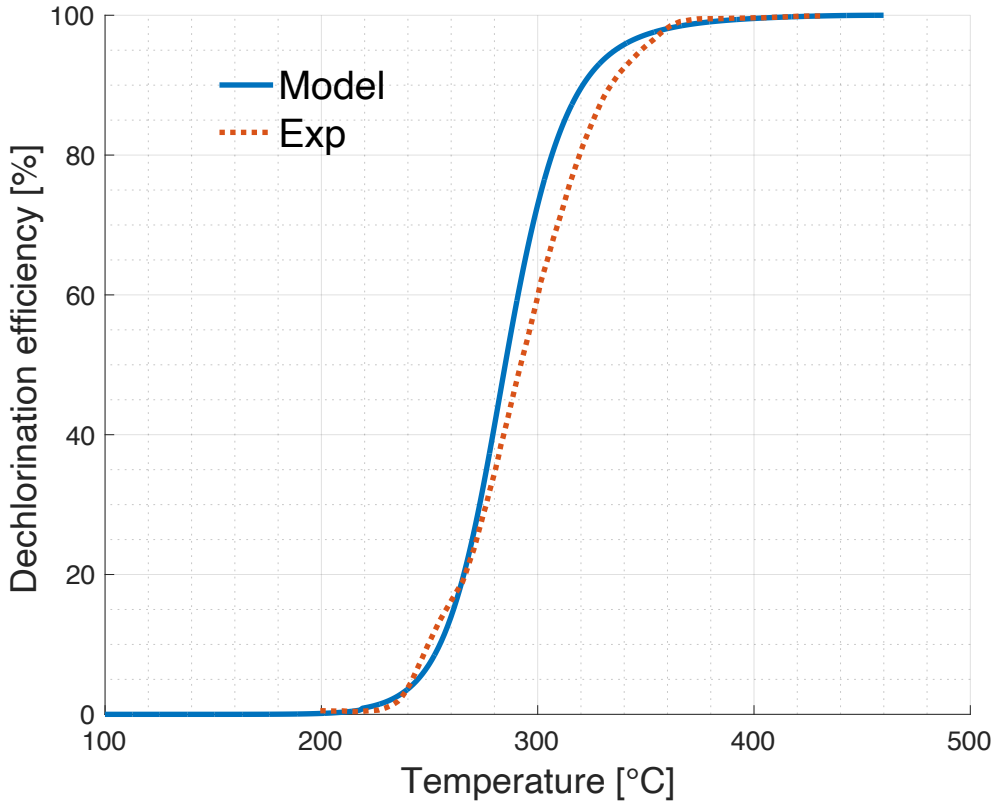

Fig. 2.4 Dechlorination efficiency of PVC shifting the model curve of 40 °C.

The figures show that the HCl release might begin during the melting stage, suggesting that measures should be taken to collect HCl emitted during this step. To prevent a mixed gas of HCl and hydrocarbons generation during the dechlorination step, experimental measurements should be taken to enhance HCl release during the first degradation step. Gas-fluid fluidized bed reactor is such a measure to help HCl release at lower temperatures [24].

Finally, thanks to the experimental data provided by the Energy Department of the Politecnico di Milano [31], an overview of the strengths and limitations of the model is shown in Fig. 2.5. The experiments were carried out from room temperature to 600 °C at different heating rates (10, 50, 100, and 150 °C/min) and with a nitrogen flow rate of 20 ml/min.

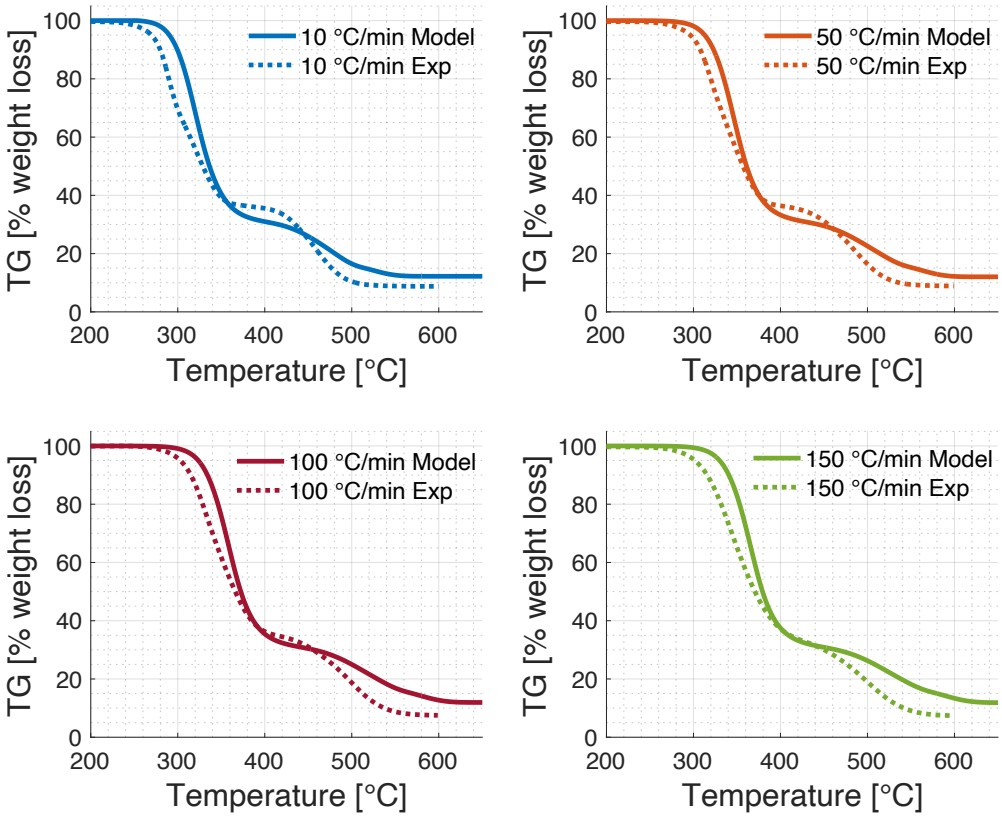

Fig. 2.5 Comparison between the model and the experimental data provided by the Energy Department of Politecnico di Milano [31] for the thermogravimetry of PVC at different heating rates (10, 50, 100, 150 °C/min).

The model appears reliable regarding the overall behavior, even if it presents some recurring differences in the various simulations proposed at different heating rates. In particular, the first step of dehydrochlorination (with the consequent formation of polyolefin chains) is delayed and more width in the model. Indeed, Fig. 2.5 shows how the release of experimental HCl stops at ~35-37% of residual massive fraction, while, in the model, it continues up to ~31-32%. However, this effect is less evident as the heating rate increases. Consequently, this lengthening of the dehydrochlorination step determines a delay in reaching the *plateau* and a second step less contracted than the experimental one.

Finally, Fig. 2.5 shows that the initiation temperature of PVC degradation increases with the heating rate in both the experimental and model simulations. However, the model is again delayed by ~40 °C compared to the experimental results.

2.2.2. Comparison with isothermal data

Although isothermal experiments are more difficult to carry out than thermogravimetric measurements, they can be another excellent tool for validating kinetic models. The only reference found regarding isothermal degradation experiments is the aforementioned work by Yuan *et al.* [24].

In this work, the chlorine removal from PVC is studied under different operating conditions. To efficiently remove Cl within a limited time before extensive generation of hydrocarbon products, different experiments were run at different operating temperatures. A hot nitrogen flow was used to fluidize the molten polymer, letting the PVC release Cl in the form of HCl. In the experimental set-up, the reactor was firstly heated to the pre-set temperature with N_2 purge all the time. The PVC, previously shredded into granules with a 2-3 mm diameter, is fed to the system and dropped to the gas distributor plate inside the reactor.

Fig. 2.6 shows the comparison of the isothermal tests, reporting the degree of dechlorination efficiency (%), already defined in the previous paragraph, as a function of time at the temperatures of 280, 290, 300, 310, and 320 °C and for a fixed N_2 flowrate of 2 l/min.

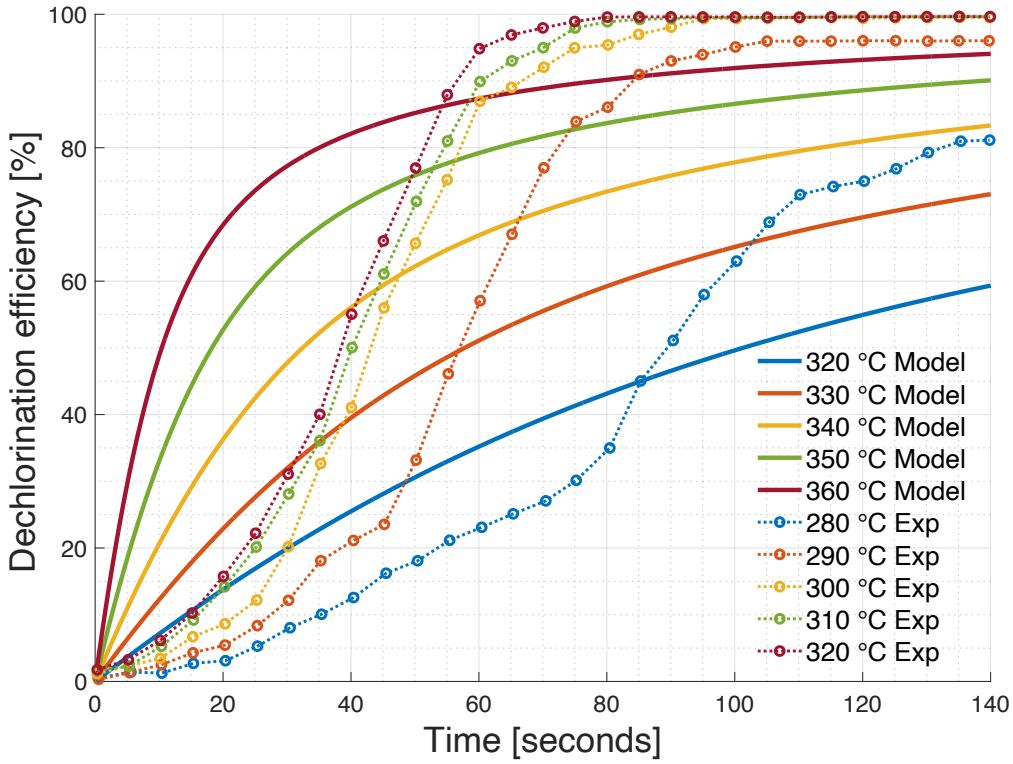

Fig. 2.6 Comparison with the isothermal data of Yuan *et al.* [24].

Fig. 2.6 shows that both for experimental and model tests, as the temperature increases, the HCl release becomes faster, and the final dechlorination efficiency higher. So, both the curves have the same qualitative trend in the function of the temperature, but the quantitative values are quite different. Indeed, in order to make possible a comparison between them, it was necessary to increase the temperature of the simulations by 40 ° C, as already highlighted in the previous paragraph (2.2.1.). In this way, the experimental curve corresponding to a temperature of 280 °C was compared to that generated by the model for a temperature of 320 °C and so on. However, it is important to note that even considering this delay in the temperature, the experimental data still has a significant discrepancy with respect to the model. However, this dispersion becomes less evident as the temperature increases, confirming the better reliability of the model in particular in the final part of the first degradation step.

2.2.3. Comparison with detailed data on product distribution

Thanks to the work carried out by Zhou *et al.* [25], the data relating to the distribution of the products obtained from the kinetic model are compared with the experimental values. In this work, Zhou *et al.* investigated the influence of the process conditions in terms of temperature and heating rate on the yield of the different product fractions and the formation of gases and polycyclic aromatic hydrocarbons (PAHs) during the pyrolysis of PVC.

As reported by the author, pure PVC samples were used in these experiments in order to eliminate the potential influence of contaminants or additives that may be found in real-world PVC waste. The pyrolysis of PVC is carried out at temperatures of 500, 600, 700, 800, and 900 °C and at fast or slow heating rates, the whole under a nitrogen atmosphere in a fixed bed reactor.

For the fast pyrolysis experiments, the reactor was initially heated to the setpoint temperature. The PVC plastic sample (~1 g) was then placed on a sample spoon and inserted into the reactor where fast pyrolysis occurred. The sample was quickly heated to the set pyrolysis temperature at an estimated heating rate of 350 °C/min.

Fig. 2.7 shows the comparison between the results obtained experimentally and those obtained from the model. Table 2.1 and Table 2.2 show the values of all the fractions at different temperatures obtained from the model and experimentally.

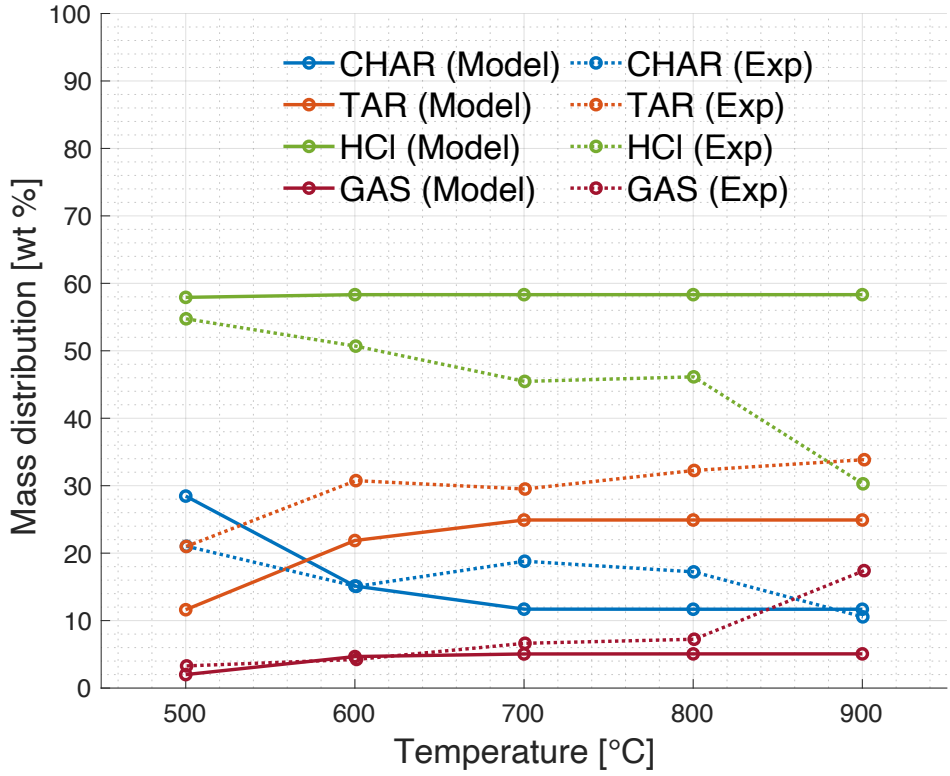

Fig. 2.7 Comparison of the model results with the distribution of the products obtained by Zhou *et al.* [25] for the fast pyrolysis.

Temperature (°C)	500	600	700	800	900
	Mass distribution [wt%]				
HCl	57.92	58.32	58.32	58.32	58.32
Gas	2.00	4.67	5.05	5.07	5.07
Tar	11.62	21.87	24.92	24.92	24.92
Residue (Char)	28.46	15.13	11.70	11.69	11.69

Table 2.1 Percentage mass distribution of the products at different temperatures obtained from the model for the fast pyrolysis.

Temperature (°C)	500	600	700	800	900
	Mass distribution [wt%]				
HCl	54.74	50.69	45.46	46.14	30.28
Gas	3.29	4.24	6.64	7.24	17.41
Tar	20.99	30.75	29.51	32.26	33.86
Residue (Char)	20.99	15.08	18.80	17.23	10.56

Table 2.1 Percentage mass distribution of the products at different temperatures obtained experimentally by Zhou *et al.* [25] for the fast pyrolysis.

As shown in Fig. 2.7 and Table 2.1 and 2.2, the biggest differences are found with the fraction of HCl released at different temperatures. In fact, experimentally, the HCl yield decreases from ~54.5 to ~30.5 wt% as the pyrolysis temperature is increased from 500 to 900 °C. However, the model predicts an approximately steady fraction of acid released at different temperatures. This disagreement is most likely due to the fact that the kinetic model predicts that almost all of the chlorine theoretically present in the polymer is eliminated as HCl, while experimentally, it is proved that the quantity of HCl released depends above all on the operating conditions.

The overestimated quantity of HCl predicted by the model influences the relative fraction of the other products, particularly the gas fraction, where the light hydrocarbons calculated by the model are present in lower quantity with respect to that actually found experimentally. Moreover, the calculated distribution of aromatic hydrocarbons (i.e. the tar fraction) is underestimated compared to the experimental data. However, the two sets of data present the same trend, showing an increase in tar yield with the temperature increase. The same considerations hold for the char fraction too. However, in this case, the model results are overestimated at low temperatures (500 °C), quite similar at 600 °C, and underestimated for higher temperatures. Finally, it is important to note that the values of the different fractions obtained from the model are constant after 700 °C, without any influence of the final temperature on the product distribution.

Moreover, from now on, it would be better not to consider the experimental results obtained at 900 °C because these results provide meaningless results. Indeed, the material balance is not correct at this temperature since the sum of all the mass fractions (HCl, Gas, Tar, and Residue) is ~92% of the initial sample mass, instead of 100%.

The figures below show the comparison between the results obtained experimentally and those obtained from the model regarding the influence of temperature on the release of

gases (Fig. 2.8), 2-ring PAHs (Fig. 2.9), and 3-ring PAHs (Fig. 2.10) during the pyrolysis of PVC.

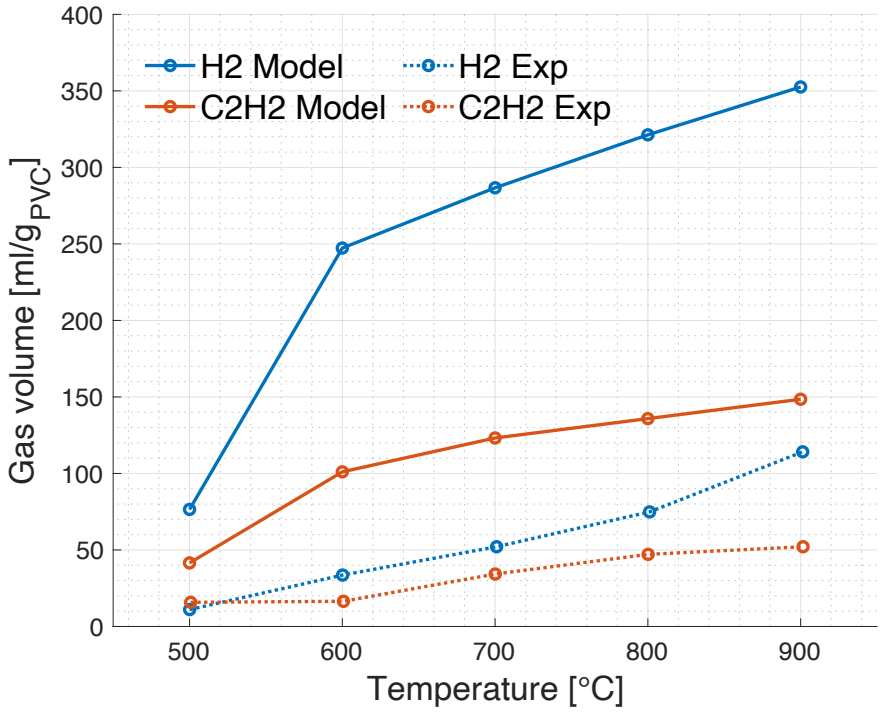

Fig. 2.8 Comparison between the gas released predicted by the model and the experimental data by Zhou *et al.* [25] for the fast pyrolysis experiments.

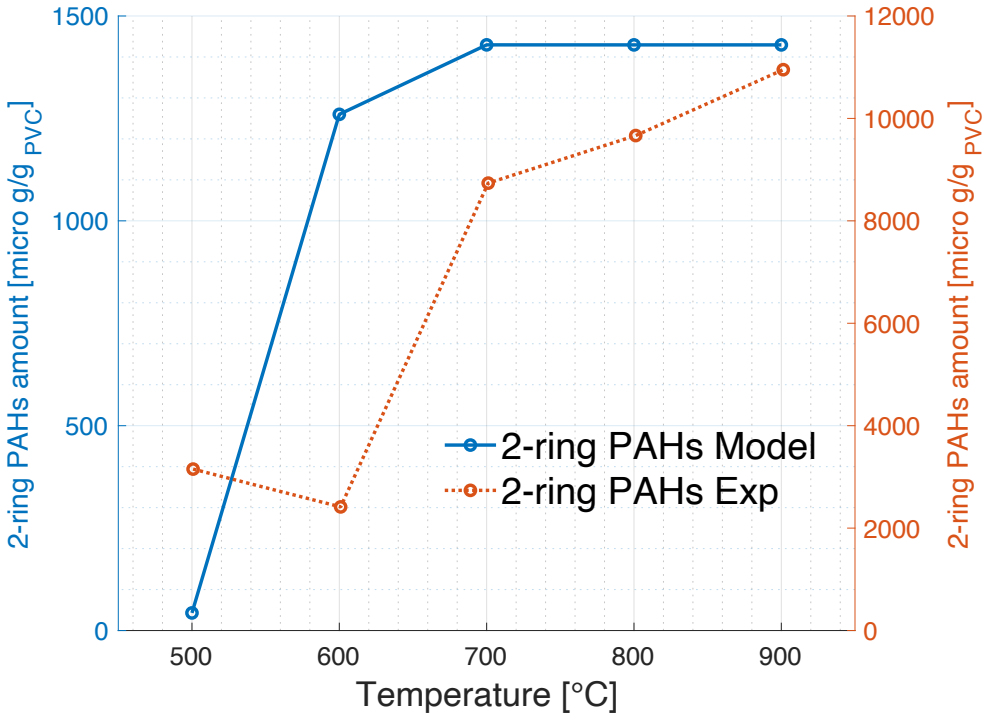

Fig. 2.9 Comparison between 2-ring PAHs formation predicted by the model and the experimental data by Zhou *et al.* [25] for the fast pyrolysis experiments.

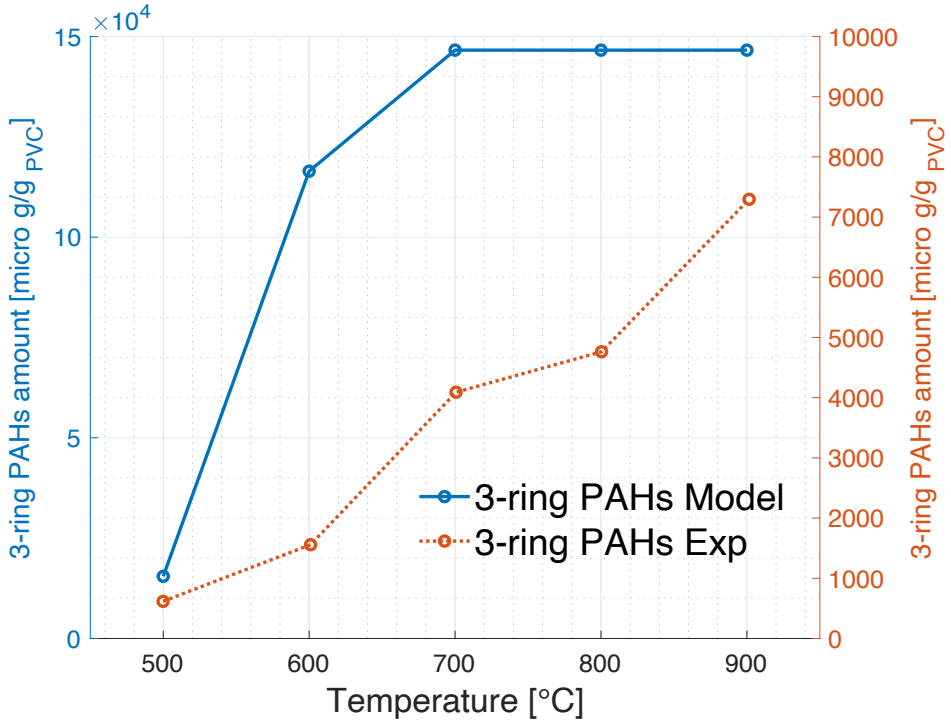

Fig. 2.10 Comparison between 3-ring PAHs formation predicted by the model and the experimental data by Zhou *et al.* [25] for the fast pyrolysis experiments.

To compute the volume of gas released predicted by the model in Fig. 2.8, the temperature-dependent gas density was considered according to the equation of state (EoS) for ideal gases:

$$\rho_i = \frac{PMW_i}{RT}$$

where P is the atmospheric pressure, T is the final operating temperature, R is the universal gas constant, and MW_i is the molecular weight of gaseous species i.

C_2H_2, shown in the figures above, is the *pseudo-species* representative of hydrocarbon gases as ethylene, propylene, and methane, produced by radical dealkylation reactions in an advanced aromatization phase, as already explained in the previous paragraph.

As seen in Fig. 2.8, both for the model and experimental results, the total gas yield increases, particularly at higher temperatures, where there is a consequent increase in all of the individual H_2 and C_2H_2 hydrocarbon gases.

Experimentally, the increase of H_2 from 11.2 to 114.1 ml/g_{PVC} is the most significant change, and this is the same for the model results, even if the model values are about three times higher. So, although the values are different from each other, the increase in the gas released with the temperature predicted by the model is consistent with the experimental results in this study. The enhancement of gas production with the increase of pyrolysis temperature can be attributed to the promotion of C–C cracking reactions [25].

Fig. 2.9 and Fig. 2.10 show the 2-ring and 3-ring PAHs quantitatively detected in the tar fraction from the pyrolysis of PVC. Due to the *lumped* approach on which the model is based (i.e. adoption of representative species rather than real molecules), not all the single products are represented in detail, but only *pseudo-species* that are representative of all the 2-ring or 3-ring PAHs. On the contrary, the experimental results provide all the single species. Therefore, in order to compare the experimental data with the model results, it was necessary to add up the quantities of all the single compounds that make up the 2-ring or 3-ring PAHs.

The figures above show an increase in 2-ring and 3-ring PAHs yield with an increase of pyrolysis temperature from 500 to 900 °C, which is consistent both experimentally and from the model. The yield of total 2–3 ring PAHs increases from ~3770 to ~18240 $\mu g/g_{PVC}$ with the increase of pyrolysis temperature from 500 to 900 °C in the experiments, while in the results obtained from the model, this value increases from ~15530 at 500 °C up to ~148030 at 900 °C. The increase of PAHs with the increase of temperature can be attributed to the promotion of secondary reactions of tar [25]. However, it should be noted that, despite having the same behavior, the results obtained by the model for the 3-ring PAHs are two orders of magnitude higher than the experimental ones. Furthermore, according to the model, for both 2-ring and 3-ring compounds, there are no longer variations in their quantity after 700 °C, while a continuously increasing trend is found in the experimental

data. Finally, it is important to note that the experimental data also proposes the results for the 4-ring PAHs (belonging to the tar fraction), while the model reports only the 2 and 3-ring compounds. This can explain the larger quantity of 3-ring PAHs obtained from the model compared to what is seen experimentally.

In order to investigate the influence of heating rate on the product distribution and on gas and PAHs formation, the results of fast pyrolysis at a heating rate of 350 °C/min and for a fixed reactor temperature of 800 °C are compared to slow pyrolysis ones, where the PVC is heated at 10 °C/min to a final temperature of 800 °C. For the slow pyrolysis experiments, again carried out by Zhou *et al.* [25], the sample spoon containing the PVC was pre-loaded into the reactor and heated from room temperature to the final temperature of 800 °C at a heating rate of 10 °C/min and held for 30 min.

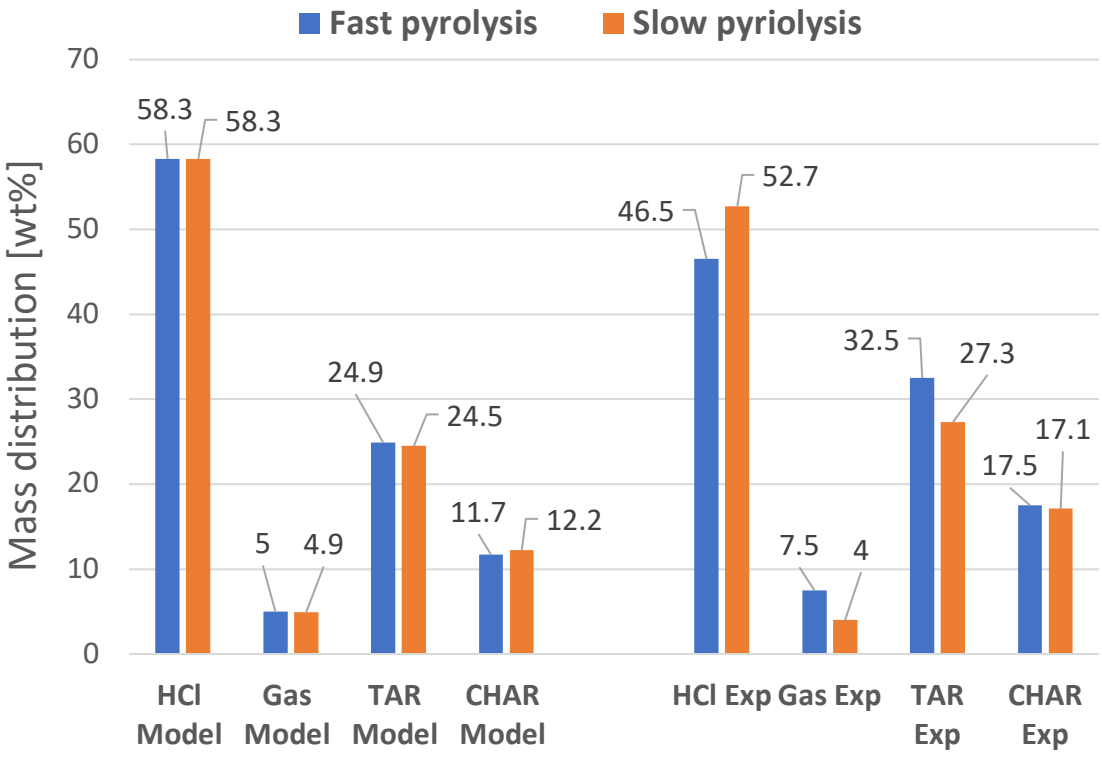

Fig. 2.11 Comparison of the model results (right) with the distribution of the products obtained by Zhou *et al.* [25] (left) for the fast and slow pyrolysis at 800 °C.

Fig. 2.11 compares the model results with the distribution of the products obtained experimentally, both for the fast and slow pyrolysis at 800 °C. From the model, the tar, char, HCl, and gas fraction do not change significantly between fast and slow pyrolysis. On the contrary, there is a more relevant difference from the experimental data, especially in terms of tar and HCl fraction. However, overall the results obtained from the model follow quite well the trend of the experimental data.

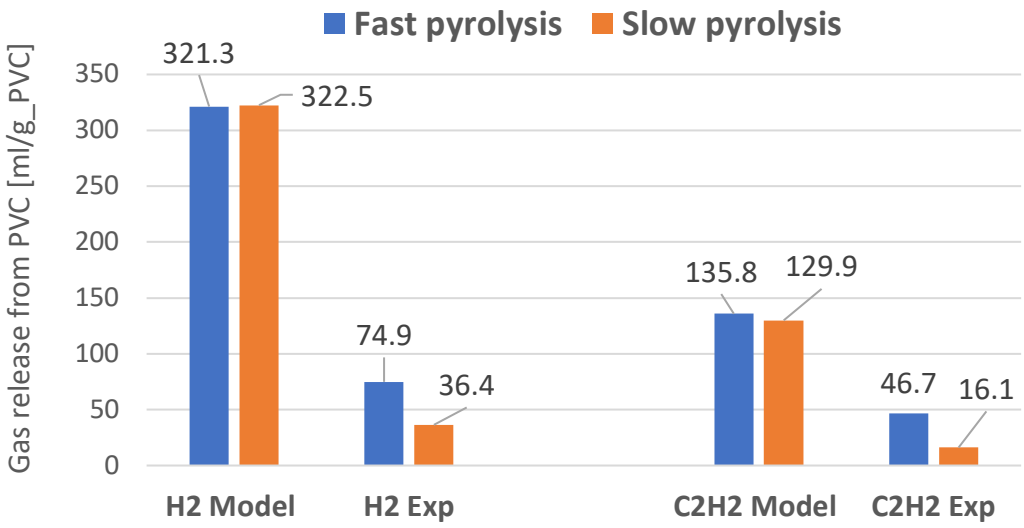

Fig. 2.12 Comparison between the gas released predicted by the model (right) and the experimental data by Zhou *et al.* [25] (left) for fast and slow pyrolysis at 800 °C.

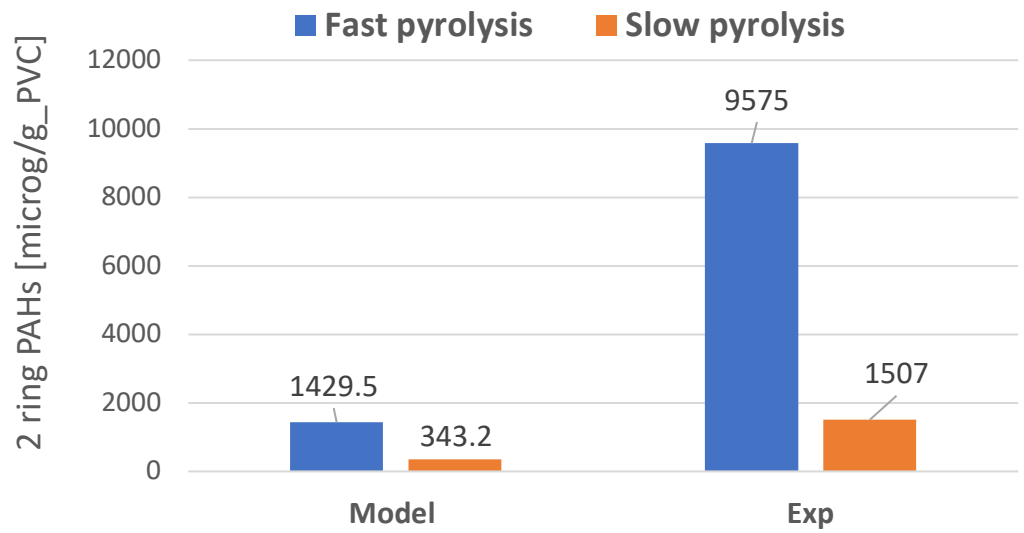

Fig. 2.13 Comparison between 2-ring PAHs formation predicted by the model (right) and the experimental data by Zhou *et al.* [25] (left) for fast and slow pyrolysis at 800 °C.

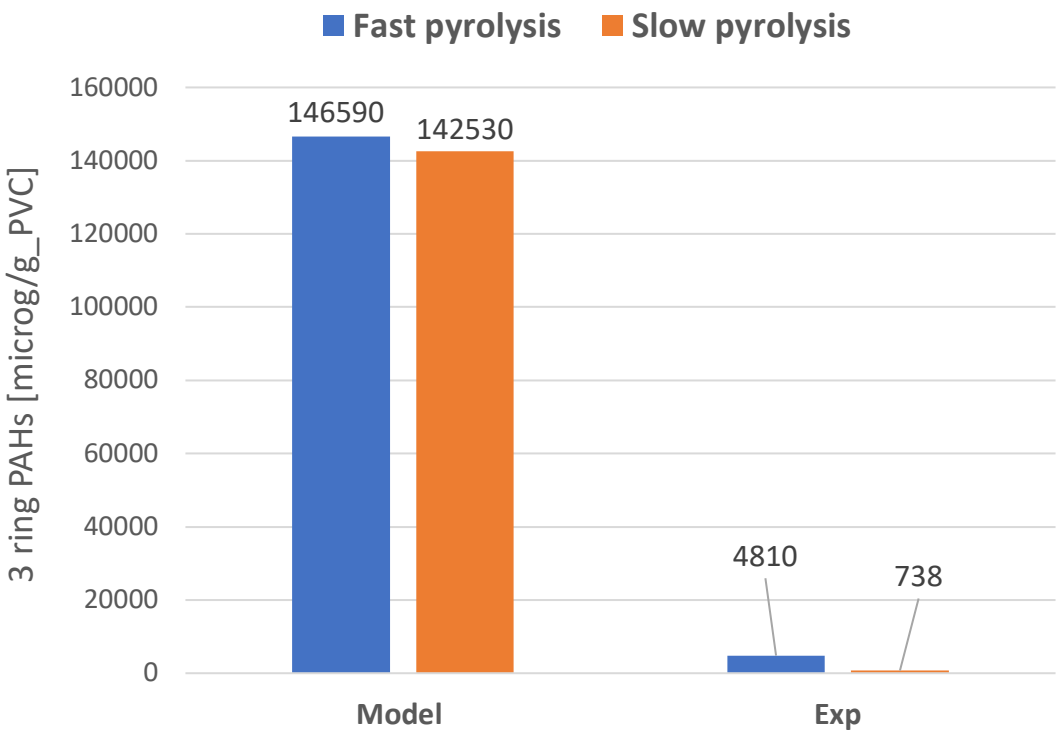

Fig. 2.14 Comparison between 3-ring PAHs formation predicted by the model (right) and the experimental data by Zhou *et al.* [25] (left) for fast and slow pyrolysis at 800 °C.

As already said above for the influence of the heating rate on the distribution of the products, looking at the results obtained by the model in Fig. 2.12, it shows that there are no significant differences even between the quantity of H_2 and the *pseudo-species* C_2H_2 released passing from fast to slow pyrolysis. In contrast, more significant differences are found in the results obtained from the experimental results. In fact, experimentally, it is shown that low pyrolysis should generate higher HCl yield and lower gas and tar yield than fast pyrolysis.

Finally, as seen in Fig. 2.13 and Fig. 2.14, also the 2-ring and 3-ring PAHs yield obtained experimentally from the slow pyrolysis is much lower than the one obtained from fast pyrolysis. On the contrary, from the results obtained by the model, the quantity of 3-ring PAHs changes very little, while the quantity of 2-ring PAHs released by passing from fast to slow pyrolysis decreases by one order of magnitude, which is therefore much more in

line with the experimental results, even if the absolute values are much lower. However, the bigger discrepancy of the model results with the experimental ones is due to the 3-ring PAHs quantity released, which is two orders of magnitude greater with respect to the experimental data.

These results are of absolute importance because they allow us to investigate the reliability of the model and its limits in an even deeper way, trying to understand where it is more appropriate to work in order to improve the model.

Chapter 3

3. PET: model description and validation

Polyethylene terephthalate is one of the most abundant plastics, and it is mainly used in food packaging products. These products have a very short life, and they are rapidly transformed into waste, accounting for 7.7 wt% of the total plastic waste generated in 2018 in Europe [1]. Therefore, new versatile alternatives for PET waste management, such as pyrolysis, should be employed to recover value-added products from this kind of waste. The modeling of PET degradation is, for this reason, of great importance in view of a future chemical recovery of *plasmix*.

In this chapter, the kinetic model of PET thermal degradation developed by the CRECK Modeling Lab of the Politecnico di Milano will be presented. Then, the model validation based on the comparison between the experimental data obtained in literature and the output data coming from the simulation will follow.

Several thermogravimetric and isothermal analyses are considered and, then, the influence of process conditions (such as the heating rate and final pyrolysis temperature) on the final product distribution, i.e. the yield of the different pyrolysis fractions and compounds, will be investigated.

3.1. Kinetic model of PET thermal degradation

PET, when treated at high temperatures, does not degrade according to a simple depolymerization mechanism. In fact, the thermal degradation of PET is the result of different chemical phenomena leading to the formation of light gaseous products, condensable vapors, waxy compounds (i.e. oxygenated aromatic compounds such as benzoic acids) and, at high temperatures, a solid residue strongly dehydrogenated (char).

The degradation of PET does not have a large availability of predictive models in the literature, but just a few studies in which some of the main degradation products are listed (such as CO, CO_2, acetaldehyde, benzoic acid, and, in small quantities, benzene).

Therefore, a kinetic model of degradation was developed and implemented by the CRECK Modeling Lab using a semi-detailed approach based on *pseudo-species* representing the functional groups present in the polymer. Such species can be real compounds or not, representing both molecules and radicals. This methodology allows describing the chemical reactions involved in the transformations of PET, including both the decomposition and the growth processes. The growth process is mainly due to the crosslinking of the aromatic structures that are responsible for the formation of char. The kinetic model just mentioned is proposed here below.

According to the model, the initial PET polymer is considered the alternating copolymer of terephthalic acid and ethylene glycol, where the two symmetrical units of monomer follow each other. These two units are represented by the reference species p−COPhCO−p and p−OCH_2CH_2O−p, where p represents the polymer chain adjacent to each unit (Fig. 3.1).

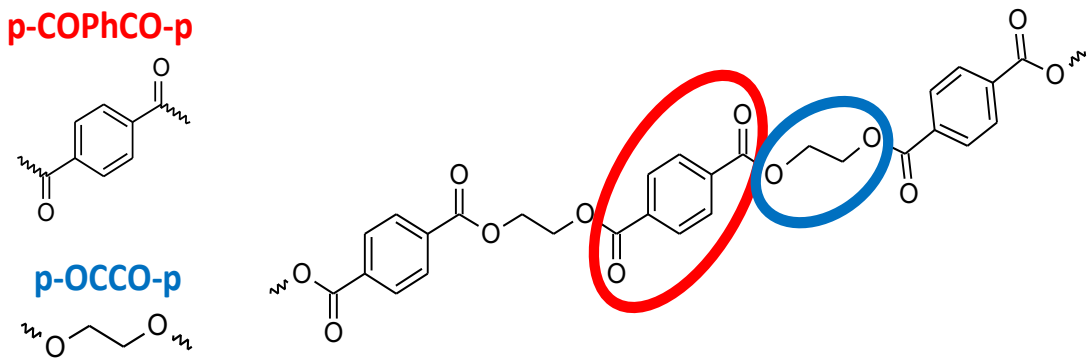

Fig. 3.1 Molecular structure of PET and molecular structure of the representative units used for its modeling.

Therefore, the processes involved in the degradation of PET can be written as reactions involving these two species and other chemical species derived during the process through numerous reactions involving different intermediates until it results in the degradation products.

Possible explanations for the formation of the main products are reported in the literature, most of which refer to molecular decomposition reactions and intramolecular addition reactions that lead to char production. However, the reactions that lead to the degradation of PET can be divided into two large groups: molecular and radical reactions. Although they are not the dominant mechanism of the degradation process, the latter are included in the model proposed because they can play an important role when the PET is mixed with more thermolabile substances that can trigger this type of mechanism.

3.1.1. Molecular reaction mechanism

Degradation of PET begins with the molecular cleavage of the polymer chain between the two constituent monomer units. This mechanism can occur through a 6-center reaction with the transfer of hydrogen from the β-carbon of the glycol to the ester group of the terephthalic acid to give two single chains, as shown in Fig. 3.2.

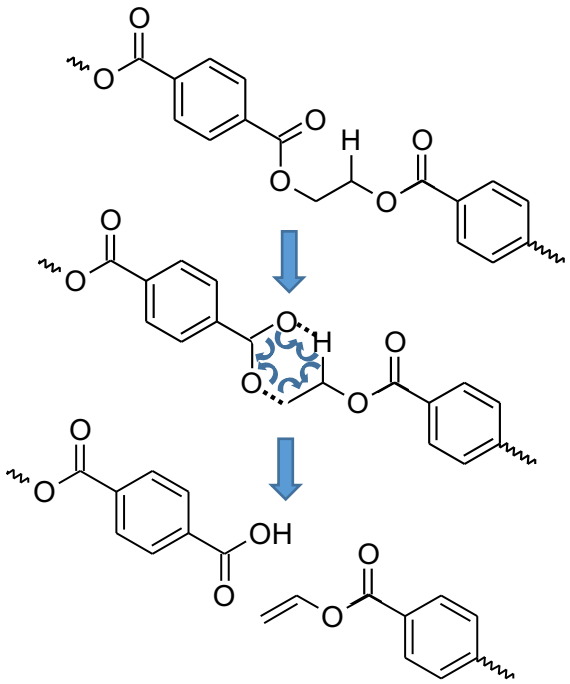

Fig. 3.2 Molecular cleavage mechanism of the polymer chain hypothesized for PET thermal degradation.

Once the polymer chain is broken, devolatilization of the polymer occurs through the degradation of the substitutions on the phenyl groups at the chain terminations. These decomposition reactions are of a molecular nature and lead to the formation of light products such as CO, CO_2, and acetaldehyde (CH_3CHO).

A further mechanism of PET degradation is represented by the formation of cyclic oligomers (dimers, trimers, or tetramers) due to the folding of the polymer chain, as shown in Fig 3.3. These compounds, which present a molecular weight between 340 and 1440 g/mol, remain in the liquid phase due to their low volatility and degrade in a similar way to what happens to longer polymer chains, producing gaseous and condensable compounds, in particular substituted benzoic acids. In its current version, the model does not distinguish between the monomers within the chain and those in the oligomeric species, providing for similar degradation reactions.

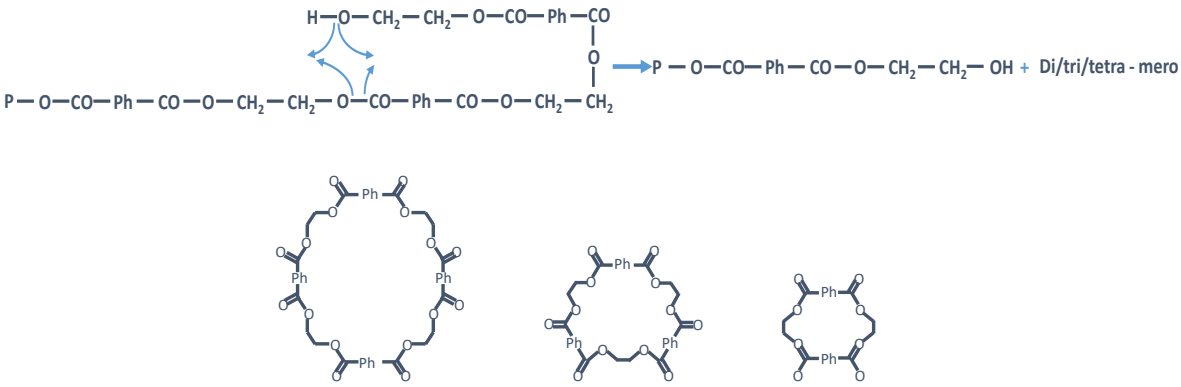

Fig. 3.3 Molecular mechanism of cyclic oligomers formation hypothesized for PET (figure above) and representation of dimers, trimers or tetramers (figure below).

3.1.2. Radical reaction mechanism

In the group of radical reactions, the initiation reactions in the thermal degradation of PET involve the homolytic cleavage of C-C or C-O bonds, reactions characterized by high activation energy. The rate constants used to describe this phenomenon were derived from analogous reactions in the gas phase by applying the proper corrections associated with the switch to the liquid phase, as done for the PVC. The high activation energy makes radical reactions for PET degradation very disadvantaged compared to molecular decompositions, particularly at low temperatures. However, the following classes of radical reaction were included in the model:

- radical initiations: these reactions lead to the formation of terminal radicals;
- hydrogen abstraction reactions with consequent migration of the radical site;
- decomposition reactions: they are β-cleavage reactions with consequent chain decomposition and formation of terminal radicals, in particular end-of-chain phenyls that are due to β-cleavage reactions involving the breaking of bonds associated with the carboxyl group, also releasing CO and CO_2. Among these reactions, the case of decarboxylation stands out due to the presence of oxygen

atoms on the chain of PET. These reactions also liberate compounds such as ethylene and benzoic acid;

- addition reactions: this class of reactions leads to the radical formation of polyaromatic hydrocarbons (PAHs) with a low degree of hydrogenation. Moreover, the radicals (in particular phenyls) can give rise to addition reactions similar to those already discussed for the thermal degradation of PVC, leading to cross-linking in the molten phase and, subsequently, to the formation of char.
- radical terminations: these reactions determine the decay of the radical concentration in the system.

3.2. Model Validation

After the brief description of the kinetic model used for the simulations, the model accuracy and reliability can be verified by exploiting the experimental data available in the literature. The comparison between the simulated thermogravimetric curves and the experimental ones, the isothermal tests, and the product distribution is reported below.

3.2.1. Comparison with thermogravimetric data

The kinetic model described in the previous paragraph can be validated based on several dynamic experiments (TGA) found in literature and carried out at different heating rates and operating conditions.

A first comparison was possible thanks to the experiments conducted by Singh *et al.* [26], which carried out the thermal degradation of different waste plastics (including HDPE, PP, PS, PET, and mixed plastic waste). The objective of this work was to investigate the effect of operating temperature and heating rate on the sample degradation and on the liquid product yields in the pyrolysis process by non-isothermal heating. To obtain the

thermogravimetric curves, the samples were pyrolyzed in a TGA analyzer. The temperature was increased from room temperature to 600 °C at a heating rate of 20 °C/min in nitrogen (N_2) atmosphere.

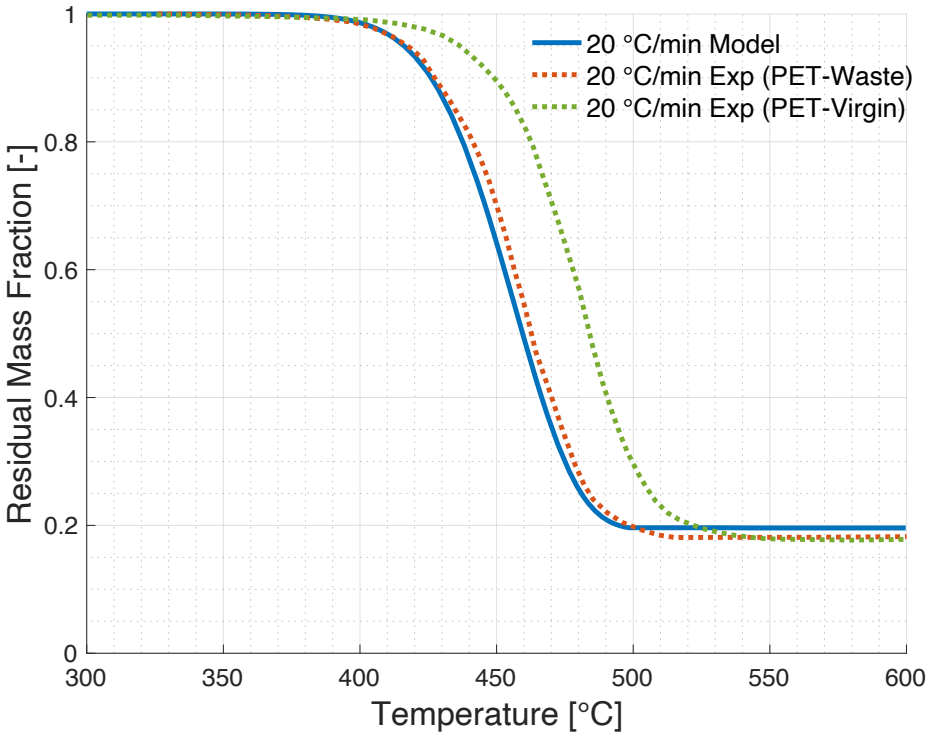

Fig. 3.4 PET thermogravimetry at 20 °C/min: comparison between the model and the experimental results by Singh *et al.* [26].

Fig. 3.4 shows the simulation results at a heating rate of 20 °C/min compared with the experimental results obtained by Singh *et al.* [26], both for the degradation of waste PET and virgin PET. The figure shows that the experimental results are very well represented by the model, demonstrating the ability of the model to capture the effect of the sample heating rate effectively. The results are in agreement, especially regarding the waste PET sample, where the differences are practically minimal, while a degradation delay of ~25 °C is present for the virgin PET sample. The same conclusions can also be extended regarding the dynamic tests with an increasing heating rate conditions carried out by Das *et al.* [27] and Dhahak *et al.* [28], reported in Fig. 3.5 and Fig. 3.6, respectively.

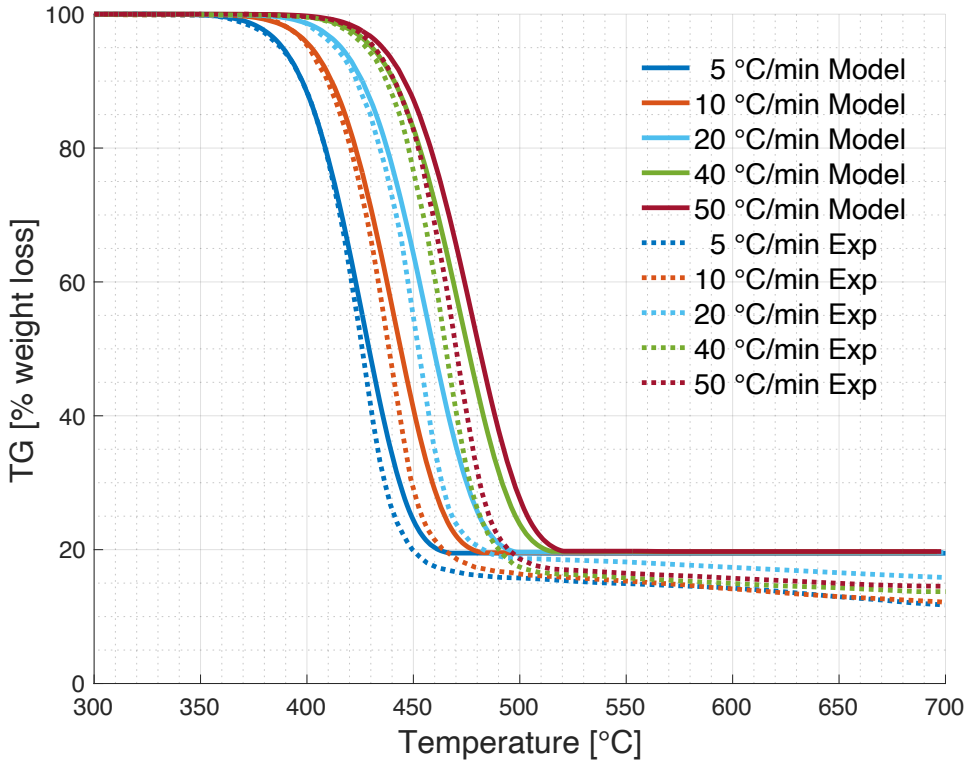

Fig. 3.5 PET thermogravimetry at different heating rates (5, 10, 20, 40 and 50 °C/min): comparison between the model and the experimental data by Das *et al.* [27].

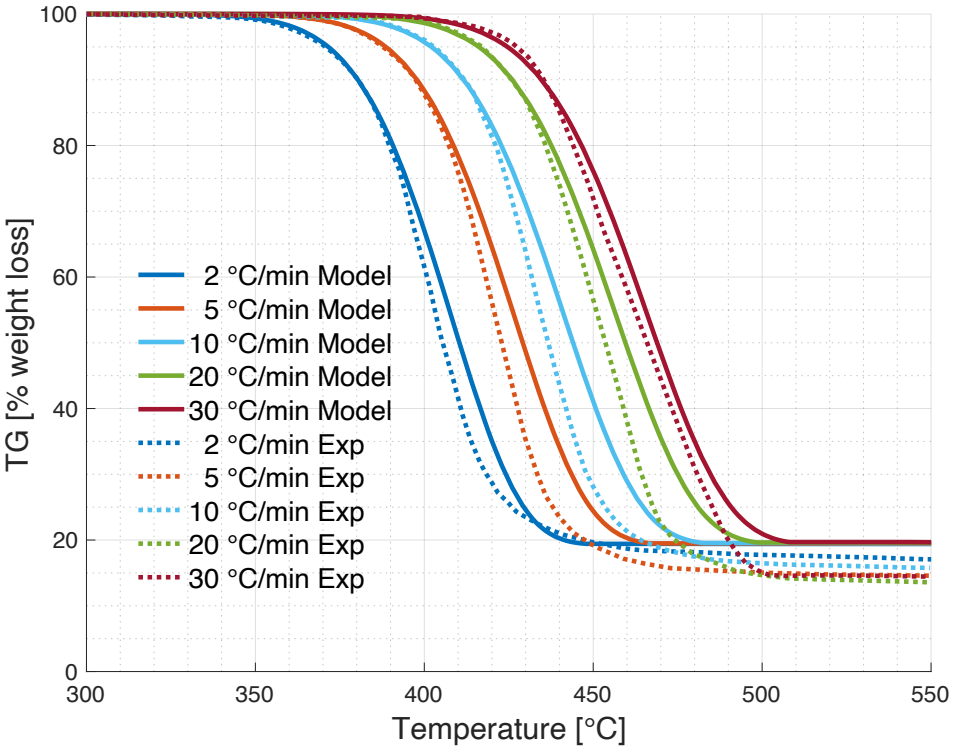

Fig. 3.6 PET thermogravimetry at different heating rates (2, 5, 10, 20 and 30 °C/min): comparison between the model and the experimental data by Dhahak *et al.* [28].

Fig. 3.5 and Fig. 3.6 show that, both for the experimental and the model curve, the degradation process begins at the same time for every different heating rate, following the same behavior. Moreover, as the heating rate increases, the TGA profiles shift to higher temperatures. This is due to lower heat transfer effectiveness, causing a delay in the decomposition rate. Therefore, the advantage of slow heating rates is the slow reaction kinetics, which makes it possible to ignore the heat and mass transfer limitations [28]. The biggest differences can be noted towards the end of the degradation, where the model appears to be in a slightly delay respect to the experimental data. Furthermore, the residual value reached at the end of the process is lower for the experimental results at every heating rate. So, the model can predict the degradation process with a good approximation, except for the final stage of degradation, where the final mass of residue obtained from the model is always larger than the one found experimentally.

Again, from the work carried out by Dhahak *et al.* [28] and from the one carried out by Osman *et al.* [29], it is possible to show the thermogravimetry analyses at different operating conditions. In the first set of experiments, Dhahak *et al.* investigated the effect of the final temperature on the slow pyrolysis of PET, carrying out TGA measurements by heating the sample at a constant heating rate of 5 °C/min to a given final temperature of 410, 430, 450 and 480 °C and, then, holding the sample at this temperature for 120 min (Fig. 3.7). In the second set of experiments, Osman *et al.* carried out TGA measurements in N_2 atmosphere at a heating rate of 0.5, 1, 2, 4, and 8 °C/min and reporting the results in the form of reaction progress in the function of the pyrolysis temperature (Fig. 3.8).

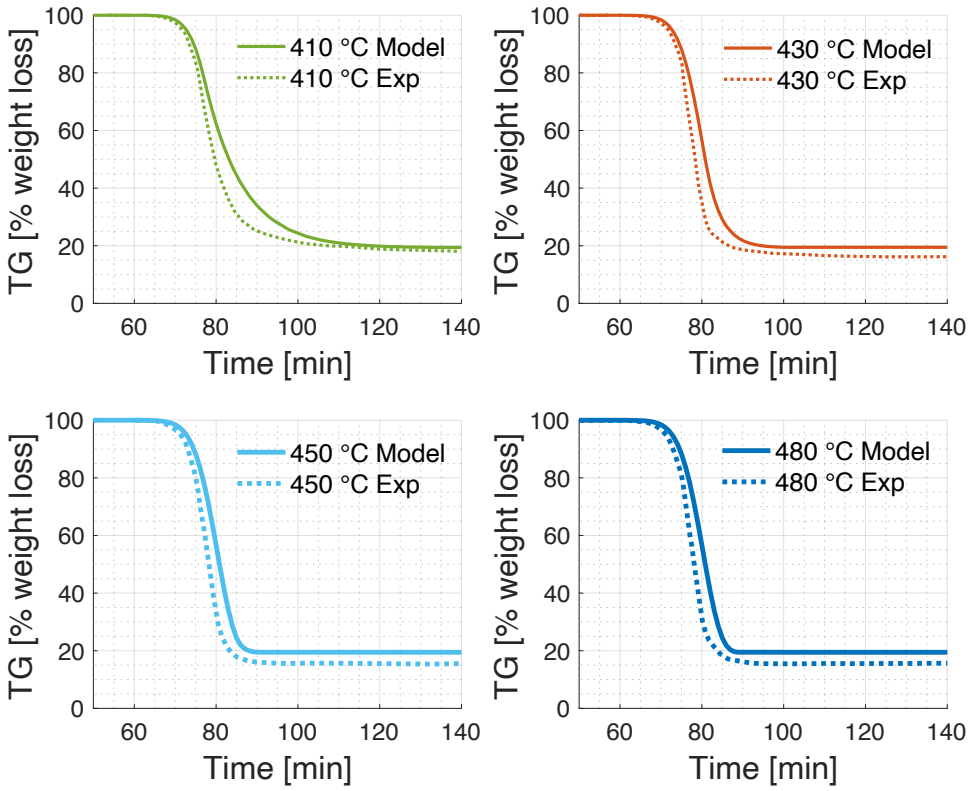

Fig. 3.7 PET thermogravimetry at a constant heating rates of 5 °C/min, final temperature of 410, 430, 450 and 480 ° and holding time of 120 min: comparison between the model and the experimental data by Dhahak *et al.* [28].

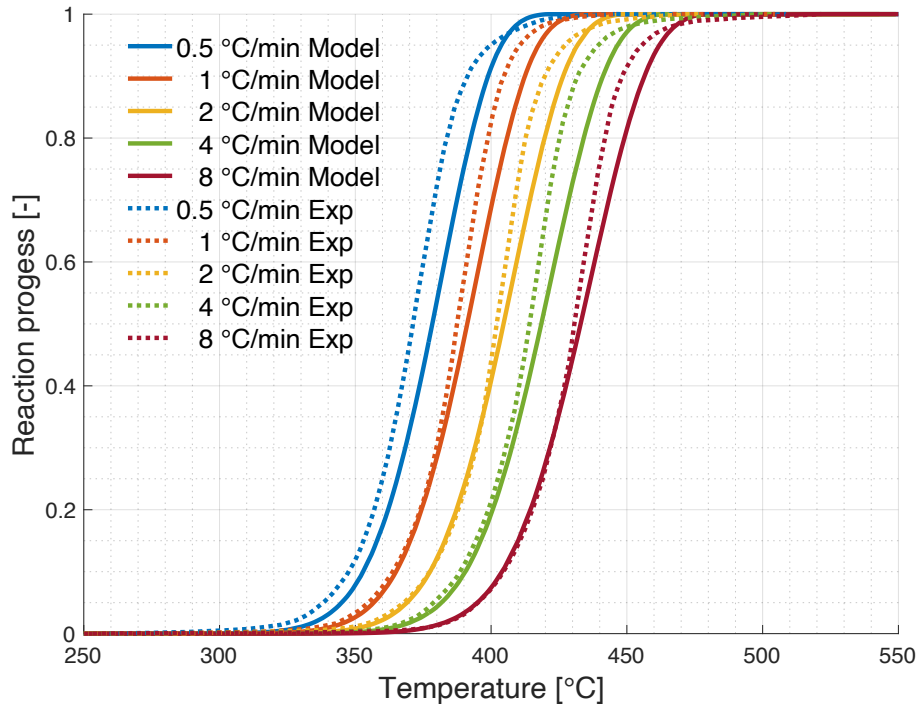

Fig. 3.8 PET reaction progress at different heating rates (0.5, 1, 2, 4 and 8 °C/min): comparison between the model and the experimental data by Osman *et al.* [29].

Fig. 3.7 shows that the mass loss begins at about the same time for both the experimental and model curve, even if the model presents a slight delay compared to the experiments, especially towards the end of the process, as already highlighted previously. For temperatures higher than 430 °C, the degradation is approximately finished after ~90 minutes. However, for 430 °C and 410 °C, more time is needed to reach a steady mass loss, especially at 410 °C, as shown both experimentally (dashed green line) and by the model (solid green line).

To conclude, Fig. 3.9 shows the comparison between the model predictions and the data collected by the Energy Department of Politecnico di Milano [31]. This comparison confirms all the observations already made in the cases previously shown. The experiments were carried out from room temperature to 600 °C, at a heating rate of 10 °C/min, and with a nitrogen flowrate of 20 ml/min.

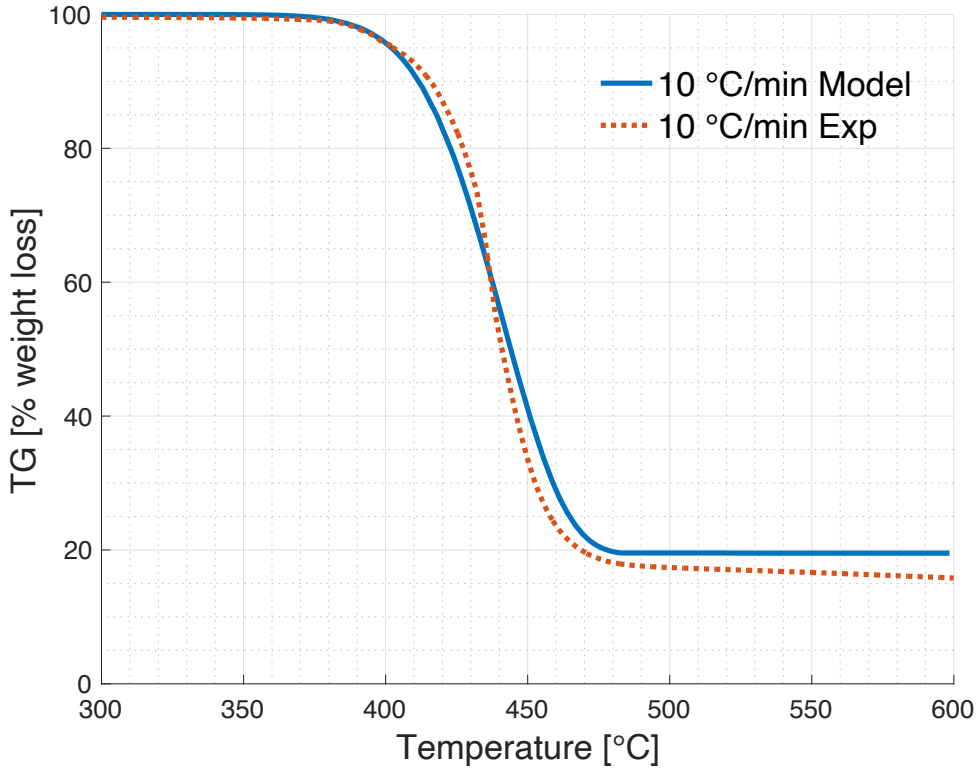

Fig. 3.9 Comparison between model and experimental data obtained by the Energy Department of Politecnico di Milano [31] at 10 ° C/min.

This last simulation offers further confirmation regarding the reliability of the model. In fact, the series of simulations shown in this paragraph demonstrates the ability of the model to effectively predict the effect of the heating rate on the mass loss of the sample. Overall, the agreement of the model with the experimental data is generally excellent. However, this is not correct at the final stage of degradation, where the final mass of residue obtained from the model is always larger than the one found experimentally. In fact, this discrepancy in the model is present during all the simulations, where the final residue quantity always assumes a constant asymptotic value of ~20% of the initial sample mass. This limit value, recurrent in every simulation carried out, is probably due to the lack of some compound in the kinetic scheme, still under development, which could evaporate under more aggressive conditions [23].

3.2.2. Comparison with isothermal data

Although isothermal experiments are more difficult to carry out than thermogravimetric measurements, they can be another excellent tool for validating kinetic models. The first reference found regarding isothermal degradation experiments is the aforementioned work by Das *et al.* [27], where isothermal analyses were carried out at four different pyrolysis temperatures (325, 350, 375, and 400 °C) with a holding time of 480 min. The maximum possible heating rate (100°C/min) was chosen to reach the desired temperature with less induction period so that the weight loss during the non-isothermal step can be neglected as the heating time is very less compared to the isothermal holding time.

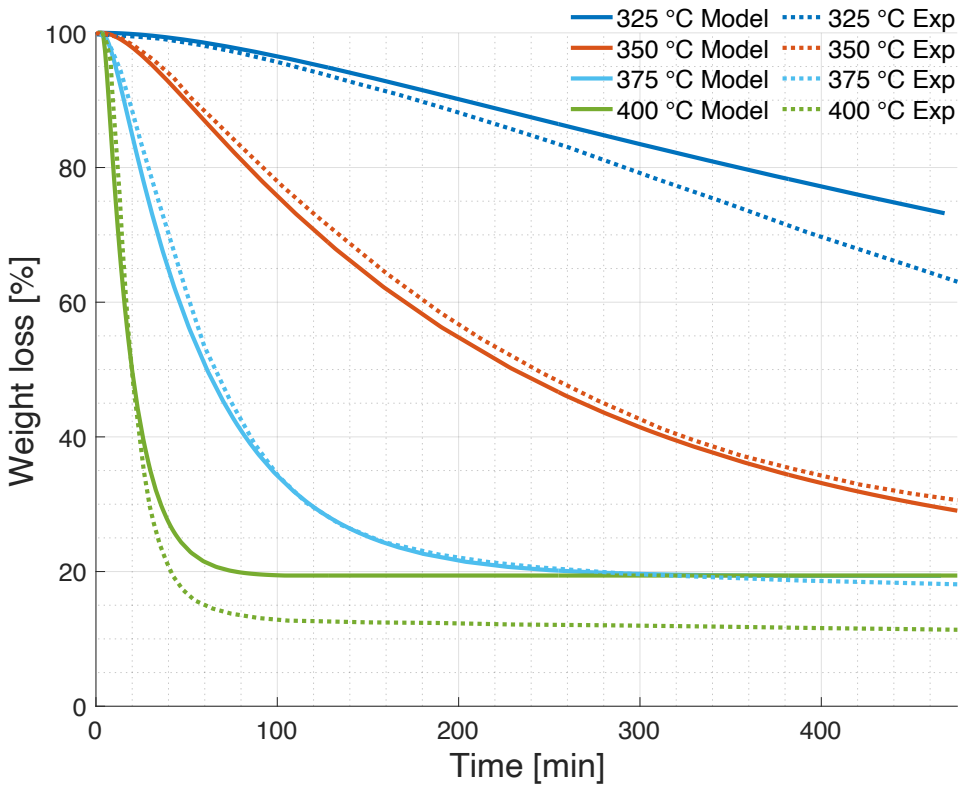

Fig. 3.10 Degradation of PET in isothermal conditions: comparison between the model and the experimental data by Das *et al.* [27].

Fig. 3.10 shows the validation of the isothermal tests carried out by Das *et al.* [27] at different pyrolysis temperatures. As for the previous thermogravimetric tests, the quality of the prediction of the model is confirmed, although there is a not negligible discrepancy concerning the isothermal test at 325 °C and 400 °C, where the error gradually increases with the pyrolysis time. Indeed, at low temperature (325 °C), incomplete conversion of PET led to a final residue mass of ~63% of the initial sample weight for the experimental results and ~73% for the model results, whereas, at high isothermal temperature (400 °C), the residue mass reached ~11% for the experimental results and ~20% for the model results. On the contrary, the results obtained from comparing the model with the work carried out by Osman *et al.* [29] present a more particular trend, where the isothermal tests are reported in the form of reaction progress in the function of the pyrolysis time. The results obtained are shown in Fig. 3.11.

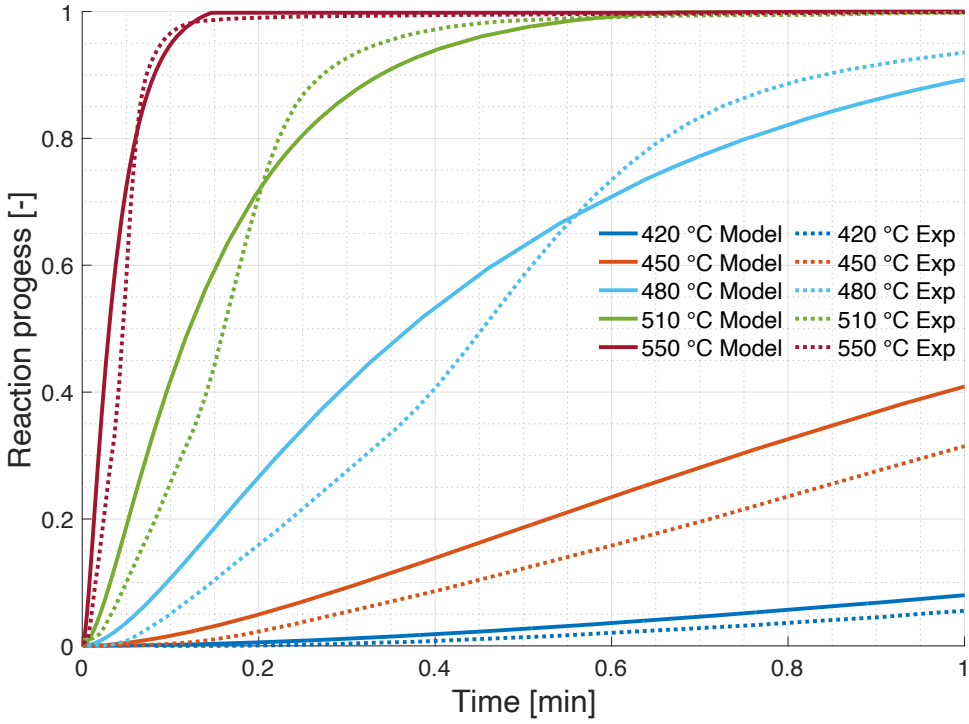

Fig. 3.11 Degradation of PET in isothermal conditions: comparison between the model and the experimental data by Osman *et al.* [29].

Fig. 3.11 shows that, at pyrolysis temperatures of 510 °C and above, the reaction reaches completion (i.e. reaction progress equal to 1) even with a short timeframe of 1 min. This rapid decomposition indicates that these temperatures would be ideal for rapid conversion. However, at temperatures of 480 °C and lower, the reaction progress does not reach unitary values after the first minute. Although with some differences, the model follows the same trend as the experimental results.

3.2.3. Comparison with detailed data on product distribution

Results related to the distribution of the products obtained from the model are compared with the experimental ones thanks to different works found in the literature.

A first comparison was possible thanks to the experiments conducted by Singh *et al.* [26], where the effect of operating temperature on the product yield is investigated by non-isothermal heating. Non-catalytic thermal pyrolysis of waste PET was carried out in a semi-

batch reactor with a nitrogen atmosphere at five different temperatures (400, 450, 500, 550, and 600 °C), where the sample was heated from room temperature to the desired temperature at 20 °C/min, and isothermal conditions were maintained thereafter. The results obtained are shown in Fig. 3.12.

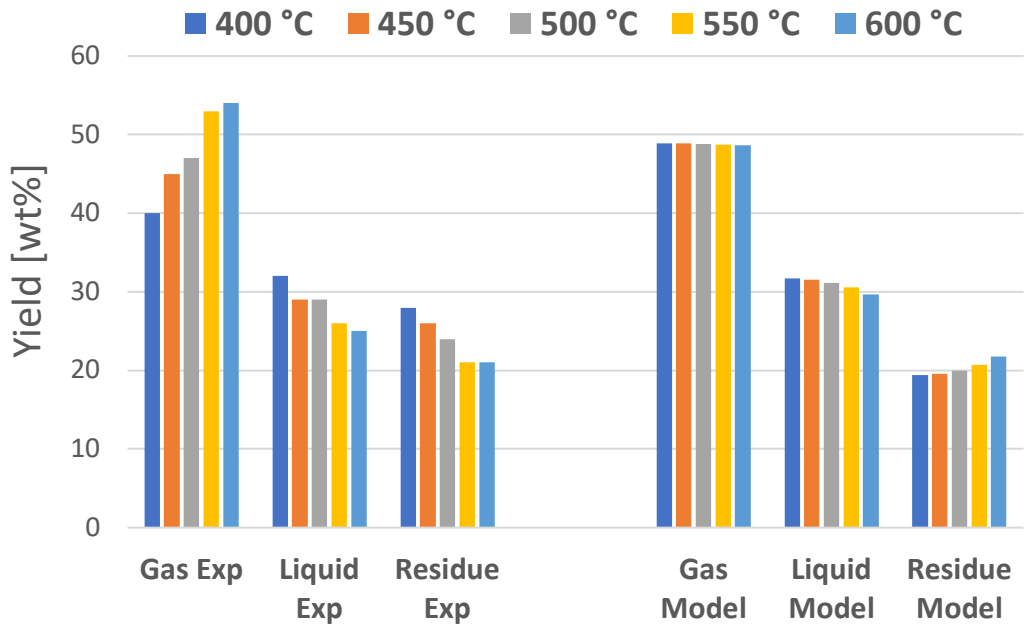

Fig. 3.12 Comparison of the model results (right) with the distribution of the products obtained by Singh *et al.* [26] (left) at different temperatures.

As seen from the figure, both the model and experimental results show the same behavior. Indeed, the yield of gas released is higher than the yield of liquid, which is higher than the residue yield. However, during the pyrolysis of waste PET, experimentally, the yield of gas increases with the increase of operating temperature, while the liquid yield and the residue decrease. On the contrary, the results obtained from the model show that the gas yield is approximately constant with the temperature, while the liquid yield decreases, and the residue increases with the rise in the operating temperature. In fact, the bigger differences are found with the residue fraction, where the results show an opposite trend between them. Another comparison was possible thanks to the work carried out by Dhahak *et al.* [28], where the slow pyrolysis of PET was investigated over a range of final temperatures from

410 °C to 480 °C. The experiments were performed at the early stages of the decomposition of PET to minimize the secondary reactions in the gas phase that could occur at high pyrolysis temperature. The work aimed to provide a thermal dependent evolution profile for the product distribution and the partial quantification of the gas and waxy products.

The slow pyrolysis of PET was performed in a horizontal tubular reactor with a heating rate of 5 °C/min, where the sample was heated up to various final temperatures (410, 430, 450, and 480 °C) with a holding time of 120, 90, 60 and 60 min, respectively. At the end of the pyrolysis, two types of products were recovered: a solid residue that remained in the sample holder and condensable waxy products recovered with two condensers and a filter. For each experiment, the sample holder, the condensers, the filter, and the connections were weighed before and after the pyrolysis. Then, the yields of solid residue and waxy products (in the condensers, filter, and connections) were calculated by dividing the mass of the products by the initial mass of PET, whereas the yield of gas was determined by difference [28]. The results obtained are shown in Fig. 3.13.

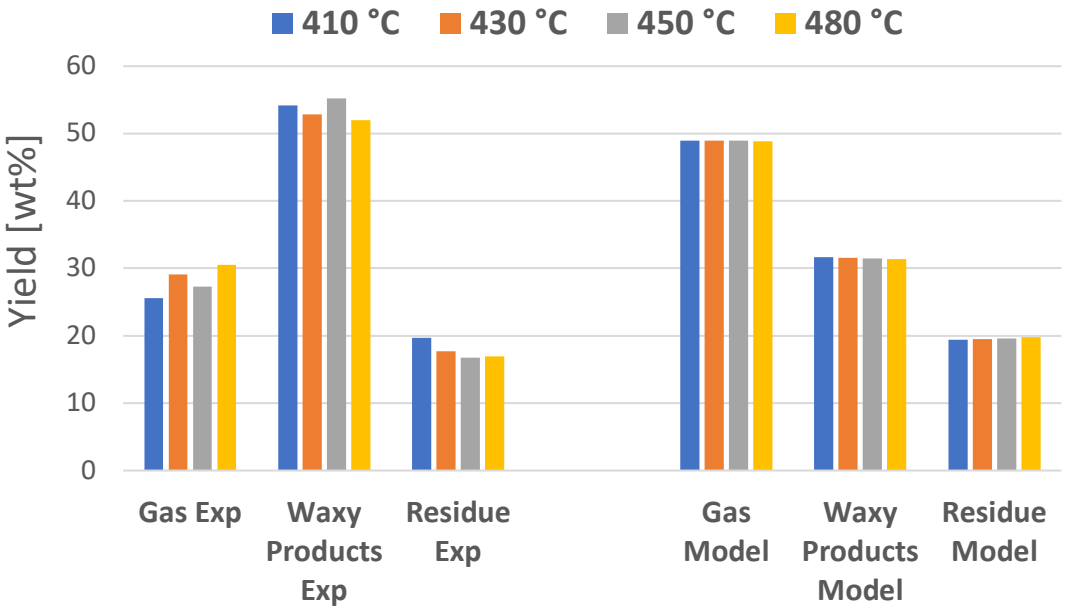

Fig. 3.13 Comparison of the model results (right) with the distribution of the products obtained by Dhahak *et al.* [28] (left) at different temperatures.

The comparison of the product yield of PET pyrolysis is shown in Fig. 3.13. No significant effect is observed in the product yield when the final temperature increases from 410 °C to 480 °C, especially for the model results. This could be due to the small range of final temperature studied and the short residence time of gases in the experimental setup, which is ~3 seconds. The experimental residue yield decreases slightly with the temperature, while the residue fraction obtained from the model shows a slight increase with the temperature. However, the greatest difference is related to the waxy fraction, where the amount of this fraction obtained experimentally is much larger than the one obtained from the model at each temperature. This could be due to the larger gas fraction predicted by the model with respect to the experimental one.

From the work carried out by Dhahak *et al.* [28], it was also possible to compare the experimental data concerning the characterization of pyrolysis gaseous products with the results obtained from the model. The results are shown in Fig. 3.14 and 3.15.

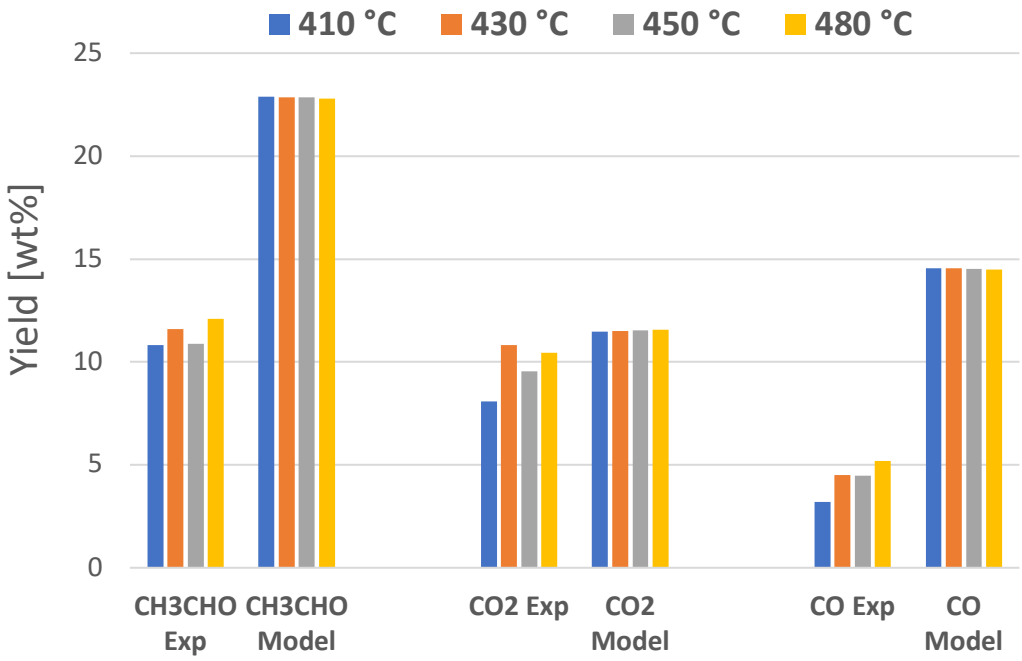

Fig. 3.14 Yields of gas at various temperatures: comparison between the model and the experimental data by Dhahak *et al.* [28].

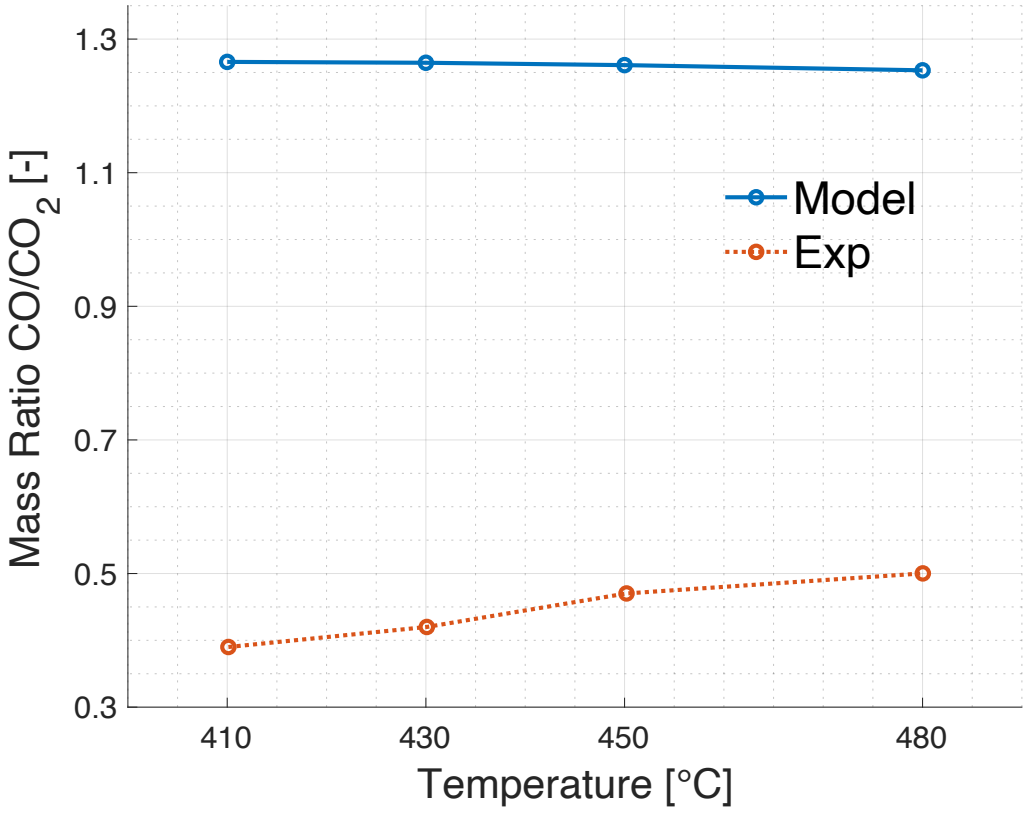

Fig. 3.15 Evolution of mass ratio CO/CO_2 as a function of final temperature: comparison between the model and the experimental data by Dhahak *et al.* [28].

In Fig. 3.14 is shown the yield of the main species that make up the gas fraction at various temperatures. As expected, the gas fraction contains mainly acetaldehyde, CO_2, and CO, but the results seem to be independent from the temperature, especially for the model. As said before, this could be due to the small range of final temperature studied. Moreover, the quantity of acetaldehyde predicted by the model is much larger than the one experimentally measured. However, the major difference between the model and the experimental data lies in the fact that the model predicts a larger final CO content, while a larger amount of CO_2 is obtained experimentally.

Experimentally, also a smaller extent of ethylene (C_2H_4) and benzene (C_6H_6) are detected, but these last two compounds are predicted by the model in negligible quantities. Indeed, increasing the temperature would promote benzene emission, but this is not predicted by

the model, where the amount of benzene formed is negligible at any temperature considered. On the contrary, benzene yield obtained experimentally increases from ~0.06 wt% at 410 °C to ~0.23 wt% at 480 °C [28]. This confirms the existence of reactions favoring the production of this compound in the whole pyrolysis temperature range that are not considered by the model.

The CO/CO_2 mass ratio is calculated and presented in Fig. 3.15. Experimentally, the ratio increases with the temperature from ~0.39 at 410 °C to ~0.5 at 480 °C, and an almost linear relationship between the CO/CO_2 ratio and the final operating temperature is shown. This highlights that the production of CO_2 is about two times larger than CO. An opposite trend is found from the model, where the quantity of CO is always higher than the quantity of CO_2 released. Moreover, the CO/CO_2 ratio shows a trend that is approximately constant with temperature.

Finally, the last comparison was possible thanks to the work carried out by Artetxe *et al.* [30], where the influence of temperature in the product distribution of PET pyrolysis was studied under isothermal conditions in the range of 500-600 °C.

In these experiments, a conical spouted-bed reactor has been used for the pyrolysis of PET, which consists of a lower conical section and an upper cylindrical section. Spouted beds with fully conical geometry combine the features of cylindrical spouted beds (such as the capacity for handling bigger particles, small pressure drop, cyclic movement of the particles, and so on) with those inherent to their geometry, such as stable operation in a wide range of gas flowrates. This versatility in the gas flow rate allows for handling particles of irregular texture, fine particles, wide size distribution, and sticky solids, whose treatment is difficult, avoiding their agglomeration [30].

The residence time inside the reactor was identified by means of the ratio between the bed height (or bed weight, W_{bed}) and the PET feed rate (Q_{PET}). Since the experimental

conditions used were $W_{bed} = 100\ g$ and $Q_{PET} = 1.5\ g/min$, a residence time of $W_{bed}/Q_{PET} = 4000\ s$ was obtained, i.e. about 1 hour. So, the experiments have been performed for 1 hour at three different isothermal temperatures (500, 550, and 600 °C), with a continuous PET feed rate of 1.5 g/min and under suitable operating conditions in order to avoid defluidization of the sample. Indeed, PET pyrolysis presents a significant risk of defluidization in fluidized bed reactors, caused by agglomerates formation. For this reason, a high nitrogen flowrate of 28 l/min was used, ensuring a good mixing in the bed too. The N_2 flow rate is twice the minimum required to maintain fluidization conditions. This led to a more vigorous movement of the particles and a better heat transfer within the PET particles (minimizing the temperature gradient within the particle itself), thus avoiding the bed defluidization. Furthermore, the authors mentioned that this type of reactor is suitable for PET pyrolysis due to its excellent performance, especially concerning heat transfer rates. Fig 3.16 shows the results obtained from the comparison between the experimental results and the model simulations.

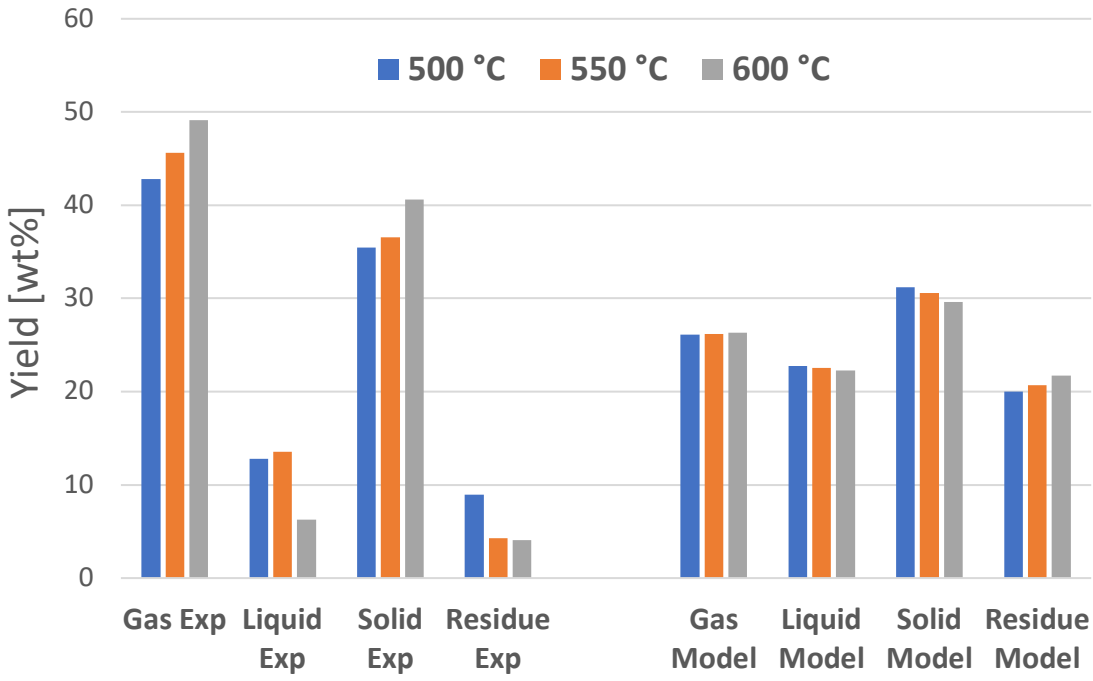

Fig. 3.16 Comparison of the model results (right) with the distribution of the products obtained by Artetxe *et al.* [30] (left) at different temperatures.

In the experiments carried out by Artetxe *et al.* [30], the pyrolysis products have been divided into four different groups: gas fraction, liquid fraction, solid fraction, and solid residue remaining in the reactor. The appearance of the solid is that of a whitish powder, mainly composed of organic acids such as benzoic acid, that is present in the form of crystals. Instead, the gas fraction obtained in these experiments is less than usual since the acetaldehyde is considered in the liquid fraction rather than the gaseous one. So, the same is also considered in the simulations in order to compare the results.

The effect of temperature on the yield of the different groups is shown in Fig. 3.16. In both cases, the main products obtained at each temperature are the gas fraction (mainly carbon monoxide and carbon dioxide) and the solid fraction, even if the quantity of these two fractions is larger in the experimental results. On the contrary, the liquid and the residue yields represent a much smaller fraction in both cases, especially in the experimental results. Experimentally, the increase in temperature leads to an evident increase in the gas fraction, which is due to the more severe thermal cracking [30], but this is not so evident by the model results. Moreover, a reduction is experimentally observed in the solid residue from ~7% at 500 °C to ~2% at 600 °C, while the residue fraction obtained from the simulations increases with the temperature. Finally, the yield of solid fraction experimentally obtained is hardly affected by temperature, showing a slight increase when the temperature is increased up to 600 °C. On the contrary, the solid fraction obtained from the model shows the opposite trend, decreasing its value with an increase in the temperature.

From the work carried out by Artetxe *et al.* [30], it is also possible to observe the comparison of CO and CO_2 released, shown in Fig. 3.17.

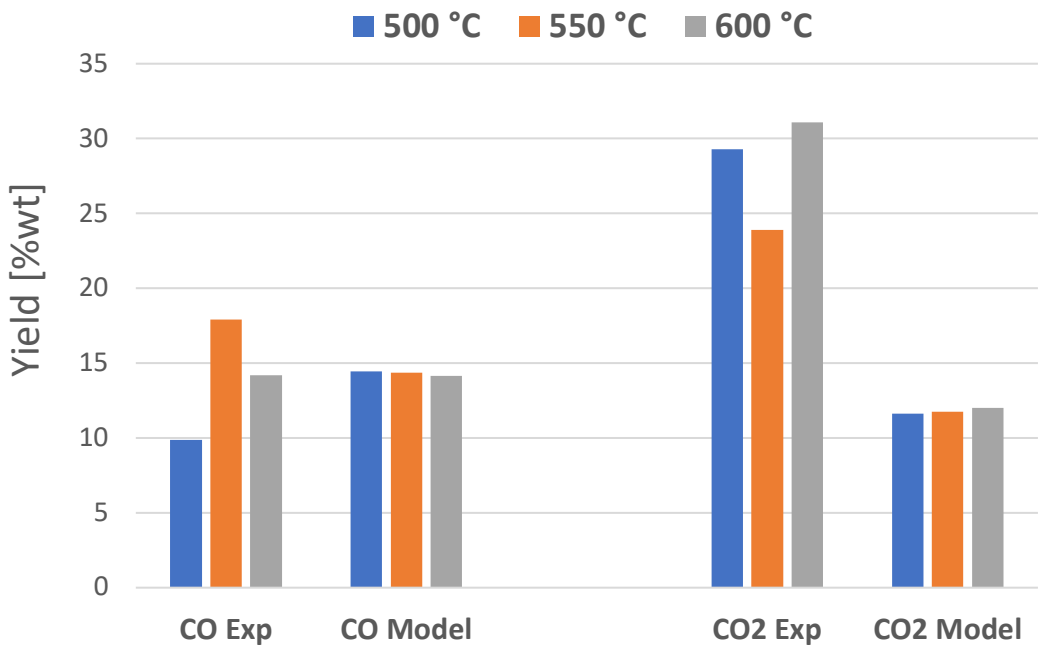

Fig. 3.17 Yields of gas at various temperatures: comparison between the model and the experimental data by Artetxe *et al.* [30].

Carbon monoxide and carbon dioxide represent the main components in the gas fraction, accounting for ~45% of product yield at 600 °C experimentally (the yield of all the gas fraction at the same temperature is ~49%, Fig. 3.16).

As already highlighted in the works carried out by Dhahak *et al.*, the major difference between the model and the experimental data lies in the fact that the model predicts a larger final CO content, while a larger amount of CO_2 is obtained experimentally.

Regarding the liquid and solid fraction, the yields of acetaldehyde and benzoic acid (the main compounds of these fractions) obtained at the three temperatures studied by Artetxe *et al.* are shown in Fig. 3.18 and Fig. 3.19, respectively.

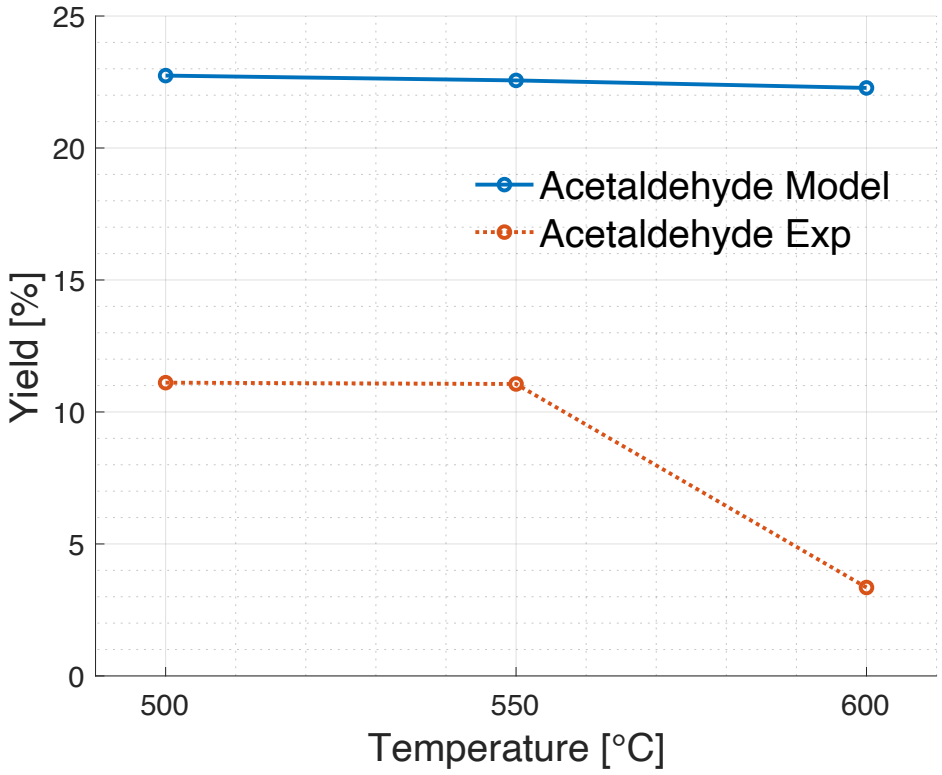

Fig. 3.18 Yields of acetaldehyde at various temperatures: comparison between the model and the experimental data by Artetxe *et al.* [30].

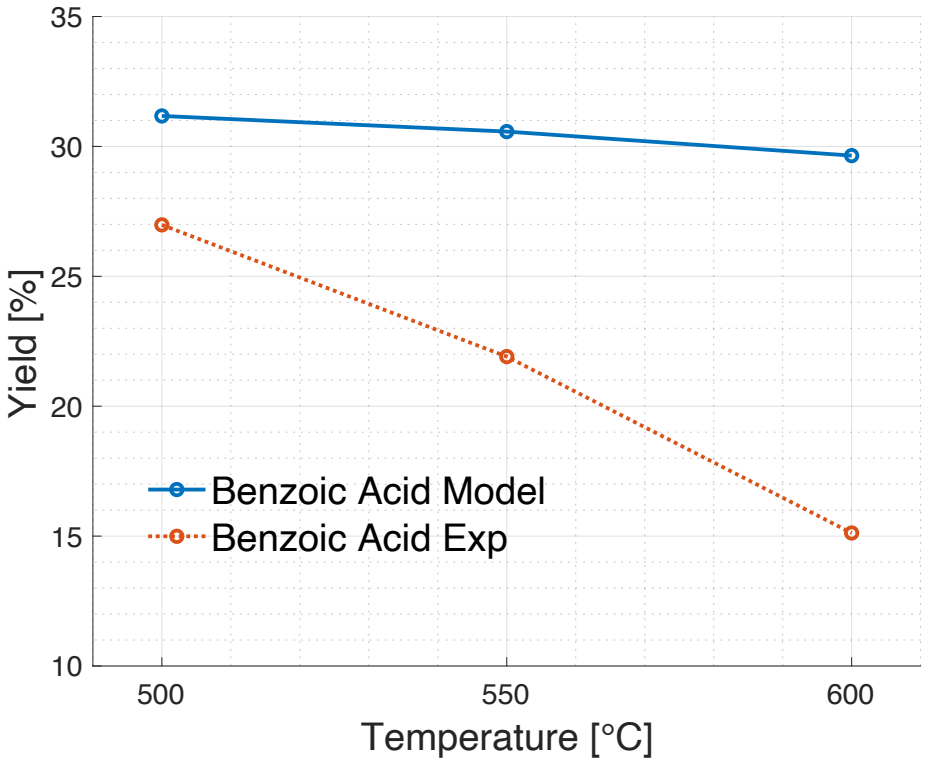

Fig. 3.19 Yields of benzoic acid at various temperatures: comparison between the model and the experimental data by Artetxe *et al.* [30].

Fig. 3.18 shows that, experimentally, the acetaldehyde yield remains approximately constant when the temperature is increased from 500 °C to 550 °C. However, it decreases considerably when a temperature of 600 °C is reached since the acetaldehyde yield undergoes a severe reduction because of thermal cracking [30]. This is not true in the model results, where the amount of acetaldehyde released remains approximately constant at each temperature. Moreover, the quantity of acetaldehyde obtained from the model is about double with respect to the one obtained experimentally.

The other main product in the pyrolysis of PET, apart from CO, CO_2, and acetaldehyde, is benzoic acid, whose experimental yield is reduced significantly when the temperature is increased to 600 °C, as shown in Fig 3.19. Indeed, at 600 °C, the pyrolysis process leads to wider product distribution in the solid fraction, which is composed of heavier products. This is due to the important effect of temperature on the cracking and secondary reactions [30]. The results obtained from the model predict the same trend, although with a less significant decrease with the temperature and a larger quantity of benzoic acid released than the experimental data, especially at 600 °C. The larger amount of benzoic acid obtained from the simulations may be due to the *lumped* approach on which the model is based. Indeed, the benzoic acid is not considered a single compound but a *pseudo-species* representative of a group of different compounds.

3.3. Final considerations

The work presented in these two last chapters consists of an analysis of the kinetic model developed by the CRECK Modeling Lab for the thermal degradation of neat PVC and PET. After a first and brief presentation of the kinetic models used for the simulations, the attention was then shifted to the comparison with the experimental data found in the literature.

Overall, the results obtained in these chapters allowed further to confirm the good predictions and reliability of the model, even if more significant deviations are observed, especially concerning the composition of the gases released during the process, which are not always in agreement with the experimental data.

The PVC model results in good agreement with the experimental data, especially in terms of TGA curves. However, minor deviations are noted in the onset points of the two degradation steps. The model provides a good prediction also in terms of product distribution, except for polyaromatic hydrocarbon compounds (PAHs).

The PET model also shows a good agreement with the experimental data, especially regarding the TGA curves, where the model can predict the onset point of the degradation very accurately. However, the model does not satisfy the actual fraction of residue at the end of the degradation, always overestimating it. Overall, the product distribution obtained from the model is in good agreement also with the experimental data. However, the model predicts a higher final CO content than CO_2, resulting in the opposite trend with respect to the experimental data. Furthermore, the release of small quantities of benzene during the experiments is observed, but the kinetic model predicts the formation of a negligible amount of this product.

After these last considerations, it is now possible to move on to the discussion of PVC-PET plastic mixtures degradation, which will be the subject of the last chapter.

Chapter 4

4. PVC and PET mixtures

This last chapter is dedicated to a sensitivity analysis of the model regarding plastic mixtures of PVC and PET. First of all, the interactions existing between these two polymers that are implemented in the process simulator will be described. After that, an analysis of the model will be carried out in order to verify the influence of the initial PVC-PET mixture composition and the operating conditions, in terms of pyrolysis temperature and heating rate, on the degradation of the sample and products distribution.

4.1. Interactions between PVC and PET

4.1.1. Polyvinyl mixtures

The treatment of complex mixtures of plastic waste, such as the *plasmix*, requires, first of all, an understanding of the behavior of the polymers subjected to mixing, and the knowledge of the possible variables that characterize a mixture, such as the composition, the mixing properties, and the practical procedures through which it is obtained (grinding, etc.). For this purpose, following the development of kinetic models for single polymers and the respective thermogravimetric and product distribution measurements for its validation (*Chapter 2* and *Chapter 3*), the approach will be extended to the analysis of binary mixtures, focusing on binary PVC-PET blends, that will be the subject of this last

chapter. This analysis is aimed at identifying and understanding the interactions between the two polymers.

The chemical treatment of plastic waste involves a preliminary mechanical grinding phase, followed by a heating and a thermal treatment phase through pyrolysis or gasification. Due to the low diffusivity and solubility of polyvinyl polymers (such as PE, PP, PS, PVC) in the liquid phase, it is evident that mechanical grinding cannot achieve mixing at the molecular level in this phase. The net result is that the radicals and intermediate species formed by the thermal degradation of one of the two polymers cannot effectively diffuse within the other component, catalyzing its degradation. Therefore, the degradation of vinyl polymers mixtures could be described by a linear combination of the mixture components. Referring to the more general case, to verify the possible non-linear nature of polymer mixtures during their thermal degradation, Faravelli and *et al.* [20] report three types of approach referring to a binary mixture of PE and PS, but extendable to all the types of plastic mixtures:

- the completely segregated model (CSM), which represents the simplest approach to reproduce the behavior of polymer mixtures. This model describes the behavior of the mixture as a linear combination of the results coming from the degradation of the two single polymers;
- the completely mixed model (CMM), which assumes the existence of a single melt phase with a mixture composition that is homogeneous and perfectly mixed, where the radicals coming from PE and PS can attack both the components of the mixture;
- the two-phase model (TPM), an intermediate approach between the first two models described, which assumes that the binary mixture is a system consisting of two completely separated liquid phases, one rich in one polymer and one rich in the other one. The composition of each of these two phases is evaluated based on the

mutual solubility of the two polymers, and the radicals generated in each of the two phases are only active inside their phase.

In the models described, from a kinetic point of view, the interactions between the polymers within the mixture occur only through H-abstractions reactions, as reactions such as cross-linking and branching reaction would lead to the formation of species (such as polyaromatic hydrocarbons and residual char) which are not experimentally observed in the pure polymer degradation. These observations confirm the hypothesis of the negligibility of these interactions.

As discussed in the work carried out by Faravelli *et al.* [20], the most rigorous approach would consist in the use of a two-phase model (TPM), subject to a more accurate estimate of the mutual solubility of the components of the mixture. However, its derivation is quite difficult and unreliable. Therefore, the CSM model represents a tool for studying the thermal degradation of plastic mixtures that provides simplicity and robustness with a good predictive capacity.

4.1.2. PVC-PET mixtures

The assumptions underlying the CSM approach are valid for PVC and vinyl polymers (PE, PP, PS) mixtures, but not for PVC and PET blends [23]. In fact, unlike the mixtures between polyvinyl polymers, the mixtures between PVC and PET show an inexplicable behavior using a completely segregated model, suggesting a possible existence of interactions between these two polymers.

Fig. 4.1 shows the thermogravimetric analysis of neat PVC and PET and their mixture (50:50 wt%) at 10 °C/min and 20 ml/min of nitrogen flowrate.

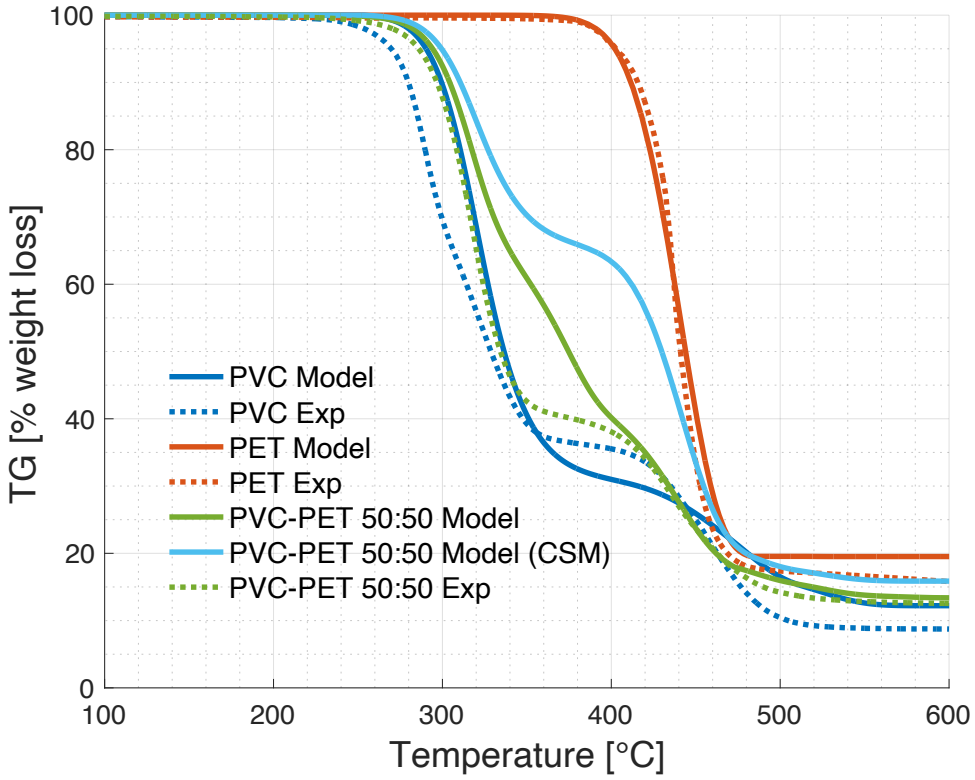

Fig. 4.1 Comparison between model and experimental TGA obtained by the Energy Department of Politecnico di Milano [31] for PVC-PET mixture (50:50 wt%) at 10 °C/min and 20 ml/min of nitrogen flowrate.

The figure highlights how, in the presence of PVC, the degradation of PET is strongly accelerated compared to the prediction of the CSM model (solid light blue line). A possible explanation for this behavior is the formation of mixtures between the two polymers favored by the presence of highly electronegative atoms that promote interactions between the chains [23]. However, the figure also highlights how the model that includes the interactions between the polymers (solid green line), despite some deviations, fits well with the experimental results, correctly capturing the temperatures of onset of degradation and the presence of inflections along the curve.

Due to these results, it has been assumed that the two polymers can be partially miscible together. Therefore, the kinetic model that describes their degradation must be considered coupled in order to be able to treat a liquid phase where both the monomers of PVC and

PET are present. To obtain this model, the kinetic mechanisms of PET and PVC were combined in a single model, and the reactions characterizing the possible interactions between them were added. In particular, abstraction reactions have been introduced between the radicals of PVC (especially the Cl radical) and the aliphatic structures of PET. Similarly, the possibility for the radicals of PET to abstract on the PVC chains was admitted.

The work carried out in this chapter includes the presentation of different combinations of PVC and PET mixtures, focusing on the influence of the operating conditions (such as heating rate and final pyrolysis temperature) on the thermogravimetric curves and the product distribution. Particular attention will also be paid to the influence of the initial PVC/PET ratio on the intensity of the iterations existing between these two compounds, comparing the results obtained from the model that considers these iterations with the CSM model.

4.2. Sensitivity analysis and comparison of model results

After validating the model for the neat polymers with the experimental data obtained in the literature (*Chapter 2* and *Chapter 3*) and the description of the iterations between PVC and PET, it is now possible to evaluate the effect of the operating conditions and the initial PVC-PET composition on the degradation process.

4.2.1. Thermogravimetric curves

This section is intended to show a sensitivity analysis of the model to the most important simulation variables, i.e. mixture composition and heating rate. If manipulated, each variable involves variations on the behavior of the simulated thermogravimetric curves, as shown in the following figures.

The main variable that determines the transformations of the analyzed mixtures is the temperature. It affects both the kinetics of reactions and thermodynamics. In fact, since the degradation of a polymer, instead of polymerization, is an overall endothermic process, it will be favored at higher temperatures [23]. The temperature can be kept constant (isothermal tests), or it can be varied over time (dynamic tests, TGA). In this last case, the heating rate is the parameter that determines the trend of the curves, establishing the evolution of the temperature over time.

Given the lack of experimental data in the literature about this specific mixture, it is interesting to examine how the model is affected depending on the heating rate and the sample initial composition.

First of all, Fig. 4.2, 4.3, and 4.4 show the comparison between the TGA coming from the model which considers the iterations between the two polymers in the mixture, and the TGA coming from the CSM model, which describes the behavior of the mixture as a linear combination of the results coming from the degradation of the two single polymers. Comparisons were made at different initial compositions of the PVC-PET mixture (20:80, 40:60, 60:40, and 80:20 wt%) and different heating rates (2, 5, and 10 ° C / min).

As already underlined above, the CSM approach allows the modeling of the thermogravimetric curve of a mixture through a simple linear combination of the TGA curves of the individual polymers.

Therefore, the predictions of the CSM model are reproduced using the following relationship:

$$m_{res,Mix}(T) = m_{res,PVC}(T)\, w_{PVC} + m_{res,PET}(T)\, w_{PET}$$

where w_{PVC} and w_{PET} are the massive fraction of PVC and PET, respectively.

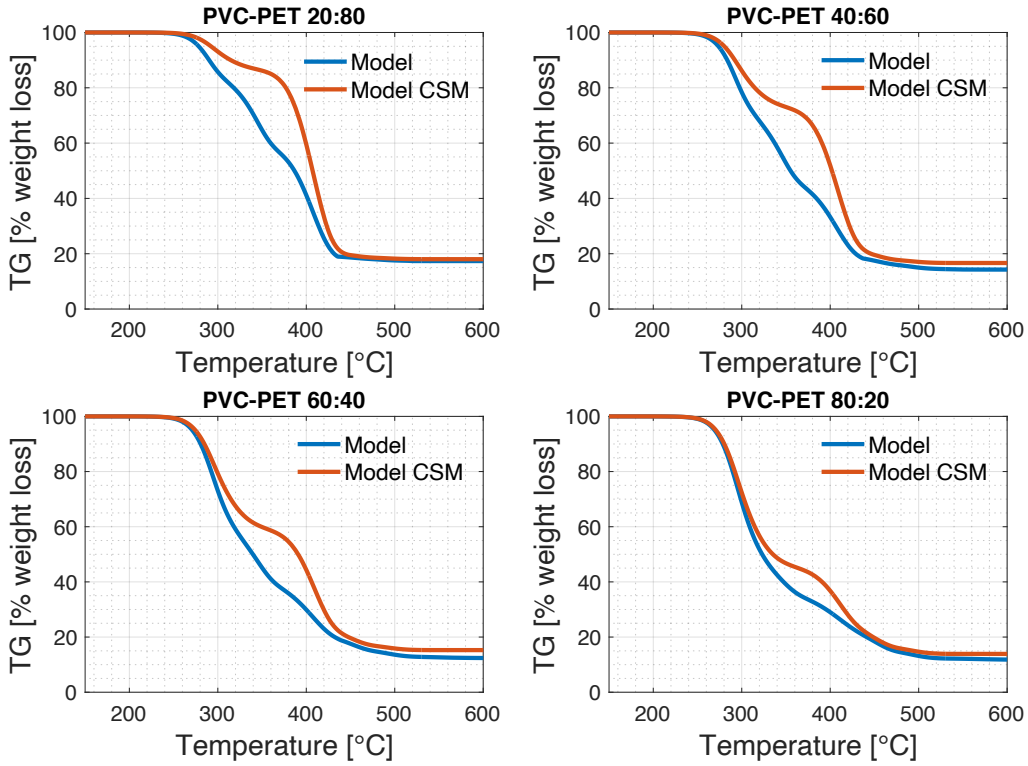

Fig. 4.2 Comparison between the model and the CSM model TGA of PVC-PET mixtures at 2 °C/min and different initial compositions.

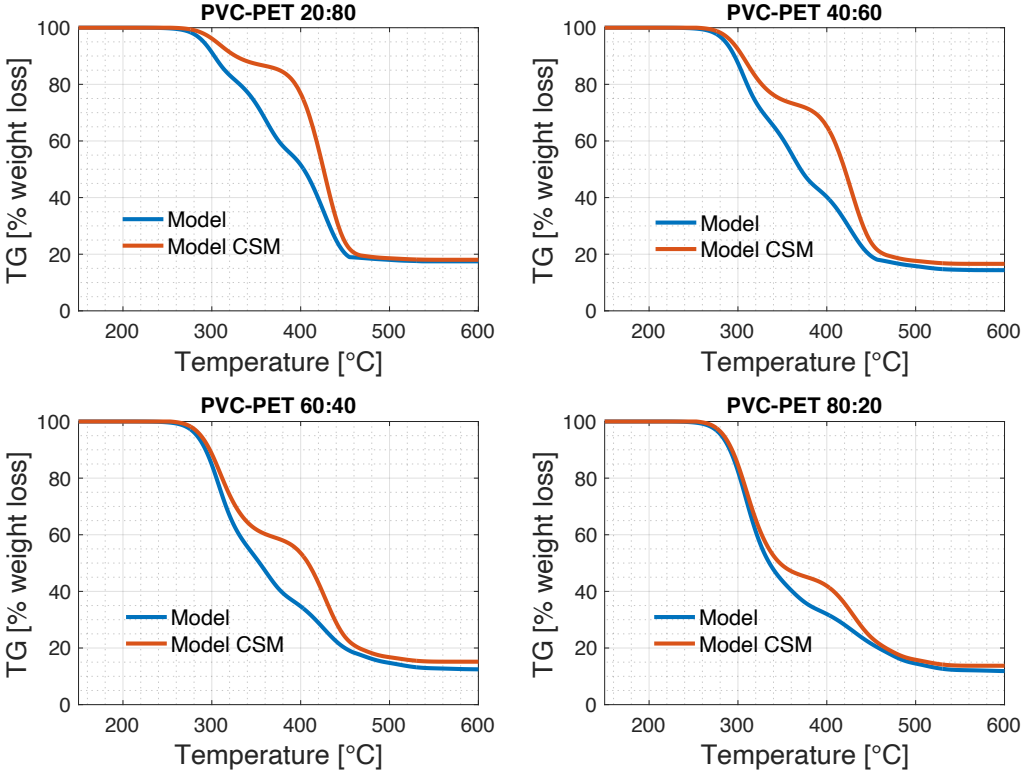

Fig. 4.3 Comparison between the model and the CSM model TGA of PVC-PET mixtures at 5 °C/min and different initial compositions.

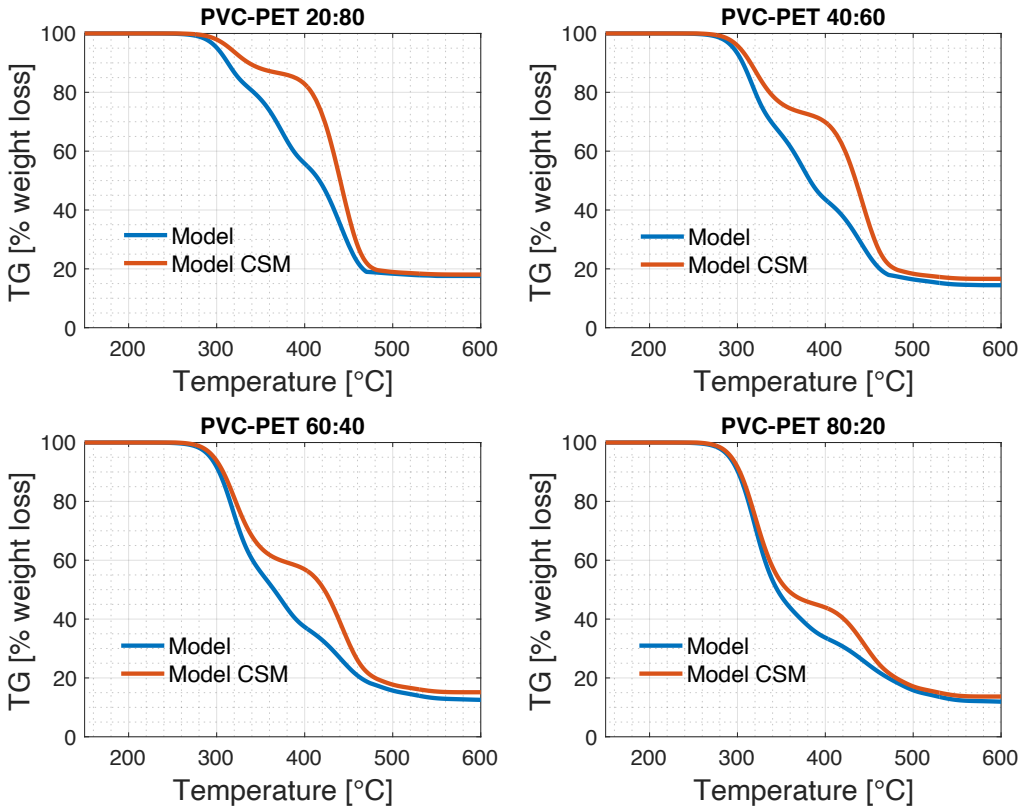

Fig. 4.4 Comparison between the model and the CSM model TGA of PVC-PET mixtures at 10 °C/min and different initial compositions.

The figures highlight how the degradation of the PVC-PET mixture predicted by the model (solid blue line) is strongly accelerated compared to the CSM model prediction (dashed orange line) at every operating condition under investigation. Moreover, the figures also show how the effect of the iterations between the two polymers is much more significant for mixtures composed mostly of PET (20:80 and 40:60 mixtures), while it becomes less evident for mixtures with a higher PVC content (60:40 and, above all, 80:20).

On the contrary, the intensity of the iterations between the two polymers does not show any particular influence with the heating rate, but only a slight translation of both the curves towards higher temperatures as the heating rate increases. From now on, only the coupled model will be used to carry out the simulations.

The effect of the heating rate on the model simulations is more evident in Fig.4.5, which shows the TGA of different PVC-PET mixtures at different heating rates (2, 5, 10 °C/min).

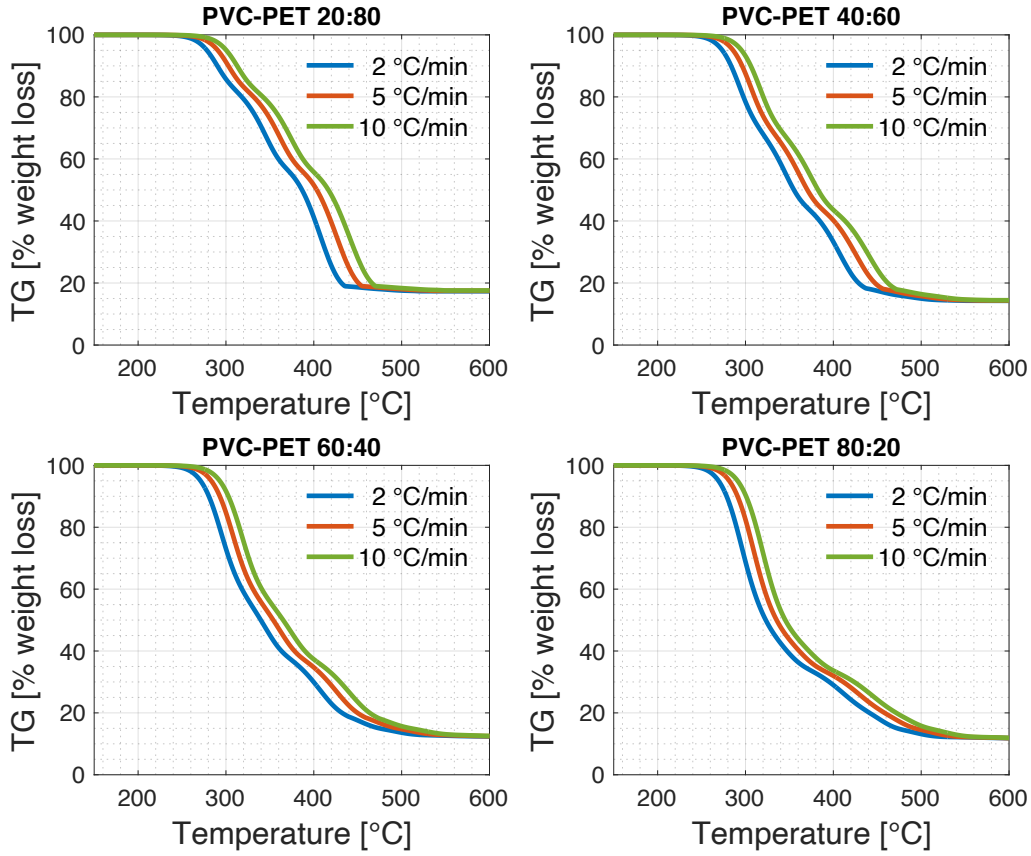

Fig. 4.5 TGA of PVC-PET mixtures at different heating rate (2, 5 and 10 °C/min) and different initial compositions.

Results obtained in Fig. 4.5 show better the translation of the degradation curves as the heating rate varies.

Finally, Fig. 4.6 shows the TGA of different PVC-PET mixtures at a heating rate of 10 °C/min. The results show the accelerating effect that the contamination of a more volatile polymer (such as PVC) has on the degradation process of a polymer that requires more extreme thermal conditions to volatilize (such as PET).

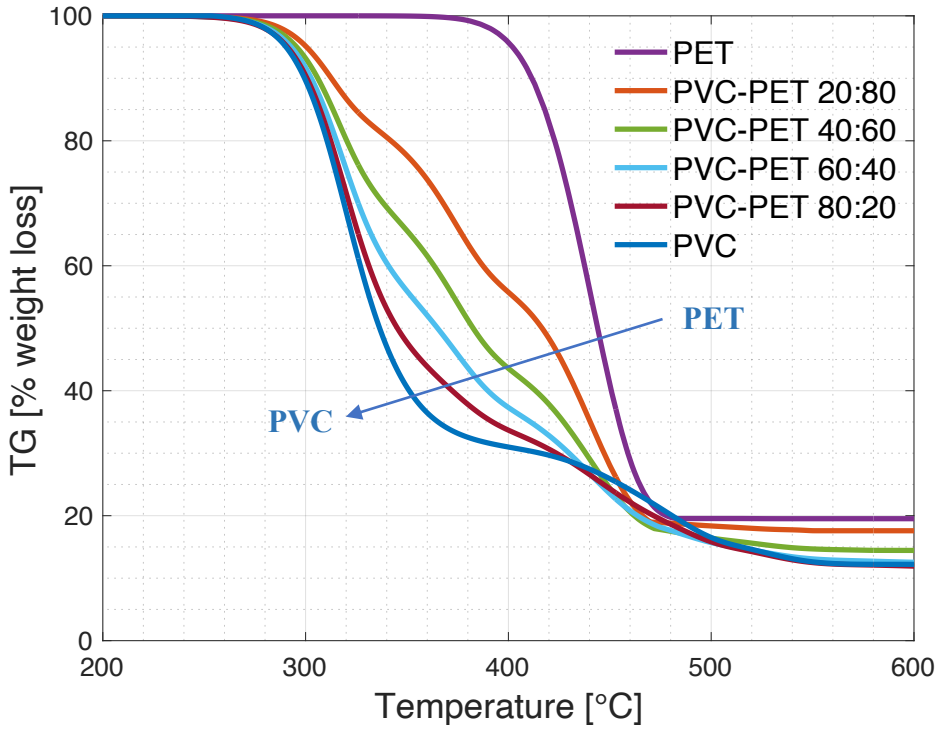

Fig. 4.6 TGA of PVC-PET mixtures at 10 °C/min and different initial compositions.

Fig. 4.6 shows how, in the initial phase of the thermal process, larger contamination of PVC in the initial sample results in a more significant acceleration of the degradation process than that of pure PET. In fact, comparing the temperatures at which a weight loss of 90% of the initial sample mass is reached, for pure PET, this value is reached at a temperature of ~410 °C, while for the mixture with 20% of PVC, this value becomes ~310 °C. This large gap of ~100 °C is equivalent to ~10 min with the simulated heating ramp (i.e. 10 °C/min).

However, after the initial phase, the mixture is strongly influenced by the resistance to volatilization of the PET, and the accelerating effect becomes less evident. In fact, this accelerating effect decreases over time and, once a weight loss of 50% of the initial sample is reached, the corresponding temperature for pure PET is ~445 °C, while for the mixture with 20% of PVC is ~415 °C, showing a difference of just 30 °C now (i.e. 3 min).

4.2.2. Evolution of volatile compounds

During the first phase of degradation, the main products released by the system are HCl and benzene (C_6H_6). Fig 4.7 shows the quantity of HCl and C_6H_6 released at a heating rate of 10 °C/min for different PVC-PET mixtures.

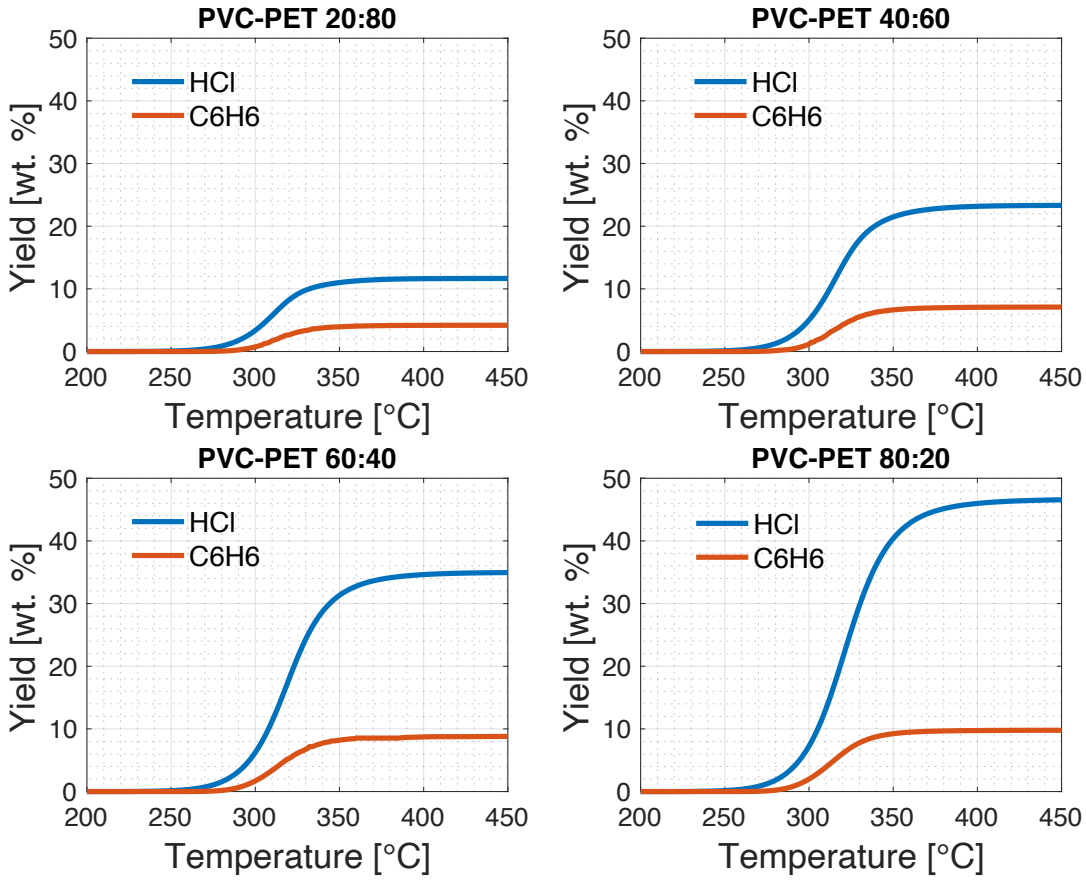

Fig. 4.7 Yield of HCl and C_6H_6 released from different PVC-PET mixtures at 10 °C/min.

Fig. 4.7 shows how, for both the compounds, the production begins at ~250 °C to ends before 350 °C (for mixtures with a lower PVC content, i.e. 20:80 and 40:60) and before 400 °C (for mixtures with a higher PVC content, i.e. 60:40 and 80:20). It is also possible to observe that, increasing the PVC content in the mixture, the yield of HCl and benzene considerably increase too, going from ~12% (HCl) and ~4% (C_6H_6) for a 20:80 PVC-PET mixture to ~47% (HCl) and ~10% (C_6H_6) for an 80:20 PVC-PET mixture.

This last consideration can also be observed in Fig. 4.8 and Fig. 4.9, which show the amount of HCl and benzene released at a heating rate of 10 °C/min for different PVC-PET mixtures.

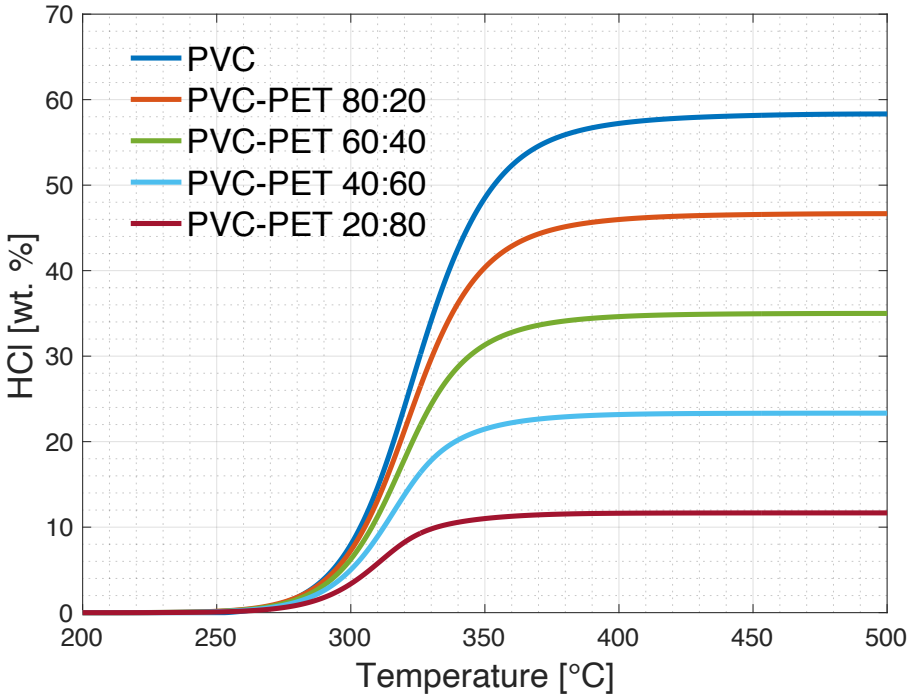

Fig. 4.8 HCl released from different PVC-PET mixtures (100:0, 80:20, 60:40, 40:60 and 20:80) at 10 °C/min.

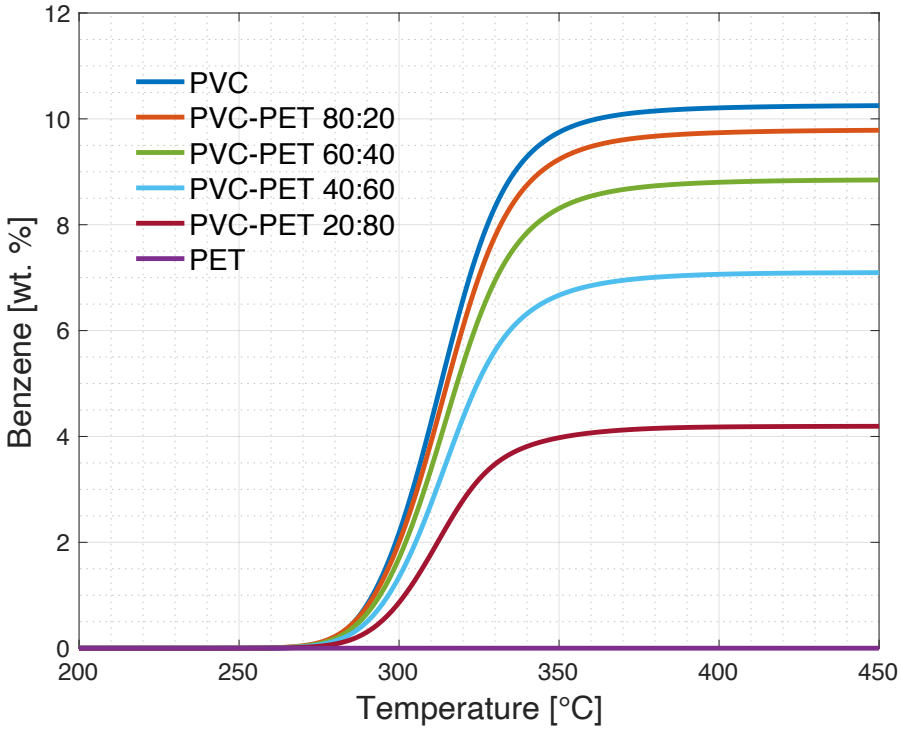

Fig. 4.9 Benzene released from different PVC-PET mixtures (100:0, 80:20, 60:40, 40:60, 20:80 and 0:100) at 10 °C/min.

In the case of benzene (Fig. 4.9), its emission curve is also reported for a sample of pure PET since the release of this compound is observed experimentally during the thermal degradation of this polymer, although in small quantities. However, as already highlighted in *Chapter 3*, the figure shows how the kinetic model of PET thermal degradation does not account for the release of benzene during the process.

Finally, the effect of the different heating rates on the quantity and rate of release of these two compounds can be observed. By performing the integration of the model at different heating rates, Fig.4.10 and Fig.4.11 are obtained. These figures show the yield of HCl and benzene, respectively, obtained at a heating rate of 2, 5, 10 °C/min for different PVC-PET mixtures.

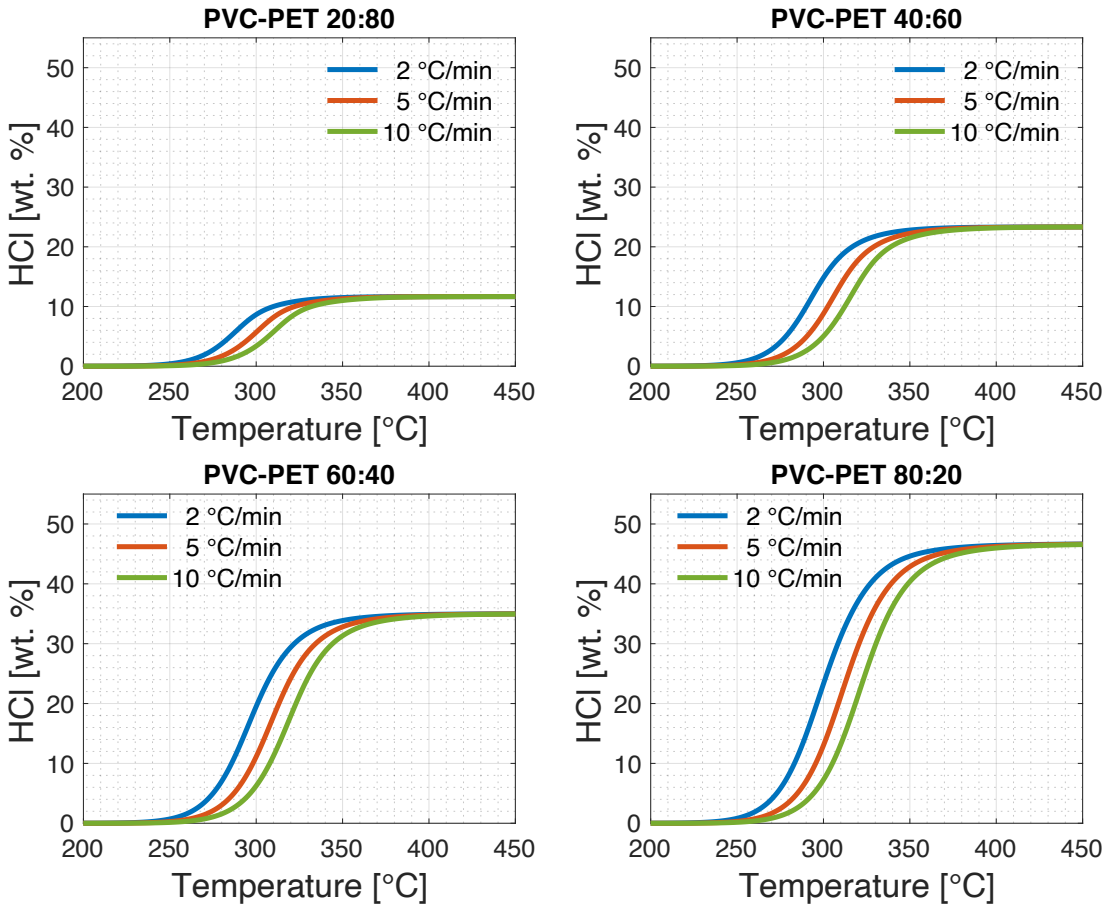

Fig. 4.10 HCl released from PVC-PET mixtures at different heating rate (2, 5 and 10 °C/min) and different initial compositions.

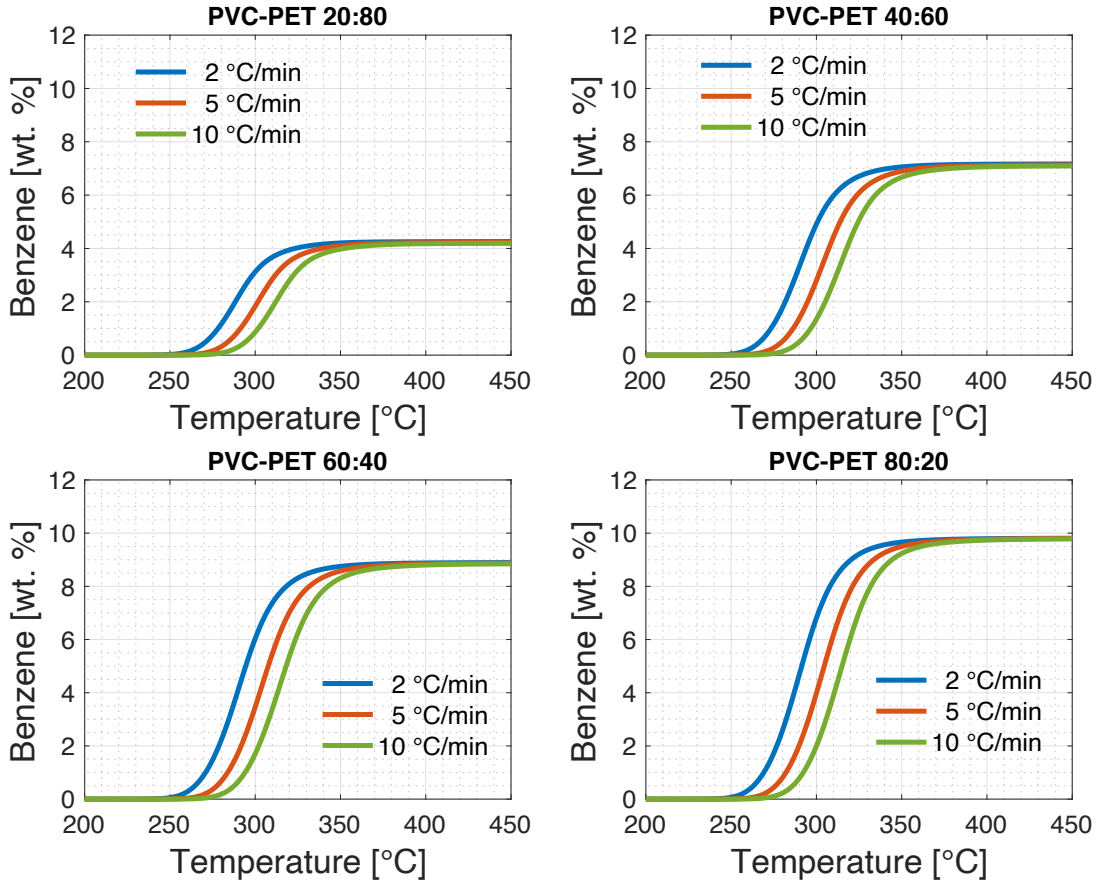

Fig. 4.11 Benzene released from PVC-PET mixtures at different heating rate (2, 5 and 10 °C/min) and different initial compositions.

As shown in Fig. 4.10, for a given initial composition of the mixture, the total amount of HCl released is always about the same as the heating rate varies. This is in accordance with the experimental data that provide for a very low amount of chlorinated compounds. However, the increase in the heating rate involves a translation of the curves toward higher temperatures (as already observed for the TGA curves), resulting in a delay in the development of HCl. In fact, by way of example, for the 40:60 PVC-PET mixture, the temperature for which 95% of the total mass of HCl is released in the gaseous phase is ~335 °C at 2 °C/min, ~350 °C at 5 °C/min and ~360 °C at 10 °C/min.

The formation of benzene was linked to the degree of chlorination of the system in the kinetic model. Therefore, the behavior at different heating rates is similar to that observed for the HCl, although the benzene is present in smaller quantities (Fig. 4.11).

Finally, even in these two last cases, it is observed that increasing the PVC content in the mixture, the yield of HCl and benzene considerably increases too.

Once the first phase of degradation is over, the main products released by the system are now CO, CO_2, acetaldehyde, and benzoic acid, whose production is delayed by ~50 °C compared to the compounds described previously (whose production started at ~250 °C). These products are characteristic of PET thermal degradation, which, being PET less volatile than PVC, requires more extreme thermal conditions to volatilize.

Fig. 4.12 shows what has just been highlighted, showing the quantity of CO and CO_2 released at 10 °C/min for different PVC-PET mixtures.

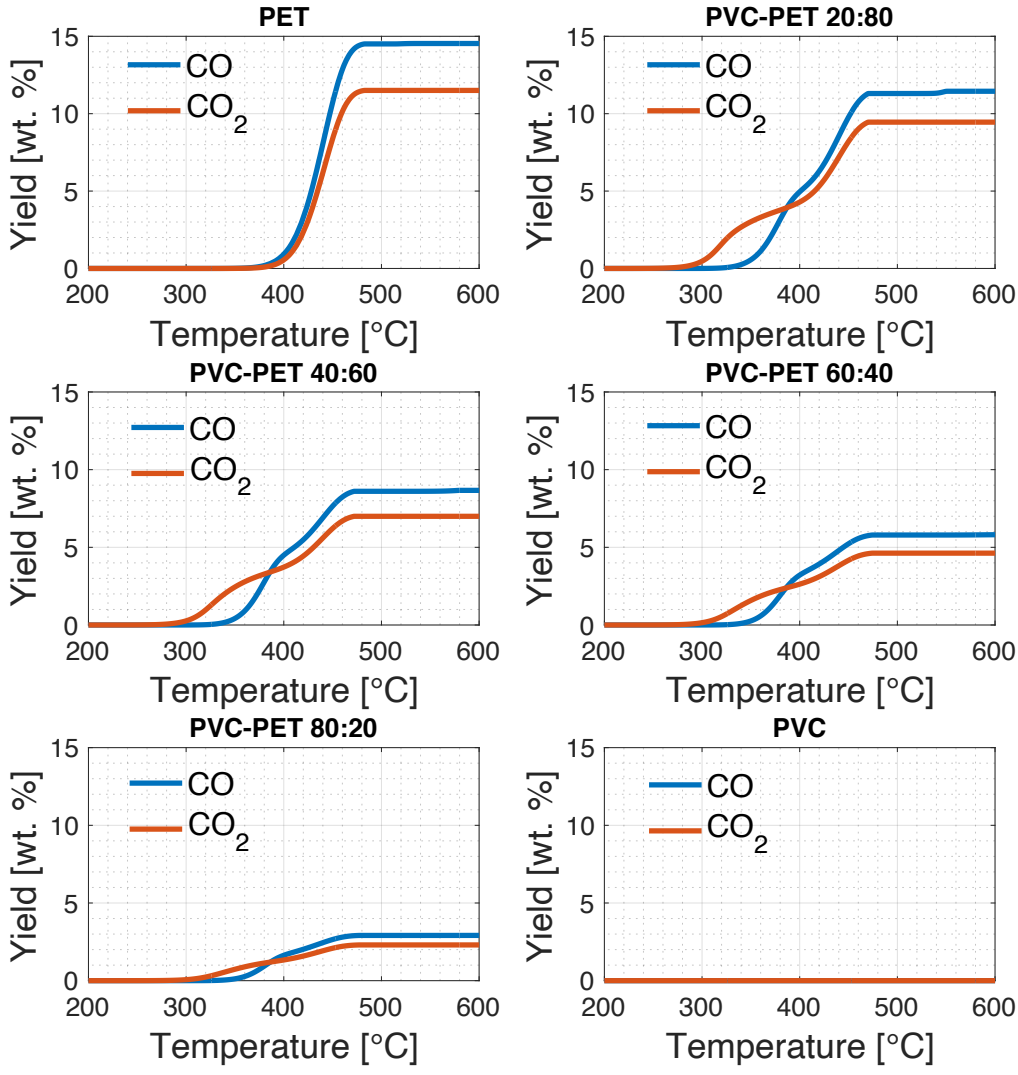

Fig. 4.12 Yield of CO and CO_2 released from different PVC-PET mixtures at 10 °C/min.

Fig.4.12 shows how, in all the mixtures considered, the production of CO_2 begins at temperatures of ~300 °C, while the production of CO results to be delayed, starting at ~350 °C. After that, the production of both the compounds stops simultaneously at ~470°C. On the other hand, the case of pure PET appears to have slightly different behavior, where the CO and CO_2 production begins and ends simultaneously at higher temperatures than the ones observed in the case of mixture. Furthermore, this latter case does not show changes in the behavior for the two compounds analyzed, where the amount of CO is always larger than that of CO_2 at all temperatures.

Finally, it is also possible to observe that, by decreasing the PET content in the mixture, the yield of CO and CO_2 decreases considerably too, going from a maximum of ~15% (CO) and ~12% (CO_2) in the case of pure PET up to vanish completely in the case of pure PVC.

Fig. 4.13 shows, instead, the quantity of acetaldehyde and benzoic acid released at 10 °C/min for different PVC-PET mixtures. In this case, Fig. 4.13 shows that the acetaldehyde and benzoic acid production begins and ends simultaneously at temperatures of ~350 °C and ~470 °C, respectively, for all the mixtures considered. However, the case of pure PET shows slightly different behavior, where the production of the two compounds begins at higher temperatures, presenting a delay of ~50 °C compared to the case of the mixture.

Finally, it is once again possible to observe how, by decreasing the PET content in the mixture, the yield of the two compounds also decreases considerably, passing from a maximum of ~32% (benzoic acid) and ~23% (acetaldehyde) in the case of pure PET up to vanish completely in the case of pure PVC.

This last consideration can be better observed in Fig. 4.14, and Fig. 4.15, which show the amount of benzoic acid and CO released at different initial mixture compositions for a heating rate of 10 °C/min.

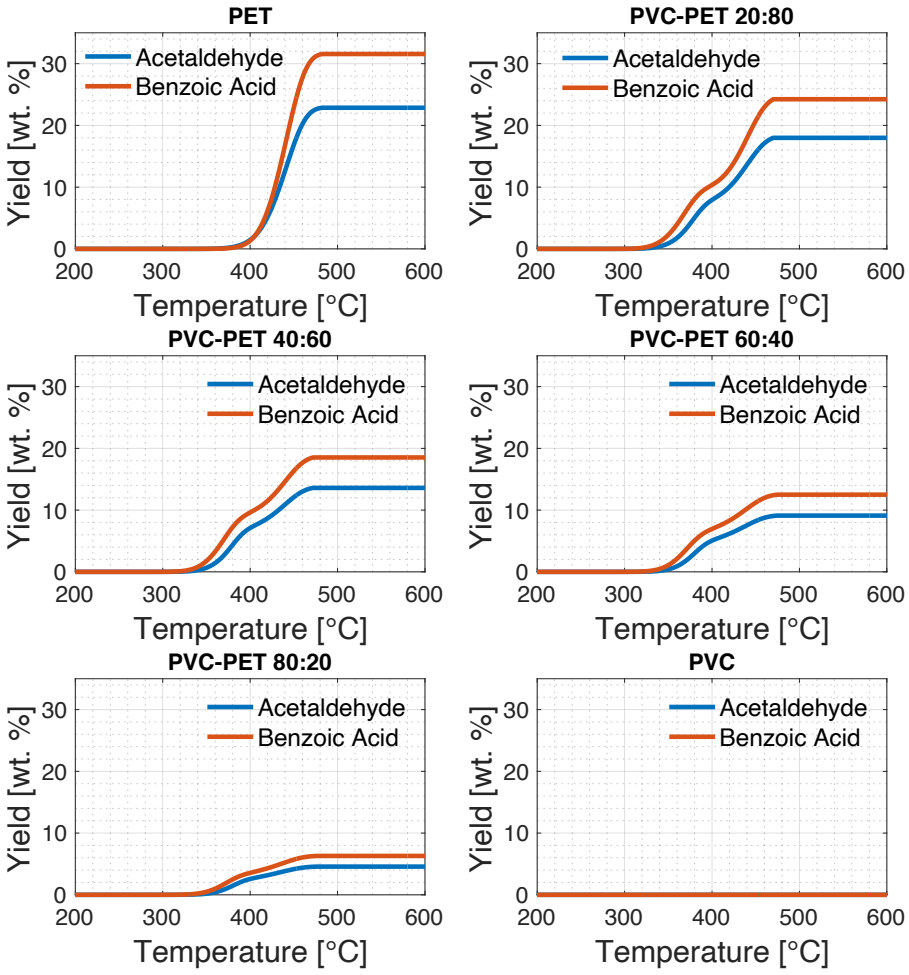

Fig. 4.13 Yield of acetaldehyde and benzoic acid released from different PVC-PET mixtures at 10 °C/min.

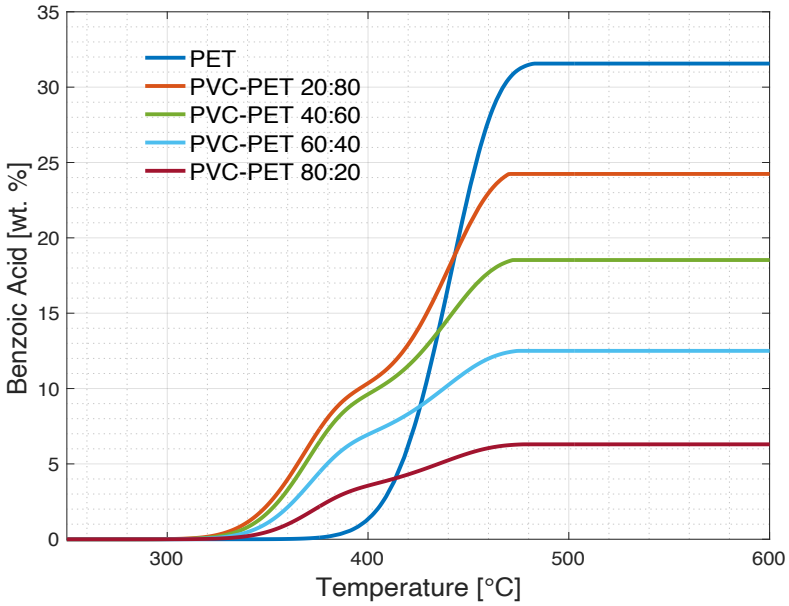

Fig. 4.14 Benzoic acid released from different PVC-PET mixtures (0:100, 20:80, 40:60, 60:40 and 80:20) at 10 °C/min.

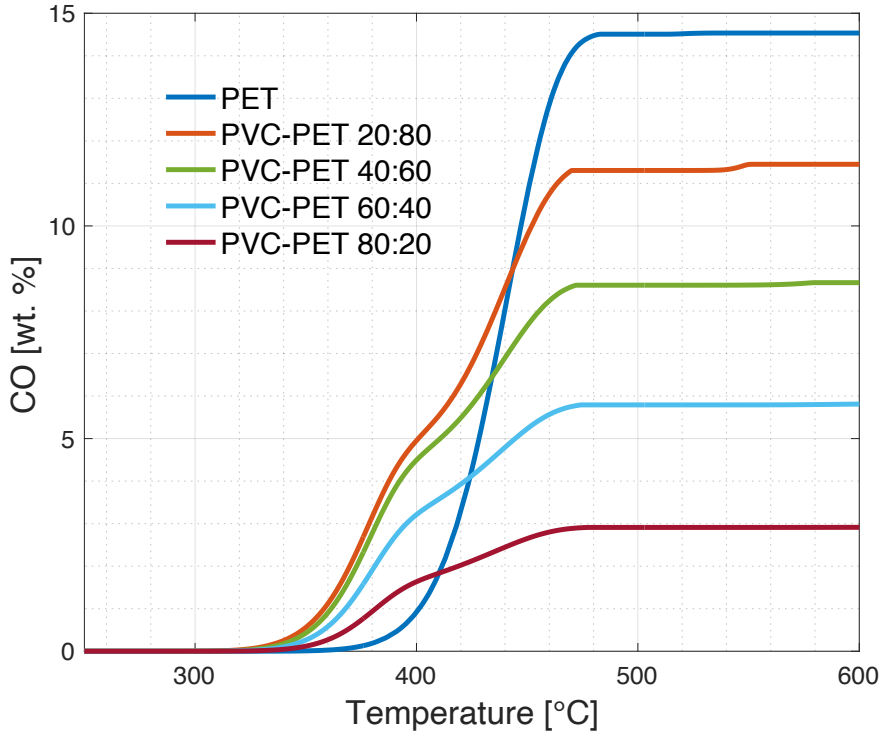

Fig. 4.15 CO released from different PVC-PET mixtures (0:100, 20:80, 40:60, 60:40 and 80:20) at 10 °C/min.

Finally, the effect of the different heating rates on the quantity and rate of volatile compounds release is observed in the figure.

By way of example, by carrying out the model integration at different heating rates, Fig. 4.16 is obtained. This figure shows the yield of benzoic acid at heating rates of 2, 5, 10 °C/min for different PVC-PET mixtures. As shown in this figure, the total amount of benzoic acid released is always about the same at different heating rates for a given mixture composition. However, an increase in the heating rate involves a translation of the curves towards higher temperatures, as already observed previously, resulting in a delay in developing the compound itself. In fact, by way of example, for the 20:80 PVC-PET mixture (i.e. the mixture where the largest development of benzoic acid is observed), the temperature for which 95% of the total mass of benzoic acid is released in the gaseous phase is ~425 °C at 2 °C/min, ~445 °C at 5 °C/min and ~460 °C at 10 °C/min.

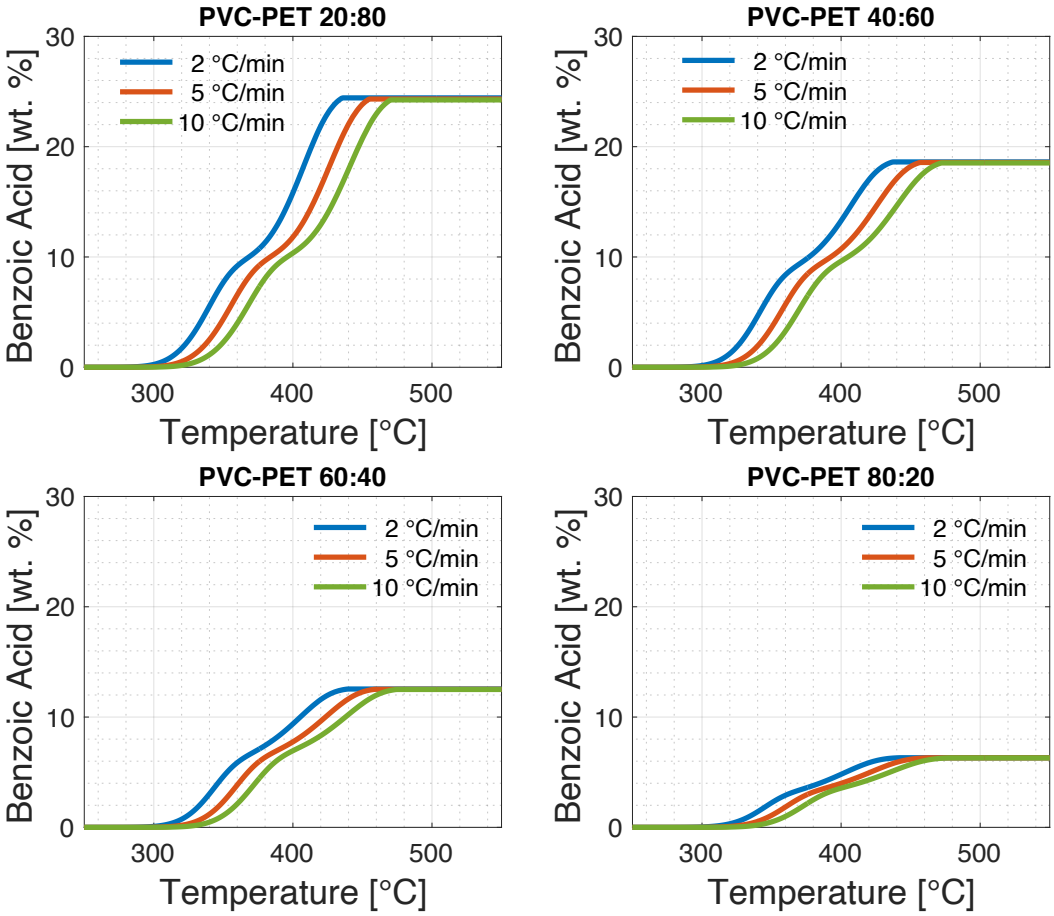

Fig. 4.16 Benzoic acid released from PVC-PET mixtures at different heating rate (2, 5 and 10 °C/min) and different initial compositions.

4.2.3. Evolution of residue

According to the kinetic scheme used for the simulations, the evolution of the residue fraction in the function of the temperature is reported here following. In particular, for each mixture considered, tests were carried out under different dynamic conditions in order to verify the effect of the heating rate on the final residue quantity.

The effect of the heating rate on the model is shown in Fig. 4.17, which shows the evolution of the residue fraction at a heating rate of 2, 5, 10 °C/min for different PVC-PET mixtures.

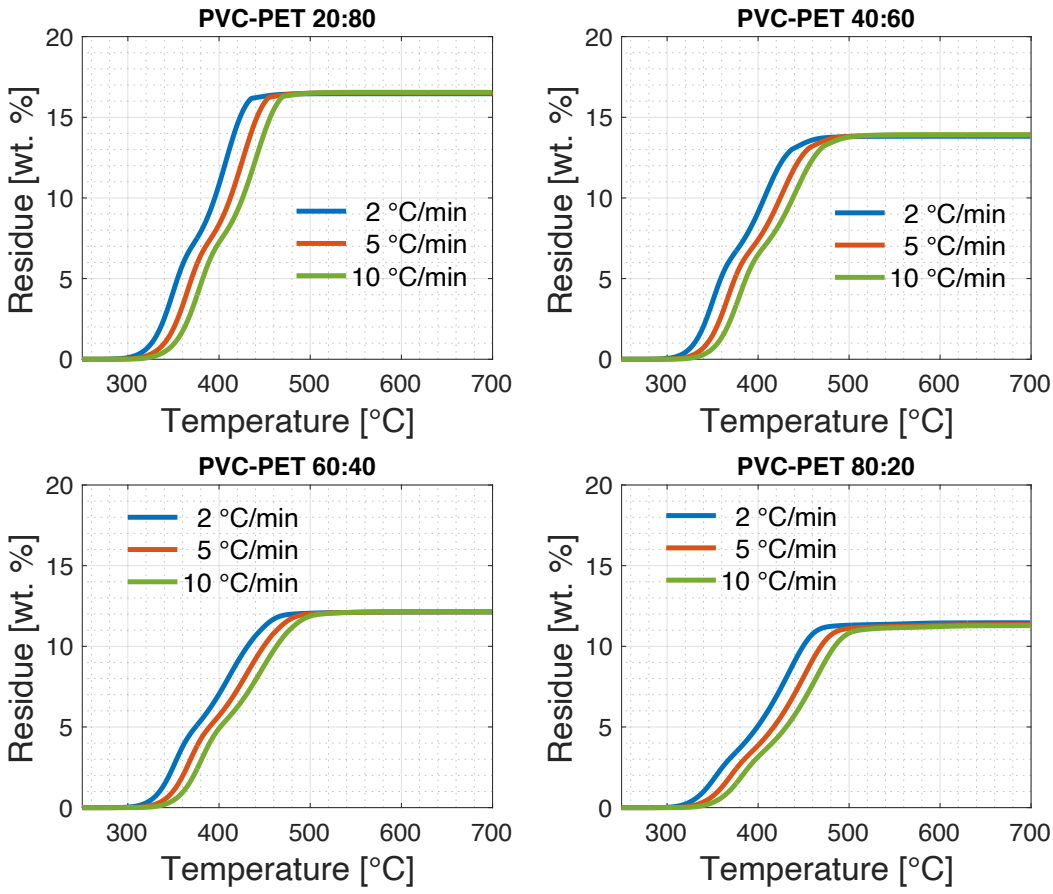

Fig. 4.17 Evolution of the residue fraction from PVC-PET mixtures at different heating rate (2, 5 and 10 °C/min) and different initial compositions.

Fig. 4.17 shows the classic translation of the curves towards higher temperatures as the heating rate increases. In fact, by increasing the heating speed, the formation of residue is delayed, while the final quantity of residue is always approximately the same.

However, it is observed that increasing the PVC content in the mixture considerably decreases the final amount of residue formed, passing from ~16% for the 20:80 PVC-PET mixture to ~11% for the 80:20 mixture. This is probably due to the larger amount of final residue predicted by the model during the thermal degradation of PET (~19%) compared to that obtained from PVC (~12%). This last consideration can also be seen in the figure below (Fig. 4.18), which shows the evolution of residue formed at a heating rate of 10 °C/min for different PVC-PET mixtures.

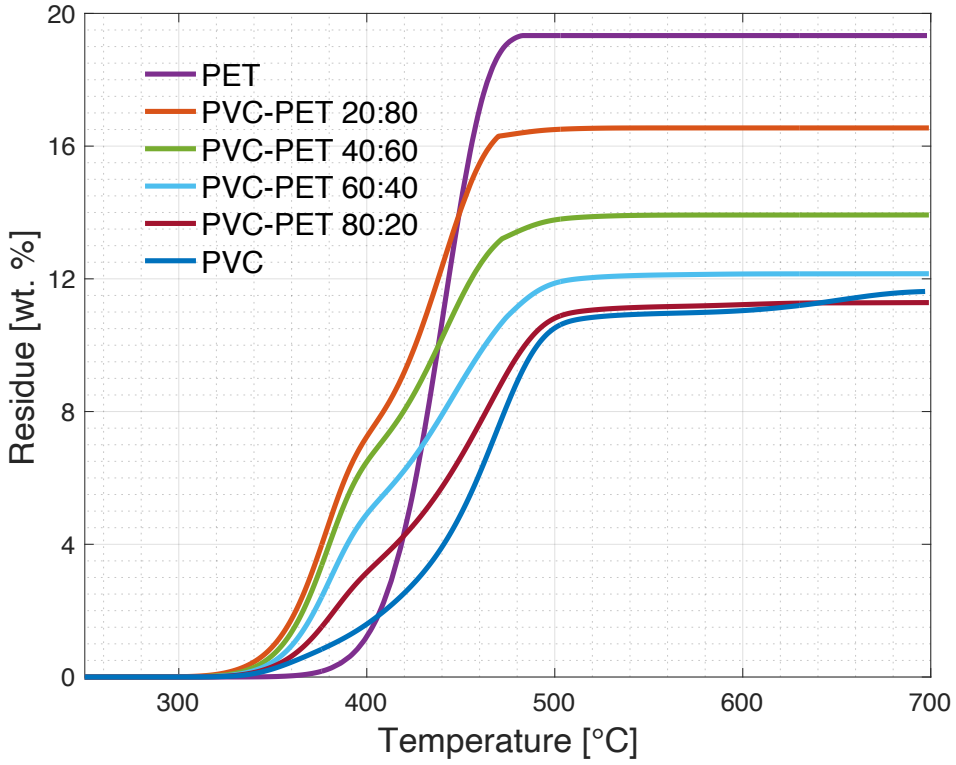

Fig. 4.18 Evolution of the residue fraction from different PVC-PET mixtures (0:100, 20:80, 40:60, 60:40, 80:20 and 100:0) at 10 °C/min.

4.2.4. Comparison with experimental data

The simulations presented in this chapter allowed quantifying the distribution of the main reaction products obtained during the process under different operating conditions. However, it was not possible to compare and verify the reliability of the results obtained due to the absence of experimental data in the literature, especially regarding the product distribution.

The only experimental data available is the TGA of PVC-PET mixture provided by the Energy Department of Politecnico di Milano [31]. Fig. 4.19 shows the TGA of the PVC-PET mixture (50:50 wt%) together with the TGA of neat PVC and PET at 10 °C/min and 20 ml/min of nitrogen flowrate, presented previously (paragraph 4.1.2).

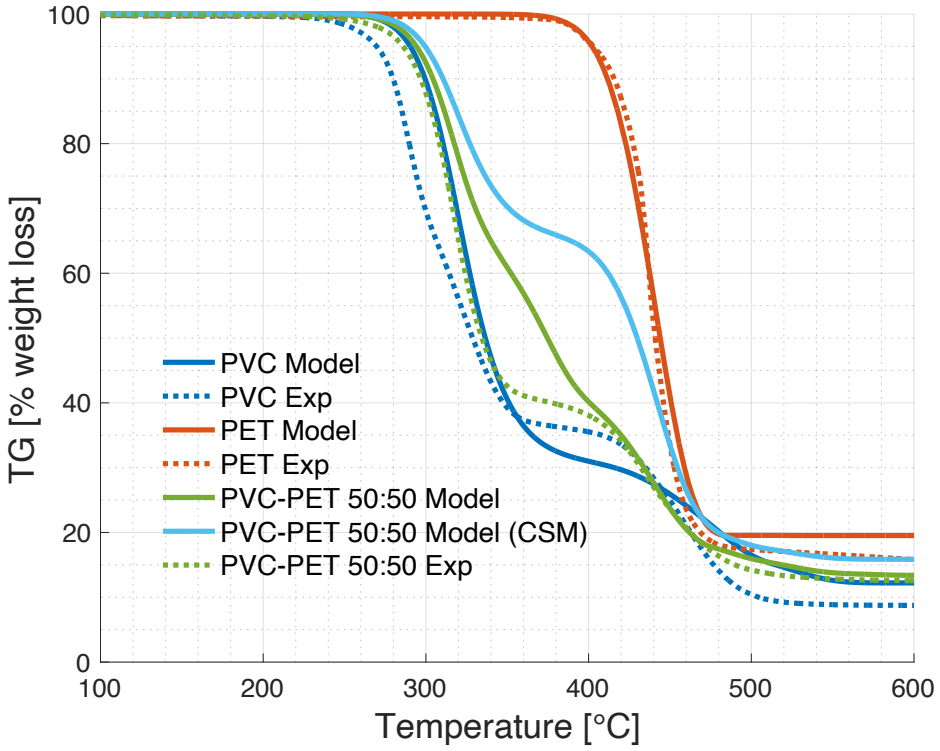

Fig. 4.19 Comparison between model and experimental TGA obtained by the Energy Department of Politecnico di Milano [31] for PVC-PET mixture (50:50 wt%) at 10 °C/min and 20 ml/min of nitrogen flowrate.

Fig. 4.19 shows how using a kinetic model that includes the chemical interactions between PET and PVC leads to results more in line with the experimental data. Experimentally, the mixture shows a final residue quantity equal to ~13%, resulting from the weighted average of the two single compounds, where the residue of PET is ~16% and that of PVC ~9%. The results obtained from the simulation show a mixture final residue value of ~12%, very consistent with the experimental results. However, the model shows moderate delay with respect to the experimental data, especially in the early stages of degradation. This indicates the possible presence of interaction reactions not currently included in the model. Moreover, Fig. 4.19 also shows how, in the initial phase of the thermal process, the presence of PVC in the mixture results in a more significant acceleration of the degradation process compared to that of pure PET. However, after the initial phase, the mixture is

strongly influenced by the resistance to volatilization of the PET, and the accelerating effect becomes less visible.

In general, the model reproduces the experimental observations quite well, with a maximum deviation of ~40 °C found at about half of the degradation process (i.e. with a residue mass of 50%). The results obtained can be considered satisfactory, considering the existence of some uncertainty in the measurements and in the composition of the polymers, such as impurities that are difficult to quantify.

4.3. Final considerations

In this last chapter, PVC-PET mixtures were analyzed in depth. After a first and brief presentation of the existing iterations between these two polymers during the degradation process, more attention was paid to the model sensitivity analysis.

The numerous simulations carried out in this chapter have highlighted the responses of the model as a function of the various operating conditions analyzed, such as the initial mixture composition and the heating rate. The behavior of the TGA curves and the evolution of the volatile products released by the system were studied in the function of the operating conditions.

Furthermore, it was also possible to make a comparison with the experimental data thanks to the TGA curve provided by the Energy Department. The simulation (presented in paragraph 4.2.4.) has allowed highlighting how using a completely segregated model (CSM) to simulate PVC-PET mixtures does not allow us to grasp the synergistic action between these two polymers, leading to significant errors in estimating the mass loss of the sample. However, using a kinetic model that includes the chemical interactions between PET and PVC leads to results more in line with the experimental data, even if the model

still shows a certain delay, especially in the early stages of degradation. This suggests the possible existence of interaction reactions not currently included in the model.

Although limited to this single experimental test, the comparison makes it possible to highlight the strengths of the kinetic model and the aspects that can be improved, still not very faithful to the mixture real behavior.

Conclusions

The work presented in these chapters consists of an analysis of the kinetic model for the plastics thermal degradation developed by the CRECK Modeling Lab of Politecnico di Milano. Starting from the study of neat polymers, i.e. PVC and PET, we then moved on to the study of the mixture between these two compounds.

Regarding neat PVC and PET, after a first and brief presentation of the kinetic model used for the simulations, we moved on to the comparison with the experimental data found in the literature. From this comparison, the main conclusions are the following:

- the PVC model is, in general, in good agreement with the experimental data, especially in terms of TGA curves. However, minor deviations are noted in the onset points of the two degradation steps. Furthermore, the model provides a good prediction also in terms of product distribution, except for polyaromatic hydrocarbon compounds (PAHs);
- the PET model also shows a good agreement with the experimental data, especially regarding the TGA curves, where the model is able to predict the onset point of the degradation excellently. However, the model does not satisfy the actual fraction of residue at the end of the degradation, always overestimating it. The product distribution obtained from the model is in good agreement with the experimental data. However, the model predicts a higher final CO content than CO_2, resulting in the opposite trend with respect to the experimental data. Finally, even if the release of small quantities of benzene is observed experimentally, the model predicts the formation of a negligible amount of this product, although it is included in the kinetic scheme.

Regarding the PVC-PET mixture, after a first and brief presentation of the existing iterations between these two polymers during the degradation process, we moved on to an analysis of the model. The effects of the initial composition of the mixture and heating rates on the behavior of the TGA curves and on the evolution of volatile compounds released by the system were studied. Furthermore, a comparison with the experimental data was possible thanks to the TGA curve provided by the Energy Department of Politecnico di Milano. From this comparison, it was possible to observe that using a completely segregated model (CSM) to simulate PVC-PET mixtures does not allow us to grasp the synergistic action between these two polymers, leading to significant errors in estimating the mass loss of the sample. However, using a kinetic model that includes the chemical interactions between PET and PVC leads to results more in line with the experimental data, even if the model still shows a certain delay, especially in the early stages of degradation. This suggests the possible existence of interaction reactions not currently included in the model.

In light of the results obtained during this work, it becomes necessary to carry out further investigations of the kinetic scheme in order to make it more reliable and precise, especially as regards the characterization of the product distribution so that, by fine-tuning the kinetic model of neat PET and PVC, it will consequently be possible to improve the model for their mixture. Unfortunately, during this work, it was not possible to make further comparisons and validations of the thermal degradation model of PVC-PET mixtures due to the lack of experimental data in the literature. So, to guarantee better reliability of the model, it would be advisable to carry out further *ad hoc* experiments, with the possibility of characterizing the distribution of the products, especially the most important compounds released during the process (i.e. HCl, benzene, CO, CO_2, acetaldehyde and benzoic acid).

Most of the experimental setups aimed at the characterization of the degradation products work in isothermal conditions, monitoring and detecting the compounds released by the process over time through mass spectrometry and gas chromatography techniques. For this reason, simulations were carried out under isothermal conditions at different pyrolysis temperatures and different initial mixture compositions in order to determine the best degradation conditions for each sample considered. This will allow outlining a possible experimental activity aimed at validating the results of the sensitivity analysis carried out in the last chapter. The results obtained from the isothermal simulations are shown in the figure below (Fig. 5.1), which shows the mass loss (%) obtained during the process for different PVC-PET mixture compositions (20:80, 40:60, 60:40 and 80:20 wt%) and at different isothermal temperatures (300, 350, 400, 450 and 500 °C).

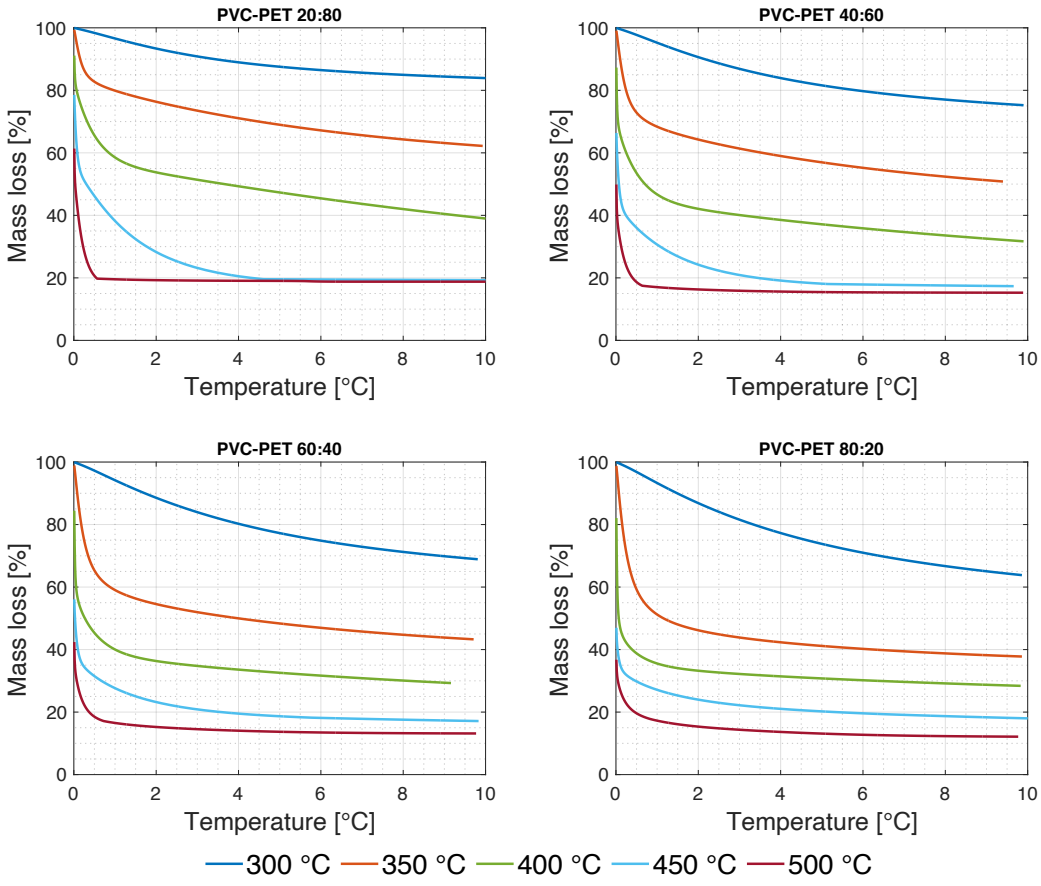

Fig. 5.1 Isothermal TGA of different PVC-PET mixtures (20.80, 40:60, 60:40, 80:20) at different temperature (300, 350, 400, 450, 500 °C).

In isothermal conditions, the TGA curves show an important increase in the rate of degradation as the process temperature increases. In order to outline an experimental plan suitable for this case, the most significant temperatures were chosen to conduct the pyrolysis experiments. These temperatures are selected based on the results obtained during the simulations shown in Fig. 5.1. For each mixture analyzed, it is advisable to choose a temperature that is high enough to allow the complete degradation of the sample (therefore, temperatures below 400 °C will not be considered) but, at the same time, too high temperatures should not be chosen so that the process does not happen too quickly. This allows for adequate detection of the compounds released during the process. Therefore, a good range of temperatures to be considered for conducting the experiments turns out to be 400-500 °C.

Once the model is satisfactorily refined, it can be coupled with the kinetic schemes already proposed by the CRECK Modeling Lab for PE, PP, and PS, allowing for improvement of the overall model for the thermal degradation of complex plastic mixtures, such as *plasmix*. This will allow the model to be used for the design of plants for the plastic waste pyrolysis.

References

[1] PlasticsEurope «Plastics - the Facts 2019» (2019).

[2] H. R. Roser, M. Roser «Plastic Pollution». *Our World Data* (2020).

[3] R. Geyer, J.R. Jambeck, K.L. Law «Production, use, and fate of all plastics ever made». *Science Advances*, Volume 3, Issue 7 (2017).

[4] B. Kunwar, H.N. Cheng, S.R. Chandrashekaran, B.K. Sharma «Plastics to fuel: a review» *Renewable and Sustainable Energy Reviews*, Volume 54, Pages 421-428 (2016).

[5] A. Rahimi, J.M. Garcia «Chemical recycling of waste plastics for new materials production» *Nature Reviews Chemistry*, Volume 1 (2017).

[6] U.S. Environmental Protection Agency, «Advancing Sustainable Materials Management: 2013 Fact Sheet» (2013).

[7] H. Zhou, A. Meng, Y. Long, Q. Li, Y. Zhang «An overview of characteristics of municipal solid waste fuel in China: Physical, chemical composition and heating value». *Renewable and Sustainable Energy Reviews*, Volume 36, Pages 107-122 (2014).

[8] A. Smith, K. Brown, S. Ogilvie, K. Rushton, J. Bates «Waste management options and climate change». *Final report to the European Commission, DG Environment* (2001).

[9] P. Attenberger, T. Kufner, O. Mieden, A. Winter «Polyvinyl chloride (PVC)». *Kunststoffe International*, Volume 2014, Issue 10, Pages 16-20 (2014).

[10] J. Yu, L. Sun, C. Ma, Y. Qiao, H. Yao «Thermal degradation of PVC: A review» *Waste Management*, Volume 48, Pages 300-314 (2016).

[11] «Global demand for PVC to rise by about 3.2%/year to 2021» *Additives for Polymers*, Volume 2014, Issue 11, Pages 10-11 (2014).

[12] J. Li-Na «Study on Preparation Process and Properties of Polyethylene Terephthalate (PET)». *Applied Mechanics and Materials*, Volume 312, Pages 406-410 (2013).

[13] Plastics Insight. «Polyethylene Terephthalate (PET): Production, Price, Market and its Properties». https://www.plasticsinsight.com/resin-intelligence/resin-prices/polyethylene-terephthalate/ (2019).

[14] T. Yoshioka, G. Grause «Feedstock Recycling of PET». *Feedstock Recycling and Pyrolysis of Waste Plastics: Converting Waste Plastics into Diesel and Other Fuels*, Pages 641-661 (2006).

[15] «Chemical Economics Handbook: PET Polymer». https://ihsmarkit.com/products/pet-polymer-chemical-economics-handbook.html (2018).

[16] K. Ragaert, L. Delva, K. Van Geem «Mechanical and chemical recycling of solid plastic waste». *Waste Management*, Volume 69, Pages 24-58 (2017).

[17] European Commission. «European Strategy on Plastic Waste in the Environment» (2013).

[18] A. F. Farzi, A. Dehnad, A.F. Fotouhi «Biodegradation of polyethylene terephthalate waste using Streptomyces species and kinetic modeling of the process» *Biocatalyst and Agricultural Biotechnology*, Volume 17, Pages 25-31 (2019).

[19] O. Dogu, M. Pelucchi, R. Van de Vijver, P.H.M. Van Steenberge, D.R. D'Hooge, A. Cuoci, M. Mehl, A. Frassoldati, T. Faravelli, K.M. Van Geem «The chemistry of Chemical Recycling of solid plastic waste: state-of-the-art, challenges, and future directions of pyrolysis and gasification» *Submitted to Progress in Energy Combustion Science* (2020).

[20] T. Faravelli, G. Bozzano, M. Colombo, E. Ranzi, M. Dente «Kinetic modeling of the thermal degradation of polyethylene and polystyrene mixtures». *Journal of Analytical and Applied Pyrolysis*, Volume 70, Issue 2, Pages 761-777 (2003).

[21] A. Marongiu, T. Faravelli, G. Bozzano, M. Dente, E. Ranzi «Thermal degradation of poly(vinyl chloride)». *Journal of Analytical and Applied Pyrolysis*, Volume 70, Issue 2, Pages 519-553 (2003).

[22] M. Mehl, A. Marongiu, T. Faravelli, G. Bozzano, M. Dente, E. Ranzi «A kinetic modeling study of the thermal degradation of halogenated polymers». *Journal of Analytical and Applied Pyrolysis*, Volume 72, Issue 2, Pages 253-272 (2004).

[23] M. Costantino, M. Borzoni «Modellazione cinetica dettagliata del degrado termico del plasmix e dei suoi componenti» (2020).

[24] G. Yuan, D. Chen, L. Yin, Z. Wang, L. Zhao, J.Y. Wang «High efficiency chlorine removal from polyvinyl chloride (PVC) pyrolysis with a gas–liquid fluidized bed reactor». *Waste Management*, Volume 34, Issue 6, Pages 1045-1050 (2014).

[25] H. Zhou, C. Wu, J.A. Onwudili, A. Meng, Y. Zhang, P.T. Williams «Influence of process conditions on the formation of 2–4 ring polycyclic aromatic hydrocarbons

from the pyrolysis of polyvinyl chloride». *Fuel Processing Technology*, Volume 144, Pages 299-304 (2016).

[26] R.K. Singh, B. Ruj, A.K. Sadhukhan, P. Gupta «Thermal degradation of waste plastics under non-sweeping atmosphere: Part 1: Effect of temperature, product optimization, and degradation mechanism». *Journal of Environmental Management*, Volume 239, Pages 395-406 (2019).

[27] P. Das, P. Tiwari «Thermal degradation study of waste polyethylene terephthalate (PET) under inert and oxidative environments». *Thermochimica Acta*, Volume 679 (2019).

[28] A. Dhahak, G. Hild, M. Rouaud, G. Mauviel, V. Burkle-Vitzthum «Slow pyrolysis of polyethylene terephthalate: Online monitoring of gas production and quantitative analysis of waxy products». *Journal of Analytical and Applied Pyrolysis*, Volume 142 (2019).

[29] A.I. Osman, C. Farrell, A.H. Al-Muhtaseb, A.S. Al-Fetesh, J. Harrison, D.W. Rooney «Pyrolysis kinetic modelling of abundant plastic waste (PET) and in-situ emission monitoring». *Environmental Sciences Europe*, Volume 32, Issue 1 (2020).

[30] M. Artetxe, G. Lopez, M. Amutio, G. Elordi, M. Olazar, J. Bilbao «Operating conditions for the pyrolysis of poly-(ethylene terephthalate) in a conical spouted-bed reactor». *Industrial and Engineering Chemistry Research*, Volume 49, Issue 5, Pages 2064-2069 (2010).

[31] A. Beretta, L. Lietti, Private Communication (2020).